

Biodegradable thermosensitive polymers:
synthesis, characterization and
drug delivery applications

Osamu Soga

Biodegradable thermosensitive polymers: synthesis, characterization and drug delivery applications

Osamu Soga

Ph. D. Thesis, with a summary in Dutch

Utrecht University, The Netherlands

March 2006

ISBN: 90-393-4188-5

Copyright: © 2006 by Osamu Soga. All rights reserved. No part of this thesis may be reproduced or transmitted in any form or by any means, without written permission from the author.

Biodegradable thermosensitive polymers: synthesis, characterization and drug delivery applications

Biodegradeerbare temperatuur-gevoelige polymeren:
synthese, karakterisering en toepassing
voor het toedienen van farmaca
(met een samenvatting in het Nederlands)

PROEFSCHRIFT

ter verkrijging van de graad van doctor aan de Universiteit Utrecht
op gezag van de Rector Magnificus, prof. dr. W.H. Gispen,
ingevolge het besluit van het College voor Promoties
in het openbaar te verdedigen op
dinsdag 21 maart 2006 des middags te 12.45 uur

door

Osamu Soga

geboren op 29 december 1970, te Gifu, Japan

Promotores: Prof. Dr. Ir. W.E. Hennink
Prof. Dr. G. Storm
Copromotores: Dr. C.F. van Nostrum
Dr. R.M. Schiffelers

The research described in this thesis was financially supported by Mitsubishi
Pharma Corporation, Osaka, Japan.

Table of contents

Chapter 1	Introduction	7
Chapter 2	Poly(<i>N</i> -(2-hydroxypropyl) methacrylamide mono/di lactate): a new class of biodegradable polymers with tuneable thermosensitivity	33
Chapter 3	Physicochemical characterization of degradable thermosensitive polymeric micelles	43
Chapter 4	Thermosensitive and biodegradable polymeric micelles for paclitaxel delivery	67
Chapter 5	<i>In vivo</i> efficacy of paclitaxel-loaded thermosensitive biodegradable polymeric micelles	87
Chapter 6	Summary and perspectives	103
Appendices	Nederlandse samenvatting	118
	List of abbreviations	120
	List of publications	122
	Curriculum vitae	124
	Acknowledgements	125

Chapter 1

Introduction

This chapter is based on: Cornelus F. van Nostrum, Cristianne J.F. Rijcken, Osamu Soga and Wim E. Hennink. *Manuscript in preparation*

General introduction

1. Nanoscopic drug carriers

Most systemically administered drugs exert their biological effects not only at their target sites but also at non-target sites, which often results in undesired side effects and hampers their therapeutic potential. This fact emphasizes the importance of drug delivery systems (DDS) which deliver biologically active compounds selectively to the pathological area. Targeted drug delivery is of particular importance for the treatment of life-threatening diseases such as cancer [1-3]. One of the main challenges in DDS research is the development of drug carriers enabling such selective tissue specific drug targeting. For this purpose, drug carriers should preferably have a high drug loading capacity, adequate stability in the bloodstream, a suitable drug release profile at the site of action, and good biocompatibility. Importantly, from an industrial viewpoint, the drug-loaded carrier systems developed for parenteral use need to be suitable for sterile manufacturing at large scale in compliance with good manufacturing practice (GMP), and should show a good stability during storage. Extensive research for the ideal, universal drug carrier system in the last quarter of the last century has resulted in a great variety of nanoscopic drug carriers [4,5]. Nanoscopic drug carriers have, as their name implies, nanoscopic dimensions (typically 10 to 200 nm), and can be categorized into particulate systems and water-soluble macromolecular systems. The first category includes systems such as liposomes [6,7] and emulsions [8,9], and systems based on synthetic polymers such as nanoparticles [10,11], polymeric micelles [12-14] and polymeric vesicles [15,16]. The second category of nanoscopic drug carrier systems encompasses polymer-drug conjugates [17,18] and dendrimers [19,20]. Some of these systems are presently on the market and many clinical evaluations are in progress to demonstrate their potential for the treatment of patients.

Due to their submicron size, nanoscopic DDS can be administered intravenously, providing possibilities to reach the pathological sites while avoiding many biological barriers in the human body, such as limited gastrointestinal absorption and high hepatic first-pass effect of orally administered drugs. After intravenous (*i.v.*) administration, nanoscopic drug carriers should deliver their payloads selectively at the target sites. It is known that the so-called enhanced permeability and retention (EPR) effect plays an important role for such targeting to e.g. tumor tissues [21,22]. The EPR effect was proposed by Maeda et al. in 1980's and is attributed to two factors. Firstly, the angiogenic tumor vasculature, as well as blood vessels in other pathological tissues, has a higher permeability compared to normal ones due to its discontinuous endothelium. Secondly, it has been shown that in tumors lymphatic drainage is not fully developed. These features lead to the fact that

colloidal particles (nanoscopic DDS) extravasate through the “leaky” endothelial layer in tumor tissues and are subsequently retained there. It should be noticed that to achieve this “passive” targeting, the nanoscopic DDS have to circulate in the bloodstream for sufficient time. In this respect, the size of nanoscopic DDS is an important factor which determines their biological fate. In general, particles with a size less than 5 to 10 nm are immediately eliminated through the renal glomerulus [23], whereas larger particles between 50 up to hundreds of nm are taken up by the liver and the spleen with the larger ones (> 250 nm) being distributed in particular to the spleen by mechanical filtration with eventual removal by the splenic macrophages [24,25]. A key issue for prolonged circulation is to reduce the rate of non-specific recognition and uptake by the mononuclear phagocyte system (MPS). It has been shown that grafting of hydrophilic polymers on the surface of particles is effective to oppose opsonization and subsequent uptake by the MPS [24,26]. Without surface coating, colloidal particles are generally speaking rapidly cleared from the bloodstream to distribute into the MPS cells of the liver, spleen and bone marrow. Another way of drug targeting, which is referred to as “active” targeting, can be accomplished by coupling a specific ligand (e.g. antibodies) to nanoscopic drug carriers [27]. Active targeting is employed to deliver the drugs into the target cells through ligand-receptor interaction and subsequent internalization of the drug-loaded vehicles, typically in combination with passive targeting. Outlined below are examples of promising nanoscopic drug carriers for targeted drug delivery.

Liposomes are vesicles composed of phospholipid bilayer membranes surrounding aqueous compartments, with a size typically between 80 to 250 nm. Hydrophilic drugs can be entrapped in the interior aqueous compartment of liposomes, while hydrophobic compounds can be incorporated into the phospholipid bilayer. Liposomes were proposed as drug carriers in cancer therapy over 30 years ago [28]. The first generation of liposomes, referred to as conventional liposomes, suffered from very fast blood clearance by the MPS [7]. A major breakthrough was the finding that coating of liposomes with a hydrophilic polymer such as poly(ethylene glycol) (PEG) provides steric stabilization of liposomes and drastically prolongs their half-lives in the bloodstream [29,30], which accelerated the development of therapeutic liposomal formulations. Pegylated liposomes are also referred to as “stealth” liposomes. At present several liposome products are on the market and a doxorubicin (DOX) formulation of liposomes bearing covalently coupled antibodies on their surface (immunoliposomes) is presently clinically evaluated [31-33]. Doxil, PEG-coated liposomal DOX marketed for the treatment of Kaposi’s sarcoma and metastatic ovarian cancer, has a 300-fold increased plasma AUC (area under the curve) [34,35] and greatly increased tumor AUC [36] compared to free DOX as a result of its “stealth” properties and the EPR

effect. Despite the excellent tumor selectivity, Doxil has only resulted in a modest increase in antitumor activity [37], likely due to too slow release of DOX from the liposomes [38]. Similar findings were reported for cisplatin-loaded PEG-coated liposomes, where almost no antitumor effect and toxicity of cisplatin was observed, although the accumulation in the tumor tissues substantially increased as compared to the free drug [39]. It can consequently be concluded that an efficient and active release mechanism is necessary for further improvement of liposomal systems.

Polymer-drug conjugates are water-soluble polymers to which drugs are covalently attached via spacers. The most well-known example is poly(*N*-(2-hydroxypropyl) methacrylamide) (pHPMAM) conjugated with DOX (PK1), developed by Kopecek and Duncan in the early 1980's [40]. PK1 has a molecular weight of around 30,000 g/mol and a DOX content of around 8.5 % (w/w). The molecular weight of PK1 was optimized to give a hydrodynamic diameter in aqueous solution of 6 nm to ensure efficient renal elimination and at the same time allowing spontaneous tumor accumulation by the EPR effect [4]. Tailoring of the polymer-drug linker is essential to create a polymer-drug conjugate that is stable in the blood circulation but allows drug liberation at the target site. PK1 employs a biodegradable peptide linker (Gly-Phe-Leu-Gly), which is a substrate for lysosomal cathepsin B, and DOX is conjugated to the linker by an amide bond. This tetrapeptide linker is cleaved by cathepsin B following endocytic uptake of the conjugate into the tumor cells. At present more than ten polymer-drug conjugates including PK1 and PK2 (the second generation of pHPMAM-DOX conjugate with galactosamine for liver targeting) are under clinical evaluation [4,41]. These formulations also include two different polymer-paclitaxel (PTX) conjugates, with clinical results which were markedly different from each other. CT-2103 is a conjugate of PTX and poly(glutamic acid), in which PTX is bound via an ester bond at loading amounts of 37 % (w/w) [42]. The polymer backbone is cleaved by cathepsin B after cellular endocytotic uptake to liberate diglutamyl-PTX, which likely is hydrolyzed intracellularly to yield PTX. Early clinical trials proved that CT-2103 is effective against e.g. non-small cell lung cancer, and PTX-resistant ovarian cancer [43]. The other formulation, PNU166945, is a pHPMAM-PTX conjugate containing PTX approximately at 5 % (w/w) [44]. PNU166945 employs the same peptide linker as PK1 (Gly-Phe-Leu-Gly), to which PTX is conjugated via an ester bond. PNU166945 showed neurotoxicity, which is typical for free PTX, in a Phase 1 study and the further clinical development of this conjugate was therefore terminated [44]. The neurotoxicity is supposed to be caused by PTX that was released in the bloodstream. These clinical results suggest that the design of the conjugates (e.g. choice of the polymer and the linker, the amount of the conjugated drugs) is critical for their therapeutic efficacy.

Polymeric micelles are self-assembled core-shell nanostructures consisting of amphiphilic block copolymers formed in an aqueous solution [45,46]. The hydrophilic blocks of the copolymers form the shell of the micelles and stabilize the micellar structure. Typically, hydrophobic blocks of the copolymers form the core of the micelles by hydrophobic interaction, although other interactions such as electrostatic interaction [47] and stereocomplex formation [48] can also be utilized as the driving force for the core formation. The application of polymeric micelles as drug delivery system was pioneered by the group of Kataoka in the early 1990's through the development of DOX-conjugated block copolymer micelles [49]. Nowadays polymeric micelles are extensively studied as a promising nanoscopic drug carrier because of their attractive features to fulfil the requirements for selective drug delivery [50-54]. Firstly, the hydrophobic core has a large capacity to accommodate hydrophobic drugs in particular. Secondly, their relatively small size (typically between 10 to 60 nm) and hydrophilic surface allow polymeric micelles prolonged circulation in the bloodstream after intravenous administration by opposing the recognition by macrophages of the MPS, and gradual extravasations through leaky capillaries, leading to their passive accumulation in e.g. tumor and other pathological areas due to the EPR effect. Thirdly, the virus-like size of the polymeric micelles enables their internalization into the cells via e.g. fluid-state endocytosis even without any targeting ligand present on their surface [55-57]. Fourthly, for pharmaceutical development it is advantageous that polymeric micelles can be easily sterilized by filtration through a 0.2 μm filter. Concerning their toxicity, polymeric micelles finally dissociate in the body into single block copolymer chains. Block copolymers for micellar applications generally have a molecular weight less than 50,000 g/mol and are therefore subject to renal clearance, preventing their long-term accumulation in the body [52,58]. Also biodegradable building blocks can be used to design polymeric micelles. Furthermore, chemical modification of block copolymers enables functionalization of polymeric micelles (e.g. the attachment of specific ligands and the introduction of stimuli-sensitive segments) for active drug targeting.

Generally amphiphilic block copolymers of the A-B type, where A represents a hydrophilic block and B represents a hydrophobic block, are used to design polymeric micelles. Other examples include A-B-A triblock copolymers [59] and graft copolymers [60,61]. Poly(ethylene glycol) (PEG) is most commonly used as the hydrophilic segment of the copolymers, since it is an FDA-approved, non-toxic polymer and its unique physicochemical properties (high water solubility, high flexibility and large exclusion volume) provide good "stealth" properties [62-64]. Also other polymers can be used as the shell forming segment, e.g. poly(*N*-vinyl-2-pyrrolidone) (PVP) [65] and poly(acrylic acid) [66]. In contrast, a larger variety of polymers has been studied as hydrophobic segment in polymeric micelles: poly(propylene glycol) (PPO, Pluronics®) [23],

poly(aspartic acid) with chemically conjugated DOX (PAsp(DOX)) [67], poly(β -benzyl-L-aspartate) (PBLA) [68], and poly(ester)s such as poly(lactic acid) (PLA) [69,70] and poly(ϵ -caprolactone) (PCL) [71,72]. The choice of the core-forming segment is the major determinant for important properties of polymeric micelles such as stability, drug loading capacity and drug release profile (described in more detail in Section 2), and explains why so many core-forming hydrophobic polymers have been used for the development of polymeric micelles.

2. Polymeric micelles as drug delivery vehicles

2-1. Critical micelle concentration

The formation of polymeric micelles in aqueous solution occurs when the concentration of the polymer increases above a certain concentration, named as the critical micelle concentration (CMC). At the CMC, hydrophobic segments of block copolymers start to associate to minimize the contact with water molecules, leading to the formation of a core-shell micellar structure. For the determination of the CMC of polymeric micelles, fluorescent probes are frequently utilized. Pyrene, a nonpolar polyaromatic molecule, preferentially partitions from a hydrophilic to more hydrophobic environment (e.g. the core of the polymeric micelles) with a concurrent change in its fluorescent properties such as a red shift in the excitation spectrum and vibrational structure changes (described as the ratio I_1/I_3) in the emission spectrum [73,74]. The CMC of polymeric micelles can be determined as the onset of these spectral changes as a function of the polymer concentration.

The CMC of polymeric micelles is typically on the order of 10^{-6} to 10^{-7} M, while that of low molecular weight surfactant micelles is on the order of 10^{-3} to 10^{-4} M [51]. This indicates that polymeric micelles, compared to surfactant micelles, are less prone to dissociation at low concentrations. This is an advantageous characteristic because polymeric micelles are subject to dilution upon intravenous administration but have to maintain the micellar form for prolonged circulation in the bloodstream and targeted drug delivery. The physical properties and the molecular weight of the core-forming block have large influence on the CMC of polymeric micelles. For example, the CMC values for polystyrene-*b*-PEG (PS-*b*-PEG) micelles range between 0.001 to 0.005 mg/mL [73], while those for some of Pluronics® (triblock copolymers of PEG-*b*-PPO-*b*-PEG) are around 0.3 mg/mL [75]. In line with expectations, longer hydrophobic blocks decrease the CMC, while the length of hydrophilic block does not significantly affect the CMC [23,50]. As described above, polymeric micelles with lower CMC are preferred as drug carriers because they are more resistant against dilution after e.g. intravenous administration. Furthermore, polymeric micelles with a “frozen” (glassy or crystalline) core

have greater kinetic stability than those with a liquid-like core, and may remain intact or dissociate very slowly into monomers even below the CMC [76].

2-2. Characterization of micellar structures

The size and the microstructure (e.g. dimension and fluidity of the core, aggregation number, density of hydrophilic coverage of the shell) of polymeric micelles largely influence their physical and biological stability. These features depend primarily on the chemical nature and the molecular weight of the segments of the block copolymers. The size of polymeric micelles and their size distribution (polydispersity) can be determined by dynamic light scattering (DLS) [77] and microscopic techniques, e.g. transmission electron microscopy (TEM) [78-80], and atomic force microscopy (AFM) [81,82]. DLS gives the hydrodynamic diameter calculated from the diffusion coefficient of the micelles using the Stokes-Einstein relation for colloidal particles, while microscopic techniques reveal the morphology of the micelles. Polymeric micelles are usually characterized by a smaller size (10 to 60 nm) and a narrower size distribution (polydispersity index < 0.1) than other nanoscopic carriers e.g. liposomes, although some polymeric micelles have a bimodal size population likely resulting from secondary aggregation of exposed hydrophobic cores [70,83,84]. The shape of polymeric micelles is mostly spherical but other shapes e.g. ellipsoid and rod-like micelles are also observed depending on the hydrophilic-hydrophobic balance of the block copolymer [46,50].

Static light scattering (SLS) provides information on the microstructure of polymeric micelles. By measuring the angular dependence of the scattered light intensity of a micellar solution, the radius of gyration (R_g) and the weight average molecular weight of the micelles ($M_w(\text{mic})$) are determined. Additional structural characteristics, e.g. the aggregation number of the micelles, the density of the micelles, the surface area of the micelles per single polymer chain, are obtained if $M_w(\text{mic})$ and other parameters such as the hydrodynamic radius of the micelles (R_{hyd} , measured by DLS) and the molecular weight of the block copolymer are known [80,85,86]. Moreover, the R_g/R_{hyd} ratio gives an indication of the shape of the polymeric micelles. The theoretical R_g/R_{hyd} ratio for homogeneous spheres is 0.775, whereas for core-shell micellar structures in which the density of the core is larger than that of the shell, the ratio is below this value [87,88]. The molar mass and the aggregation number of the micelles are significantly affected by the molecular weight of the block copolymer [89]. For example, at a fixed PEG molecular weight of 5,000 g/mol, the aggregation number of PLA-*b*-PEG micelles ranges from 30 to 1,100 by varying the molecular weight of the PLA block from 2,000 to 45,000 g/mol [85]. Large aggregation numbers are generally associated with a low surface area per single polymer chain, which is a favourable property for prolonged blood circulation [70,90].

Regarding the fluidity of the core, ^1H NMR provides information on the mobility of the polymer chains in their micellar form. The presence of solid-like core of the micelles in D_2O results in the disappearance of the proton signals from the core-forming segments due to a restricted chain mobility within the core [91,92]. It has been reported that the core of PLA-*b*-PEG micelles becomes more viscous and solid-like with increasing molecular weight of the PLA block [85]. In contrast, proton peaks of the hydrophobic PPO blocks of Pluronics® micelles are observed in D_2O with ^1H -NMR, indicating a high segmental motion of the PPO chains in the hydrophobic core [14].

2-3. Drug loading into polymeric micelles

Drugs can be incorporated into polymeric micelles by chemical conjugation (covalent attachment of the drug to the core-forming polymer via e.g. amide bond) or by physical entrapment. There are several means for loading drugs physically into the core of polymeric micelles. The simplest way is by direct dissolution of the drugs and the block copolymers in aqueous solution, but this method is applicable only when both are readily soluble in water (e.g. Pluronics®). In most cases, drug-loaded polymeric micellar systems consist of hydrophobic drugs and water-insoluble block copolymers, and then loading procedures with organic solvents such as o/w emulsion [54], dialysis [93] and solid dispersion [94,95] are utilized. In an o/w emulsion procedure, the drug and the polymer are dissolved in a water-immiscible volatile solvent (e.g. chloroform) and this solution is subsequently emulsified in an aqueous phase. Due to its amphipathic nature, the block copolymer partitions at the solvent/water interface and the drug is incorporated in the hydrophobic core of the micelle once the solvent had evaporated. In the dialysis procedure, the drug and the polymer are dissolved in a water-miscible organic solvent (e.g. acetonitrile) and this solution is subsequently dialyzed against water. As the organic solvent is replaced by water, the polymer associates with the drug to form drug-loaded micelles. The solid dispersion procedure consists of dissolving the drug and the polymer in an organic solvent and the formation of solid polymer matrix by removing the solvent under reduced pressure. The addition of water to the preheated polymer matrix and subsequent stirring also leads to the formation of drug-loaded micelles. Although high loading capacity of hydrophobic drugs (typically more than 10 % (w/w)) has been achieved by these approaches, these procedures can not be easily scaled up for GMP manufacturing. Leroux et al. recently reported a simple loading method which is potentially applicable for large-scale production. A *tert*-butanol/water mixture containing the drug and the polymer is sterilized through filtration and is then lyophilized. Next, the freeze-dried cake is rehydrated in water and drug-loaded micelles are obtained [96,97].

Polymeric micelles have been loaded with a great variety of drugs such as DOX [49,57,98-102], PTX [56,69,95,103-108], cisplatin [109,110], amphotericin B [111], indomethacin [112,113], photosensitizers [114-116] and a new cytotoxic drug candidate (KRN 5500) [117,118]. Especially PTX, a typical hydrophobic anticancer drug with a low solubility of 0.3 $\mu\text{g}/\text{mL}$ in water [119-121], has been frequently used in recent years as a drug for newly developed polymeric micellar systems, because the current commercial PTX formulation (Taxol®) causes adverse effects by the presence of Cremophor EL (a polyethoxylated castor oil) and alternative formulations are consequently urgently needed [122,123]. Besides, polymeric micellar formulations of PTX may achieve prolonged circulation in the bloodstream and result in increased tumor accumulation compared to Taxol, as described in Section 2-5 [106]. Furthermore, active targeting of PTX is possible with polymeric micelles to which tumor specific antibodies such as 2C5 are conjugated [103].

Most efficient drug loading can be achieved when the compatibility (e.g. assessed by the Flory-Huggins interaction parameter [50]) between the drug and the core-forming segment of the block copolymer is high. For example, the partition coefficient of pyrene is of the order of 10^2 for Pluronics® [75], 10^4 for PBLA-*b*-PEG [124] and 10^5 for PS-*b*-PEG [73,125], showing that the extreme hydrophobic pyrene partitions, as expected, preferentially into the hydrophobic core of polymeric micelles. Further, the affinity of a drug for the hydrophobic drug can be optimized by a proper selection of the hydrophobic block of a block copolymer. Examples include poly(*N*-(6-hexylstearate)-L-aspartamide)-*b*-PEG (PHSA-*b*-PEG) for amphotericin B [126,127] and poly(C16-benzyl-L-aspartate)-*b*-PEG for KRN 5000 [117]. It is even possible to covalently link the drug to the core-forming block in order to stabilize the micellar core. This was demonstrated for PAsp(DOX)-*b*-PEG, which stably incorporated DOX by π - π stacking between conjugated and non-conjugated molecules [67,84], and this formulation (NK911) is presently under clinical evaluation (see Section 2-5). Park et al. recently reported an interesting and rational approach to the design of a polymer with a core-forming block that has a high affinity for the drug to be entrapped. They first screened a large number of hydrotropic agents to identify their ability to enhance the solubility of PTX in water, and *N,N*-diethylnicotinamide (NNDENA) was found to be the most effective hydrotropic agent for PTX [121]. Next, monomers containing NNDENA, 2-(4-vinylbenzyloxy)-*N,N*-diethylnicotinamide (DENA monomer) and their block copolymers with PEG were synthesized. The resulting PDENA-*b*-PEG block copolymer solubilized PTX up to 37 % (w/w) to form polymeric micelles with a size of 100 nm, which were stable for months without giving leakage and subsequent precipitation of PTX [107].

2-4. Drug release from polymeric micelles

Drug-loaded micelles should have sufficient stability in the bloodstream to enable them to reach their target site. This also implies that the release of the drug from the micelles has to be minimal in the bloodstream. The release of physically entrapped drugs from polymeric micelles is controlled by diffusion of the drug through the micellar core and the partition coefficient of the drug over the micellar core and the aqueous phase, provided that the micelles remain intact. The release of pyrene from polymeric micelles with a glassy core such as poly(styrene) ($T_g = 100\text{ }^\circ\text{C}$) and poly(*tert*-butyl acrylate) ($T_g = 40\text{-}43\text{ }^\circ\text{C}$) was slow, indicated by very small diffusion constants of 10^{-18} to $10^{-16}\text{ cm}^2/\text{s}$ [128]. On the other hand, the release of pyrene from poly(2-vinylpyridine)-*b*-PEG, whose core is liquid-like under the experimental conditions, was too fast to be assessed [128]. This indicates that polymeric micelles with a solid-like core at body temperatures are preferable for targeted drug delivery. Other factors influencing drug release are the length of core-forming polymer segment and the amount of the loaded drug. It was shown that the release rate of indomethacin from PCL-*b*-PEG micelles decreased as the molecular weight of the PCL block and the amount of entrapped indomethacin increased [129].

The release of chemically conjugated drugs is usually very slow compared to that of physically loaded drugs, since the release is dependent on the chemical or enzymatic hydrolysis of the bond between the drug and the polymer backbone. In fact, the release of DOX from PAsp(DOX)-*b*-PEG, where DOX is chemically bound to the polymer via an amide bond, is so slow that the chemically conjugated DOX did not exert antitumor activity [67,84]. To enhance the release of chemically bound DOX, the use of an acid labile hydrazone linkage between the drug and the polymer has been recently reported, and accelerated release of DOX at acidic pH *in vitro* was indeed demonstrated [101,130,131]. Although these systems have not been evaluated *in vivo* yet, such acid sensitive spacers might be beneficial for tumor targeting since the extracellular pH of tumors as well as the endosomal and lysosomal compartments of the cells are more acidic than that of blood and normal tissues [12,132].

2-5. *In vivo* preclinical and clinical evaluation of polymeric micelles

A number of *in vivo* evaluations of polymeric micelles (without drug as well as drug-loaded) have been performed until now [133]. In general, polymeric micelles with good physical stability (e.g. low CMC, dense hydrophilic shell) show acceptable prolonged circulation in the bloodstream after *i.v.* administration [134,135], although their half-lives in their distribution phase (more than 40 % of the injected dose is cleared within one hour [135]) are shorter than those of PEG-coated liposomes (more than 50 % of the injected dose remains in the circulation after 4 hours [26]). However, due to their smaller

size, polymeric micelles may have an increased possibility to accumulate in the regions that are poorly accessible for liposomes [136].

After administration of drug-loaded polymeric micelles, the *in vivo* biodistribution of the drugs is largely influenced by the nature of the core segment. It has been shown that PTX-loaded polymeric micelles with a PLA core did not show improved target distribution of PTX compared to Taxol [97,137], while those with a core of polyaspartate modified with 4-phenyl-1-butanol significantly increased the plasma AUC (90-fold versus Taxol) and the tumor AUC (25-fold versus Taxol) of PTX [106]. These results would suggest that a micellar core which contains more hydrophobic and more compatible groups to PTX (e.g. phenyl groups) is preferable for strong interaction with PTX and its stable retention *in vivo*.

At present several drug-loaded polymeric micellar systems are being clinically evaluated and these include DOX (NK911 [138] and Pluronic P85 [139]), KRN 5500 [140] and PTX (Genexol-PM [108,141]). The plasma AUC of DOX for NK911 (see Section 2-3) in patients with solid tumors was two-fold greater than that for the conventional DOX formulation but was 100-fold lower than that for Doxil (PEG-coated liposomal DOX), indicating that NK911 is less stable or more rapidly cleared in the bloodstream than Doxil [138]. A phase I study for Genexol-PM (a PLA-*b*-PEG micellar formulation of PTX) showed that the plasma AUC and the plasma half-life of PTX for Genexol-PM were relatively lower than those for Taxol, which is consistent with the results of animal experiments [108,137]. However, acute hypersensitivity reactions, which frequently occur for Taxol due to Cremophor EL, were not observed for any patients administered with Genexol-PM [108].

2-6. Polymeric micelles with controlled instability

The ideal polymeric micellar system stably retains the entrapped drug in the bloodstream, and releases the drug, preferably in a relatively short time, only after reaching the site of action. To balance these conflicting requirements (retention and release), polymeric micellar systems where the release of the entrapped drugs occurs in a controlled way have been developed. One strategy concerns the use of external stimuli such as light [142], ultrasound [57,143] and temperature [144,145] to (temporarily) destabilize the micelles and simultaneously release the entrapped drug. However, in clinical practice, the use of externally applied stimuli is not always feasible. Furthermore, this kind of treatment requires the identification of the precise localization of the pathological site, so this approach is not feasible for treatment of e.g. undetected metastases. Consequently, it is more advantageous to exploit naturally occurring differences and conditions in the human bodies (e.g. pH differences, chemical or biological degradation) for destabilization of the micelles and release of the loaded drug.

One sophisticated and rational approach for such “spontaneous” systems is the conversion of core-forming segment of polymeric micelles from hydrophobic to a more hydrophilic state under physiological conditions, which causes the hydrophilization of the amphiphilic block copolymer and eventual dissolution of the micelles. When the drug initially is stably associated with the hydrophobic core, the release of the drug is expected to occur concurrently with the destabilization of the micelles. In recent years, such conversion has been achieved by protonation or degradation of the originally hydrophobic block of the micelle-forming polymer. Relatively many examples of “protonation” approaches have been reported and include block copolymers which contain L-histidine [146,147], pyridine [148] and tertiary amine groups [149,150] in their hydrophobic segments. With these block copolymers polymeric micelles are formed at pH above the pKa of the protonatable group, where the hydrophobic segment essentially is unprotonated. As the pH decreases below the pKa, the ionization of the polymer causes increased hydrophilicity and electrostatic repulsions of the polymers, leading to the destabilization of the micelles. The control of the transition pH is possible by a combination of different block copolymers. It has been shown that poly(L-histidine)-*b*-PEG (pHis-*b*-PEG) micelles destabilized at physiological pH (7.4) [146], whereas mixed polymeric micelles consisting of a mixture of pHis-*b*-PEG and PLA-*b*-PEG showed improved micellar stability at pH 7.4 and were dissociated at pH 6.0 to 7.2, depending on the amount of PLA-*b*-PEG blended [147].

On the other hand, only one example has been reported so far as to the “degradation” approach to hydrophilize and thus destabilize polymeric micelles. Frechet et al. recently reported on a block copolymer of PEG and poly(aspartic acid) functionalized with trimethoxybenzylidene acetals as acid-labile linkages [151]. Cyclic benzylidene acetals increased the hydrophobicity of the core by stacking of the aromatic rings and masked the polarity of the diol by the acetal groups. These micelles were quite stable at physiological pH, but once the acidity of the solution was lowered to pH 5, hydrolysis of acetal bonds occurred. The generation of diols increased the hydrophilicity of the polymers and dissolution of the micelles occurred, followed by the release of a hydrophobic dye. They also synthesized linear-dendritic block copolymers of PEG and polylysine/polyester dendron, to whose periphery cyclic benzylidene acetals were attached (Figure 1) [100,152]. The dendritic block copolymers formed polymeric micelles with a size 20 to 50 nm [152], and an accelerated release of the entrapped DOX at acidic pH was observed *in vitro* as a result of micelle disruption [100].

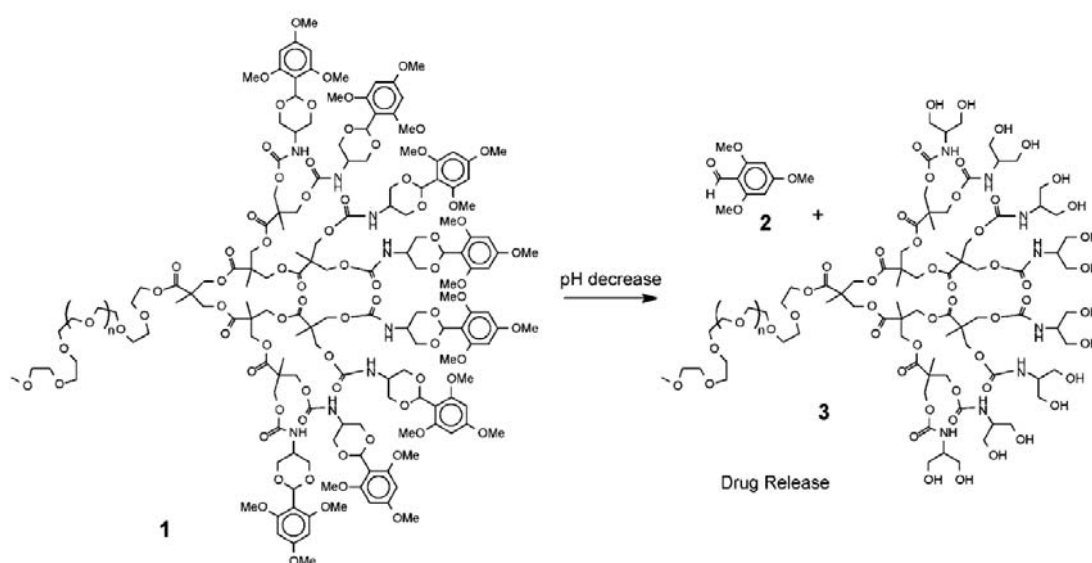


Figure 1. Structure of a linear-dendritic block copolymer of a PEG and a third generation polyester dendrimer with cyclic acetals of 2,4,6-trimethoxybenzaldehyde attached to the periphery (1). Hydrolysis of the cyclic acetals on the dendrimer periphery releases 2,4,6-trimethoxybenzaldehyde (2) and reveals polar 1,3-diol moieties on the dendrimer periphery to provide (3) [100].

A few other “degradation” approaches have been reported for nanoparticles [153] and polymeric vesicles [154,155]. Couvreur et al. prepared nanoparticles of poly(methylidene malonate 2.1.2.) (Figure 2) [153]. When incubated at basic pH the release of ethanol from the nanoparticles was observed due to the hydrolysis of the ester bond in the side chains. The resulting polymers were more hydrophilic than the starting polymers owing to the presence of free carboxyl groups, leading to the eventual solubilization of the nanoparticles. Hubbell et al. synthesized A-B-A block copolymers consisting of poly(propylene sulfide) and PEG (PEG-*b*-PPS-*b*-PEG), which formed polymeric vesicles in water [154]. The PPS block is oxidized to poly(propylene sulphoxide) and eventually to poly(propylene sulphone), leading to the hydrophilization of the polymer (Figure 3). Accordingly, the polymeric vesicles eventually destabilized upon incubation with H₂O₂, as evidenced by the turbidity change and cryo-TEM. The oxidative conversion was also achieved by encapsulating glucose oxidase (GOx) into the polymeric vesicles [155]. When the GOx-containing polymeric vesicles were incubated in 0.1 M glucose solution, glucose which diffused across the membrane of the polymeric vesicles into their inner spaces was oxidized by GOx to produce H₂O₂, leading to the dissolution of the GOx-encapsulated polymeric vesicles. Thermosensitive polymers with degradable side chains are also applicable to such “hydrophobic to hydrophilic” conversion (as described in detail in Section 3) [156].

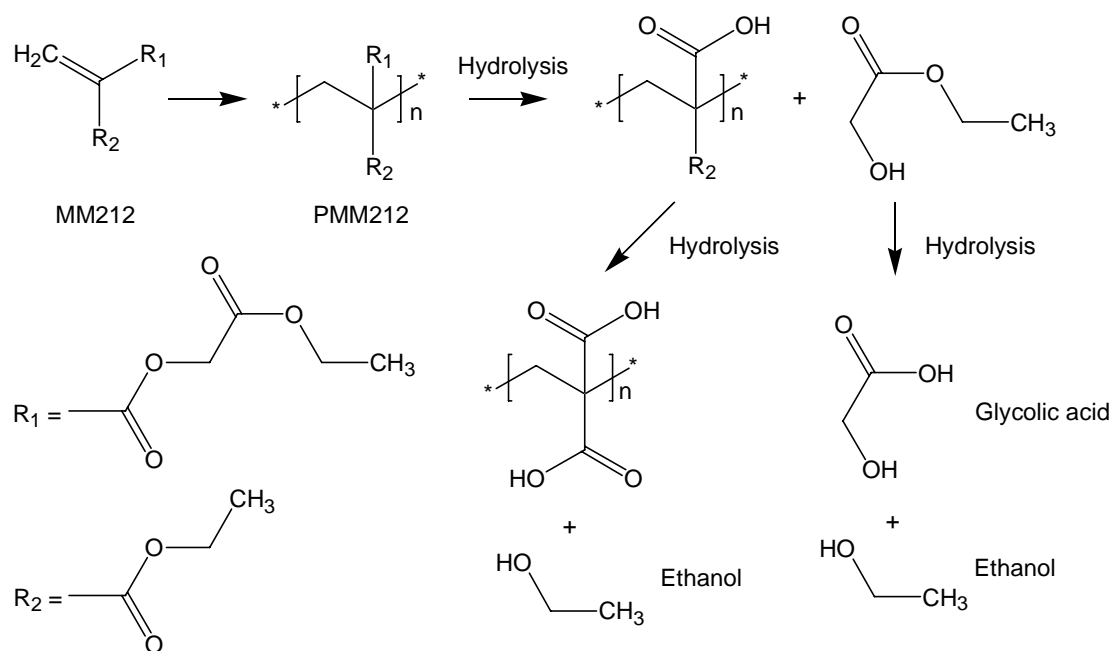


Figure 2. Structure of poly(methylidene malonate 2.1.2.) and its degradation (hydrophilization) process via ester hydrolysis of the polymer side chains [153].

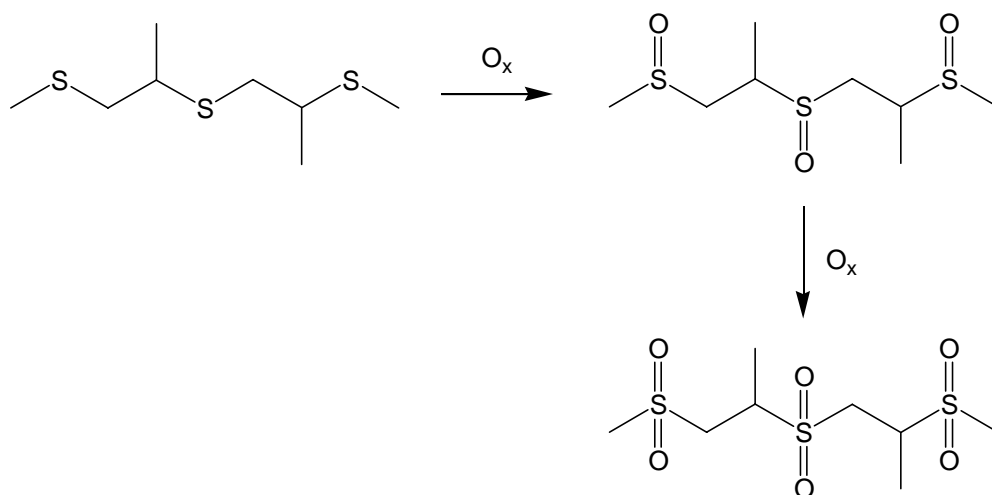


Figure 3. Scheme of the oxidation reaction for poly(propylene sulfide) to poly(propylene sulfoxide) and to poly(propylene sulphone) [154].

3. Thermosensitive polymeric micelles

Thermosensitive polymers with a lower critical solution temperature (LCST) are presently under investigation for biomedical and pharmaceutical applications [23,157-159]. The temperature at which the phase transition (precipitation of the polymers) occurs is called the cloud point (CP). Below the CP, water is bound to the hydrophilic moieties of the polymer and the presence of hydrated water prevents the interaction between different polymer chains as well as intrapolymer association. This means that below the CP the polymer exists in a water-soluble form. Once the polymer solution is heated above the CP, the hydrogen bonds between water molecules and the hydrophilic moieties in the polymer chain are disrupted and water is expelled from the polymer chains. As a result, interactions between the hydrophobic moieties of the polymer chain increase, which is associated with the collapse of the polymer and finally results in aggregation/precipitation of the polymer. Poly(*N*-isopropylacrylamide) (PNIPAAm), which has a reversible and sharp phase transition around 32 °C in water, has been most extensively investigated among a variety of LCST polymers [160-162]. Since the CP of PNIPAAm in water is slightly below body temperature, it is very attractive for pharmaceutical use and is widely used for the design of thermosensitive drug delivery systems such as hydrogels [163,164], nanoparticles [165], films [166] and surface-modified liposomes [167,168]. The phase transition behavior of PNIPAAm has been studied with a variety of techniques including FT-IR, SLS, DLS and DSC [169-172]. The CP of PNIPAAm can be modulated by copolymerizing with hydrophobic or hydrophilic comonomers. Hydrophobic comonomers decrease the CP whereas hydrophilic comonomers have the opposite effect [173,174]. This makes it possible to design polymers with their CP around body temperature. In addition, various polymers having PNIPAAm-related structures (*N*-substituted acrylamide and methacrylamide polymers) and different CP's are also investigated as thermosensitive polymers [175,176].

PNIPAAm (and its random copolymers with other monomers) can be used either as a hydrophilic segment or as a hydrophobic segment of polymeric micelles. In the former case, PNIPAAm functions as hydrophilic outer shells of micelles below the CP. Okano et al. prepared DOX-loaded polymeric micelles of poly(butyl methacrylate)-*b*-PNIPAAm (PBMA-*b*-PNIPAAm) and PS-*b*-PNIPAAm, which showed a core-shell micellar structure below the CP of PNIPAAm (20 °C) [145]. Upon heating above the CP, a rapid release of DOX from the PBMA-*b*-PNIPAAm micelles was observed as a result of the structural distortion of the relatively flexible PBMA core (T_g of PBMA is 20 °C) due to the collapse of the PNIPAAm shell. In contrast, PS-*b*-PNIPAAm micelles did not show any enhanced DOX release after increasing the temperature above the

CP because the rigid PS core (T_g of PS is 100 °C) was insensitive for the collapse of PNIPAAm. Since PNIPAAm is in its precipitated form at body temperature, this system is not suitable for *in vivo* application without modification. By copolymerizing NIPAAm with the hydrophilic dimethylacrylamide (DMAAm), the resulting random copolymer (poly(NIPAAm-*co*-DMAAm)) showed a CP of 40 °C, which is slightly above body temperature [177]. The release of DOX from PLA-*b*-poly(NIPAAm-*co*-DMAAm) micelles was very slow at 37 °C, while an increase in DOX release rate was observed at 42.5 °C, suggesting this system might be appropriate for hyperthermia treatment.

When PNIPAAm is used as a hydrophobic segment of polymeric micelles, PNIPAAm is attached to a hydrophilic polymer e.g. PEG [144]. The PNIPAAm-*b*-PEG block copolymer is hydrophilic and soluble in aqueous solution below the CP of PNIPAAm, but above this temperature it forms polymeric micelles with a collapsed PNIPAAm core and a PEG outer shell due to the dehydration of PNIPAAm. The temperature at which the micelles are formed is called critical micelle temperature (CMT). The advantage of PNIPAAm-*b*-PEG system is that polymeric micelles can be simply prepared by heating an aqueous polymer solution of sufficient concentration (above the CMC) above the CP of the PNIPAAm block. Thus, in contrast to other methods to prepare polymeric micelles (see Section 2-3), PNIPAAm-*b*-PEG micelles can be prepared without using organic solvents. The heating rate is a critical parameter for the size of PNIPAAm-*b*-PEG micelle. A fast heating rate resulted in micelles with a smaller size than when a slow heating rate was applied [178,179]. The formation of thermosensitive micelles upon heating is a competitive process between intrapolymer coil-to-globule transition (collapse) of thermosensitive segments and interpolymer association (aggregation) of polymers. A higher heating rate causes a rapid dehydration of the thermosensitive segments, and therefore the subsequent collapse of these segments precedes the aggregation between polymers. As a result, micelles with a well-defined core-shell structure are formed. Our group further found that an extremely rapid pass through the CMT (“heat shock procedure”) leads to the formation of PNIPAAm-*b*-PEG micelles with a size around 50 nm [180].

A major disadvantage of PNIPAAm-based systems is that thermal treatment (hyperthermia or hypothermia) is required for the controlled destabilization of the micelles and concurrent drug release, which is not always feasible in clinical practice as mentioned earlier. Furthermore, PNIPAAm is not biodegradable and its biocompatibility is not well understood at present. Insoluble PNIPAAm might cause some serious adverse effects. Consequently, thermosensitive polymeric micelles which spontaneously destabilize at physiological conditions are more promising since the use of external stimuli is not required in clinical

practice. There are two possible approaches for destabilization of thermosensitive polymeric micelles:

- 1) Degradation of the backbone of thermosensitive polymers. Examples of such polymers include poly(amino acid)s [181] and PEG-*b*-PCL-*b*-PEG [182]. An increase in CP in time is not likely to occur for this type of system.
- 2) Degradation of the side chains of thermosensitive polymers so that the hydrophilicity of the polymers increases and results in the increase of the CP of the polymers in time.

An example of the second approach has been reported by Katayama et al. They synthesized the copolymer of NIPAAm and *N*-methacryloyl-GLRRASLG (*N*-methacryloylpeptide), a PNIPAAm-based polymer with peptide side chains [156]. The GLRRASLG peptide was phosphorylated by protein kinase A, which resulted in an increase of the CP of the copolymers from 36.7 °C to 40 °C due to the hydrophilization of the peptide chains. But this polymer is probably not suitable for *in vivo* application, since the change of the CP before hydrophilization is already too close to body temperature. For this approach thermosensitive polymers with CP changing from below to above body temperature are required.

SCOPE OF THE THESIS

As described above, “hydrophobic to hydrophilic” conversion of the core of polymeric micelles is an interesting strategy to destabilize polymeric micelles and release their payload in a controlled way. One possible approach to achieve such conversion is to combine the convenient micelle formation procedure of thermosensitive polymers with the increase of its CP from below to above body temperature in time. This idea led our group to develop novel thermosensitive copolymers of NIPAAm and *N*-(2-hydroxypropyl) methacrylamide lactate (poly(NIPAAm-*co*-HPMAm-lactate)) and their block copolymers with PEG (poly(NIPAAm-*co*-HPMAm-lactate)-*b*-PEG) (Figure 4) [183]. When 35 mol % HPMAm-lactate was copolymerized with NIPAAm, the CP of poly(NIPAAm-*co*-HPMAm-lactate) was around 15 °C in phosphate buffered saline and thus below body temperature. The ester bond of HPMAm-lactate monomer is hydrolytically sensitive, and, importantly, the resulting HPMAm is a more hydrophilic monomer than NIPAAm. Indeed, the CP of the hydrolyzed polymer, poly(NIPAAm-*co*-HPMAm) was 45 °C, making this polymer soluble in water at body temperature [183]. Owing to this unique property, polymeric micelles formed with poly(NIPAAm-*co*-HPMAm-lactate)-*b*-PEG block copolymers showed controlled instability at body temperature. In other words, the block copolymers formed polymeric micelles with a core of poly(NIPAAm-*co*-

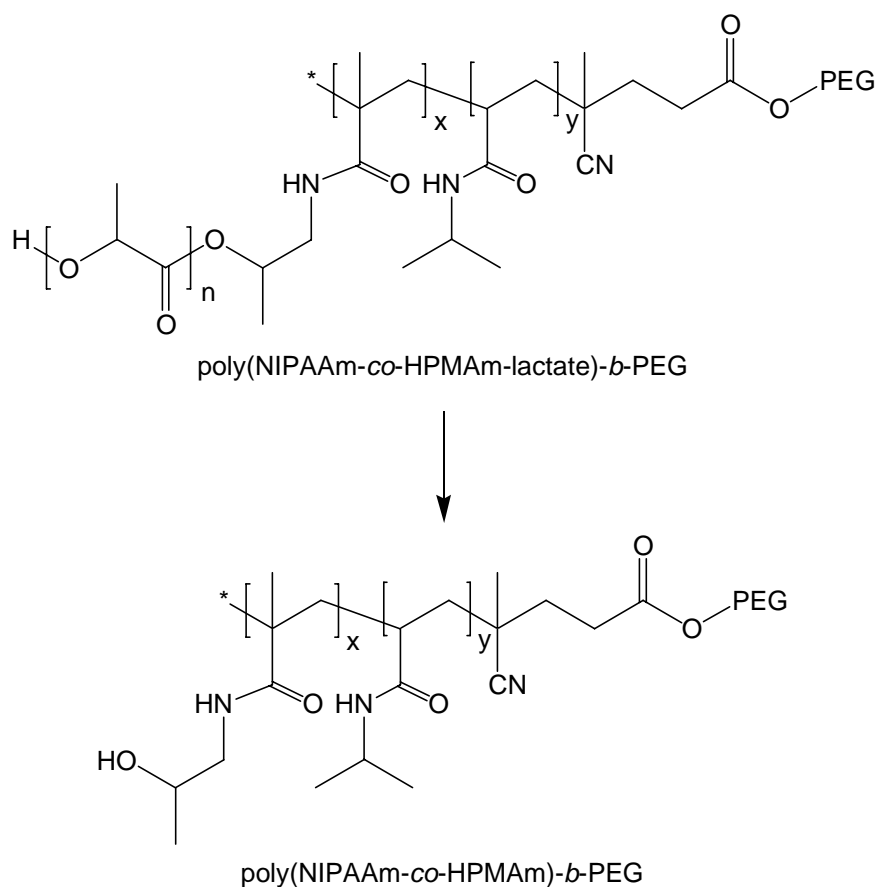


Figure 4. Structure of poly(NIPAAm-co-HPMAm-lactate)-b-PEG. Hydrolysis of the lactic acid side chains of the polymer leads to poly(NIPAAm-co-HPMAm)-b-PEG with increased hydrophilicity, as indicated by its increased CP [183].

HPMAm-lactate), since the CP of this block is below 37 °C. Then, due to the hydrolysis of the lactic acid side chains, the CP of the thermosensitive block increased in time, and when the CP comes above body temperature, the polymer became soluble in water and the dissolution of the micelles occurred [183,184].

The aim of the research described in this Thesis is to further investigate the possibilities of this novel polymeric micellar system and to demonstrate its utility as a drug delivery vehicle. The first step is the design of novel and biocompatible thermosensitive polymers without the use of PNIPAAm, since PNIPAAm is not biodegradable and its biocompatibility is not well understood at present. Next, polymeric micelles from these thermosensitive polymers are evaluated for their controlled dissolution properties and drug loading capacity. Finally, the *in vivo* performance of the drug-loaded polymeric micelles is evaluated.

In **Chapter 2** the synthesis of a novel class of thermosensitive and biodegradable polymers, poly(*N*-(2-hydroxypropyl) methacrylamide mono/di lactate) (poly(HPMAm-mono/di lactate)), is reported. The CP of these polymers

in water varies between 13 °C and 65 °C, depending on the ratio of HPMAM-monolactate and HPMAM-dilactate. Since poly(HPMAM-dilactate), having a CP of 13 °C, is converted in time to poly(HPMAM-monolactate) (CP of 65 °C) or more hydrophilic pHPMAM, this polymer is supposed to be suitable for “hydrophobic to hydrophilic” conversion at body temperature.

Therefore, in **Chapter 3**, block copolymers of poly(HPMAM-dilactate) and PEG (pHPMAMDL-*b*-PEG) are synthesized, and polymeric micelles formed from these polymers are physicochemically characterized by DLS, SLS, cryo-TEM, ¹H NMR and FT-IR. Most importantly, the pHPMAMDL-*b*-PEG micelles show controlled dissolution at body temperature as a result of the hydrophilization of the core due to the hydrolysis of the lactic acid side chain.

In **Chapter 4** the loading of PTX into pHPMAMDL-*b*-PEG micelles is reported. A simple loading method taking advantage of the thermosensitivity of pHPMAMDL-*b*-PEG is established, and the PTX-loaded pHPMAMDL-*b*-PEG micelles are characterized regarding morphology, drug release, stability, and *in vitro* cytotoxicity. To get insight into the mechanism of the cytotoxicity of the PTX-loaded micelles, CLSM and FACS studies with fluorescently labeled micelles are also performed.

In **Chapter 5** data are presented regarding an introductory *in vivo* study of pHPMAMDL-*b*-PEG micelles and PTX-loaded pHPMAMDL-*b*-PEG micelles performed to assess their feasibility as a drug delivery carrier. Their biodistribution in mice and rats after *i. v.* administration, and the therapeutic effect of PTX-loaded micelles in tumor bearing mice after *i. v.* and intraperitoneal (*i. p.*) administration are presented.

In **Chapter 6** the results are summarized and perspectives for future research are given.

References

1. D.J.A. Crommelin, G. Scherphof, G. Storm. *Adv Drug Deliv Rev* 17 (1995) 49-60.
2. L. Gros, H. Ringsdorf, H. Schupp. *Angew Chem Int Ed Engl* 20 (1981) 305-325.
3. M.A. Moses, H. Brem, R. Langer. *Cancer Cell* 4 (2003) 337-341.
4. R. Duncan. *Nat Rev Drug Discov* 2 (2003) 347-360.
5. D.J.A. Crommelin, G. Storm, W. Jiskoot, R. Stenekes, E. Mastrobattista, W.E. Hennink. *J Control Release* 87 (2003) 81-88.
6. D.J.A. Crommelin, G. Storm. *J Liposome Res* 13 (2003) 33-36.
7. D.C. Drummond, O. Meyer, K. Hong, D.B. Kirpotin, D. Papahadjopoulos. *Pharmacol Rev* 51 (1999) 691-743.
8. T. Yamaguchi, Y. Mizushima. *Crit Rev Ther Drug Carrier Syst* 11 (1994) 215-229.
9. S. Tamilvanan. *Prog Lipid Res* 43 (2004) 489-533.

10. I. Bala, S. Hariharan, M.N. Kumar. *Crit Rev Ther Drug Carrier Syst* 21 (2004) 387-422.
11. J. Panyam, V. Labhasetwar. *Adv Drug Deliv Rev* 55 (2003) 329-347.
12. R. Haag. *Angew Chem Int Ed Engl* 43 (2004) 278-282.
13. K. Kataoka, A. Harada, Y. Nagasaki. *Adv Drug Deliv Rev* 47 (2001) 113-131.
14. G.S. Kwon. *Crit Rev Ther Drug Carrier Syst* 20 (2003) 357-403.
15. D.E. Discher, A. Eisenberg. *Science* 297 (2002) 967-973.
16. F. Ahmed, D.E. Discher. *J Control Release* 96 (2004) 37-53.
17. A. Nori, J. Kopecek. *Adv Drug Deliv Rev* 57 (2005) 609-636.
18. R. Satchi-Fainaro, M. Puder, J.W. Davies, H.T. Tran, D.A. Sampson, A.K. Greene, G. Corfas, J. Folkman. *Nat Med* 10 (2004) 255-261.
19. E.R. Gillies, J.M.J. Frechet. *Drug Discovery Today* 10 (2005) 35-43.
20. F. Aulenta, W. Hayes, S. Rannard. *Euro Polym J* 39 (2003) 1741-1771.
21. Y. Matsumura, H. Maeda. *Cancer Res* 46 (1986) 6387-6392.
22. H. Maeda, J. Wu, T. Sawa, Y. Matsumura, K. Hori. *J Control Release* 65 (2000) 271-284.
23. A.V. Kabanov, E.V. Batrakova, V.Y. Alakhov. *J Control Release* 82 (2002) 189-212.
24. S. Stolnik, L. Illum, S.S. Davis. *Adv Drug Deliv Rev* 16 (1995) 195-214.
25. R.M. Schiffelers, I.A. Bakker-Woudenberg, S.V. Sniijders, G. Storm. *Biochim Biophys Acta* 1421 (1999) 329-339.
26. J.M. Metselaar, P. Bruin, L.W. de Boer, T. de Vringer, C.J. Snel, C. Oussoren, M.H. Wauben, D.J.A. Crommelin, G. Storm, W.E. Hennink. *Bioconjug Chem* 14 (2003) 1156-1164.
27. T.M. Allen. *Nat Rev Cancer* 2 (2002) 750-763.
28. G. Gregoriadis, E.J. Wills, C.P. Swain, A.S. Tavill. *Lancet* 1 (1974) 1313-1316.
29. T.M. Allen, A. Chonn. *FEBS Lett* 223 (1987) 42-46.
30. A.L. Klibanov, K. Maruyama, V.P. Torchilin, L. Huang. *FEBS Lett* 268 (1990) 235-237.
31. T.M. Allen, P.R. Cullis. *Science* 303 (2004) 1818-1822.
32. S. Hosokawa, T. Tagawa, H. Niki, Y. Hirakawa, K. Nohga, K. Nagaike. *Br J Cancer* 89 (2003) 1545-1551.
33. Y. Matsumura, M. Gotoh, K. Muro, Y. Yamada, K. Shirao, Y. Shimada, M. Okuwa, S. Matsumoto, Y. Miyata, H. Ohkura, K. Chin, S. Baba, T. Yamao, A. Kannami, Y. Takamatsu, K. Ito, K. Takahashi. *Ann Oncol* 15 (2004) 517-525.
34. A. Gabizon, R. Shiota, D. Papahadjopoulos. *J Natl Cancer Inst* 81 (1989) 1484-1488.
35. A. Gabizon, R. Catane, B. Uziely, B. Kaufman, T. Safra, R. Cohen, F. Martin, A. Huang, Y. Barenholz. *Cancer Res* 54 (1994) 987-992.
36. J. Vaage, E. Barbera-Guillem, R. Abra, A. Huang, P. Working. *Cancer* 73 (1994) 1478-1484.
37. K.J. Harrington, C. Lewanski, A.D. Northcote, J. Whittaker, A.M. Peters, R.G. Vile, J.S. Stewart. *Eur J Cancer* 37 (2001) 2015-2022.
38. T.M. Allen, D.R. Mumbengegwi, G.J. Charrois. *Clin Cancer Res* 11 (2005) 3567-3573.

39. S. Bandak, D. Goren, A. Horowitz, D. Tzemach, A. Gabizon. *Anticancer Drugs* 10 (1999) 911-920.
40. R. Duncan, L.W. Seymour, K.B. O'Hare, P.A. Flanagan, S. Wedge, I.C. Hume, K. Ulbrich, J. Strohalm, V. Subr, F. Spreafico. *J Control Release* 19 (1992) 331-346.
41. J. Kopecek, P. Kopeckova, T. Minko, Z. Lu. *Eur J Pharm Biopharm* 50 (2000) 61-81.
42. J.W. Singer, B. Baker, P. De Vries, A. Kumar, S. Shaffer, E. Vawter, M. Bolton, P. Garzone. *Adv Exp Med Biol* 519 (2003) 81-99.
43. C.J. Langer. *Expert Opin Investig Drugs* 13 (2004) 1501-1508.
44. J.M. Meerum Terwogt, W.W. ten Bokkel Huinink, J.H. Schellens, M. Schot, I.A. Mandjes, M.G. Zurlo, M. Rocchetti, H. Rosing, F.J. Koopman, J.H. Beijnen. *Anticancer Drugs* 12 (2001) 315-323.
45. S. Forster, T. Plantenberg. *Angew Chem Int Ed Engl* 41 (2002) 689-714.
46. G. Riess. *Prog Polym Sci* 28 (2003) 1107-1170.
47. A. Harada, K. Kataoka. *Science* 283 (1999) 65-67.
48. N. Kang, M.E. Perron, R.E. Prud'homme, Y.B. Zhang, G. Gaucher, J.C. Leroux. *Nano Letters* 5 (2005) 315-319.
49. M. Yokoyama, G.S. Kwon, T. Okano, Y. Sakurai, T. Seto, K. Kataoka. *Bioconjug Chem* 3 (1992) 295-301.
50. C. Allen, D. Maysinger, A. Eisenberg. *Colloids Surf B: Biointerfaces* 16 (1999) 3-27.
51. M.L. Adams, A. Lavasanifar, G.S. Kwon. *J Pharm Sci* 92 (2003) 1343-1355.
52. A. Lavasanifar, J. Samuel, G.S. Kwon. *Adv Drug Deliv Rev* 54 (2002) 169-190.
53. V.P. Torchilin. *J Control Release* 73 (2001) 137-172.
54. M.C. Jones, J.C. Leroux. *Eur J Pharm Biopharm* 48 (1999) 101-111.
55. R. Savic, L. Luo, A. Eisenberg, D. Maysinger. *Science* 300 (2003) 615-618.
56. X. Shuai, T. Merdan, A.K. Schaper, F. Xi, T. Kissel. *Bioconjug Chem* 15 (2004) 441-448.
57. N. Rapoport. *Int J Pharm* 277 (2004) 155-162.
58. L.W. Seymour, R. Duncan, J. Strohalm, J. Kopecek. *J Biomed Mater Res* 21 (1987) 1341-1358.
59. A.V. Kabanov, P. Lemieux, S. Vinogradov, V. Alakhov. *Adv Drug Deliv Rev* 54 (2002) 223-233.
60. M.F. Francis, L. Lavoie, F.M. Winnik, J.C. Leroux. *Eur J Pharm Biopharm* 56 (2003) 337-346.
61. Y. Kakizawa, K. Kataoka. *Adv Drug Deliv Rev* 54 (2002) 203-222.
62. M.C. Woodle, D.D. Lasic. *Biochim Biophys Acta* 1113 (1992) 171-199.
63. G. Molineux. *Cancer Treat Rev* 28 (2002) 13-16.
64. J.H. Lee, H.B. Lee, J.D. Andrade. *Prog Polym Sci* 20 (1995) 1043-1079.
65. A. Benahmed, M. Ranger, J.C. Leroux. *Pharm Res* 18 (2001) 323-328.
66. T. Inoue, G. Chen, K. Nakamae, A.S. Hoffman. *J Control Release* 51 (1998) 221-229.
67. M. Yokoyama, S. Fukushima, R. Uehara, K. Okamoto, K. Kataoka, Y. Sakurai, T. Okano. *J Control Release* 50 (1998) 79-92.

68. G.S. Kwon, M. Naito, M. Yokoyama, T. Okano, Y. Sakurai, K. Kataoka. *Pharm Res* 12 (1995) 192-195.
69. R.T. Liggins, H.M. Burt. *Adv Drug Deliv Rev* 54 (2002) 191-202.
70. S.A. Hagan, A.G.A. Coombes, M.C. Garnett, S.E. Dunn, M.C. Davis, L. Illum, S.S. Davis, S.E. Harding, S. Purkiss, P.R. Gellert. *Langmuir* 12 (1996) 2153-2161.
71. C. Allen, J. Han, Y. Yu, D. Maysinger, A. Eisenberg. *J Control Release* 63 (2000) 275-286.
72. K. Letchford, J. Zastre, R. Liggins, H. Burt. *Colloids Surf B: Biointerfaces* 35 (2004) 81-91.
73. M. Wilhelm, C.L. Zhao, Y.C. Wang, R.L. Xu, M.A. Winnik, J.L. Mura, G. Riess, M.D. Croucher. *Macromolecules* 24 (1991) 1033-1040.
74. G. Kwon, M. Naito, M. Yokoyama, T. Okano, Y. Sakurai, K. Kataoka. *Langmuir* 9 (1993) 945-949.
75. A.V. Kabanov, I.R. Nazarova, I.V. Astafieva, E.V. Batrakova, V.Y. Alakhov, A.A. Yaroslavov, V.A. Kabanov. *Macromolecules* 28 (1995) 2303-2314.
76. G.S. Kwon, T. Okano. *Adv Drug Deliv Rev* 21 (1996) 107-116.
77. R. Finsy. *Adv Colloid Interface Sci* 52 (1994) 79-143.
78. G. Cavallaro, L. Maniscalco, M. Licciardi, G. Giammona. *Macromol Biosci* 4 (2004) 1028-1038.
79. A.K. Gupta, S. Madan, D.K. Majumdar, A. Maitra. *Int J Pharm* 209 (2000) 1-14.
80. C. Konak, D. Oupicky, V. Chytrý, K. Ulbrich, M. Helmstedt. *Macromolecules* 33 (2000) 5318-5320.
81. J. Liaw, T. Aoyagi, K. Kataoka, Y. Sakurai, T. Okano. *Pharm Res* 15 (1998) 1721-1726.
82. F. Kohori, K. Sakai, T. Aoyagi, M. Yokoyama, Y. Sakurai, T. Okano. *J Control Release* 55 (1998) 87-98.
83. S. Cammas, K. Suzuki, C. Sone, Y. Sakurai, K. Kataoka, T. Okano. *J Control Release* 48 (1997) 157-164.
84. M. Yokoyama, T. Okano, Y. Sakurai, K. Kataoka. *J Control Release* 32 (1994) 269-277.
85. T. Riley, S. Stolnik, C.R. Heald, C.D. Xiong, M.C. Garnett, L. Illum, S.S. Davis, S.C. Purkiss, R.J. Barlow, P.R. Gellert. *Langmuir* 17 (2001) 3168-3174.
86. X.H. Wang, X.P. Qiu, C. Wu. *Macromolecules* 31 (1998) 2972-2976.
87. M.R. Talingting, P. Munk, S.E. Webber, Z. Tuzar. *Macromolecules* 32 (1999) 1593-1601.
88. J. Yun, R. Faust, L.S. Szilagyi, S. Keki, M. Zsuga. *Macromolecules* 36 (2003) 1717-1723.
89. S.L. Nolan, R.J. Phillips, P.M. Cotts, S.R. Dungan. *J Colloid Interface Sci* 191 (1997) 291-302.
90. S. Stolnik, B. Daudali, A. Arien, J. Whetstone, C.R. Heald, M.C. Garnett, S.S. Davis, L. Illum. *Biochim Biophys Acta* 1514 (2001) 261-279.

91. C.R. Heald, S. Stolnik, K.S. Kujawinski, C. De Matteis, M.C. Garnett, L. Illum, S.S. Davis, S.C. Purkiss, R.J. Barlow, P.R. Gellert. *Langmuir* 18 (2002) 3669-3675.
92. J.S. Hrkach, M.T. Peracchia, A. Domb, N. Lotan, R. Langer. *Biomaterials* 18 (1997) 27-30.
93. J. Taillefer, M.C. Jones, N. Brasseur, J.E. van Lier, J.C. Leroux. *J Pharm Sci* 89 (2000) 52-62.
94. X. Zhang, J.K. Jackson, H.M. Burt. *Int J Pharm* 132 (1996) 195-206.
95. S.C. Kim, D.W. Kim, Y.H. Shim, J.S. Bang, H.S. Oh, S.W. Kim, M.H. Seo. *J Control Release* 72 (2001) 191-202.
96. E. Fournier, M.H. Dufresne, D.C. Smith, M. Ranger, J.C. Leroux. *Pharm Res* 21 (2004) 962-968.
97. D. Le Garrec, S. Gori, L. Luo, D. Lessard, D.C. Smith, M.A. Yessine, M. Ranger, J.C. Leroux. *J Control Release* 99 (2004) 83-101.
98. T. Nakanishi, S. Fukushima, K. Okamoto, M. Suzuki, Y. Matsumura, M. Yokoyama, T. Okano, Y. Sakurai, K. Kataoka. *J Control Release* 74 (2001) 295-302.
99. E.S. Lee, K. Na, Y.H. Bae. *Nano Lett* 5 (2005) 325-329.
100. E.R. Gillies, J.M. Frechet. *Bioconjug Chem* 16 (2005) 361-368.
101. M. Hruby, C. Konak, K. Ulbrich. *J Control Release* 103 (2005) 137-148.
102. A.V. Kabanov, E.V. Batrakova, V.Y. Alakhov. *Adv Drug Deliv Rev* 54 (2002) 759-779.
103. V.P. Torchilin, A.N. Lukyanov, Z. Gao, B. Papahadjopoulos-Sternberg. *Proc Natl Acad Sci U S A* 100 (2003) 6039-6044.
104. A. Krishnadas, I. Rubinstein, H. Onyuksel. *Pharm Res* 20 (2003) 297-302.
105. G. Cavallaro, M. Licciardi, G. Giammona, P. Caliceti, A. Semenzato, S. Salmaso. *J Control Release* 89 (2003) 285-295.
106. T. Hamaguchi, Y. Matsumura, M. Suzuki, K. Shimizu, R. Goda, I. Nakamura, I. Nakatomi, M. Yokoyama, K. Kataoka, T. Kakizoe. *Br J Cancer* 92 (2005) 1240-1246.
107. K.M. Huh, S.C. Lee, Y.W. Cho, J. Lee, J.H. Jeong, K. Park. *J Control Release* 101 (2005) 59-68.
108. T.Y. Kim, D.W. Kim, J.Y. Chung, S.G. Shin, S.C. Kim, D.S. Heo, N.K. Kim, Y.J. Bang. *Clin Cancer Res* 10 (2004) 3708-3716.
109. N. Nishiyama, S. Okazaki, H. Cabral, M. Miyamoto, Y. Kato, Y. Sugiyama, K. Nishio, Y. Matsumura, K. Kataoka. *Cancer Res* 63 (2003) 8977-8983.
110. N. Nishiyama, Y. Kato, Y. Sugiyama, K. Kataoka. *Pharm Res* 18 (2001) 1035-1041.
111. A. Lavasanifar, J. Samuel, S. Sattari, G.S. Kwon. *Pharm Res* 19 (2002) 418-422.
112. W.J. Lin, L.W. Juang, C.C. Lin. *Pharm Res* 20 (2003) 668-673.
113. J. Djordjevic, M. Barch, K.E. Uhrich. *Pharm Res* 22 (2005) 24-32.
114. C.F. van Nostrum. *Adv Drug Deliv Rev* 56 (2004) 9-16.
115. G.D. Zhang, A. Harada, N. Nishiyama, D.L. Jiang, H. Koyama, T. Aida, K. Kataoka. *J Control Release* 93 (2003) 141-150.

116. D. Le Garrec, J. Taillefer, J.E. Van Lier, V. Lenaerts, J.C. Leroux. *J Drug Target* 10 (2002) 429-437.
117. M. Yokoyama, A. Satoh, Y. Sakurai, T. Okano, Y. Matsumura, T. Kakizoe, K. Kataoka. *J Control Release* 55 (1998) 219-229.
118. Y. Matsumura, M. Yokoyama, K. Kataoka, T. Okano, Y. Sakurai, T. Kawaguchi, T. Kakizoe. *Jpn J Cancer Res* 90 (1999) 122-128.
119. E.K. Rowinsky, R.C. Donehower. *N Engl J Med* 332 (1995) 1004-1014.
120. J. Crown, M. O'Leary. *Lancet* 355 (2000) 1176-1178.
121. J. Lee, S.C. Lee, G. Acharya, C.J. Chang, K. Park. *Pharm Res* 20 (2003) 1022-1030.
122. H. Gelderblom, J. Verweij, K. Nooter, A. Sparreboom. *Eur J Cancer* 37 (2001) 1590-1598.
123. A.K. Singla, A. Garg, D. Aggarwal. *Int J Pharm* 235 (2002) 179-192.
124. G.S. Kwon, M. Naito, K. Kataoka, M. Yokoyama, Y. Sakurai, T. Okano. *Colloids Surf B: Biointerfaces* 2 (1994) 429-434.
125. J.X. Zhao, C. Allen, A. Eisenberg. *Macromolecules* 30 (1997) 7143-7150.
126. A. Lavasanifar, J. Samuel, G.S. Kwon. *J Control Release* 79 (2002) 165-172.
127. A. Lavasanifar, J. Samuel, G.S. Kwon. *Colloids Surf B: Biointerfaces* 22 (2001) 115-126.
128. Y. Teng, M.E. Morrison, P. Munk, S.E. Webber, K. Prochazka. *Macromolecules* 31 (1998) 3578-3587.
129. S.Y. Kim, I.G. Shin, Y.M. Lee, C.S. Cho, Y.K. Sung. *J Control Release* 51 (1998) 13-22.
130. Y. Bae, N. Nishiyama, S. Fukushima, H. Koyama, M. Yasuhiro, K. Kataoka. *Bioconjug Chem* 16 (2005) 122-130.
131. Y. Bae, S. Fukushima, A. Harada, K. Kataoka. *Angew Chem Int Ed Engl* 42 (2003) 4640-4643.
132. K. Engin, D.B. Leeper, J.R. Cater, A.J. Thistlethwaite, L. Tupchong, J.D. McFarlane. *Int J Hyperthermia* 11 (1995) 211-216.
133. D. Le Garrec, M. Ranger, J.C. Leroux. *Am J Drug Deliv* 2 (2004) 15-42.
134. G. Kwon, S. Suwa, M. Yokoyama, T. Okano, Y. Sakurai, K. Kataoka. *J Control Release* 29 (1994) 17-23.
135. Y. Yamamoto, Y. Nagasaki, Y. Kato, Y. Sugiyama, K. Kataoka. *J Control Release* 77 (2001) 27-38.
136. V. Weissig, K.R. Whiteman, V.P. Torchilin. *Pharm Res* 15 (1998) 1552-1556.
137. H.M. Burt, X.C. Zhang, P. Toleikis, L. Embree, W.L. Hunter. *Colloids Surf B: Biointerfaces* 16 (1999) 161-171.
138. Y. Matsumura, T. Hamaguchi, T. Ura, K. Muro, Y. Yamada, Y. Shimada, K. Shirao, T. Okusaka, H. Ueno, M. Ikeda, N. Watanabe. *Br J Cancer* 91 (2004) 1775-1781.
139. E.V. Batrakova, S. Li, Y. Li, V.Y. Alakhov, W.F. Elmquist, A.V. Kabanov. *J Control Release* 100 (2004) 389-397.
140. Y. Mizumura, Y. Matsumura, M. Yokoyama, T. Okano, T. Kawaguchi, F. Moriyasu, T. Kakizoe. *Jpn J Cancer Res* 93 (2002) 1237-1243.

141. S.R. Park, D.Y. Oh, D.W. Kim, T.Y. Kim, D.S. Heo, Y.J. Bang, N.K. Kim, W.K. Kang, H.T. Kim, S.A. Im, J.H. Suh, H.K. Kim. *Oncol Rep* 12 (2004) 1059-1064.
142. J. Jiang, X. Tong, Y. Zhao. *J Am Chem Soc* 127 (2005) 8290-8291.
143. N. Rapoport, W.G. Pitt, H. Sun, J.L. Nelson. *J Control Release* 91 (2003) 85-95.
144. M.D.C. Topp, P.J. Dijkstra, H. Talsma, J. Feijen. *Macromolecules* 30 (1997) 8518-8520.
145. J.E. Chung, M. Yokoyama, T. Okano. *J Control Release* 65 (2000) 93-103.
146. E.S. Lee, H.J. Shin, K. Na, Y.H. Bae. *J Control Release* 90 (2003) 363-374.
147. E.S. Lee, K. Na, Y.H. Bae. *J Control Release* 91 (2003) 103-113.
148. T.J. Martin, K. Prochazka, P. Munk, S.E. Webber. *Macromolecules* 29 (1996) 6071-6073.
149. A.S. Lee, A.P. Gast, V. Butun, S.P. Armes. *Macromolecules* 32 (1999) 4302-4310.
150. Y. Tang, S.Y. Liu, S.P. Armes, N.C. Billingham. *Biomacromolecules* 4 (2003) 1636-1645.
151. E.R. Gillies, J.M. Frechet. *Chem Commun (Camb)* (2003) 1640-1641.
152. E.R. Gillies, T.B. Jonsson, J.M. Frechet. *J Am Chem Soc* 126 (2004) 11936-11943.
153. F. Lescure, C. Seguin, P. Breton, P. Bourrinet, D. Roy, P. Couvreur. *Pharm Res* 11 (1994) 1270-1277.
154. A. Napoli, M. Valentini, N. Tirelli, M. Muller, J.A. Hubbell. *Nat Mater* 3 (2004) 183-189.
155. A. Napoli, M.J. Boerakker, N. Tirelli, R.J. Nolte, N.A. Sommerdijk, J.A. Hubbell. *Langmuir* 20 (2004) 3487-3491.
156. Y. Katayama, T. Sonoda, M. Maeda. *Macromolecules* 34 (2001) 8569-8573.
157. B. Jeong, Y.H. Bae, D.S. Lee, S.W. Kim. *Nature* 388 (1997) 860-862.
158. A. Chilkoti, M.R. Dreher, D.E. Meyer, D. Raucher. *Adv Drug Deliv Rev* 54 (2002) 613-630.
159. A.S. Hoffman, P.S. Stayton, V. Bulmus, G. Chen, J. Chen, C. Cheung, A. Chilkoti, Z. Ding, L. Dong, R. Fong, C.A. Lackey, C.J. Long, M. Miura, J.E. Morris, N. Murthy, Y. Nabeshima, T.G. Park, O.W. Press, T. Shimboji, S. Shoemaker, H.J. Yang, N. Monji, R.C. Nowinski, C.A. Cole, J.H. Priest, J.M. Harris, K. Nakamae, T. Nishino, T. Miyata. *J Biomed Mater Res* 52 (2000) 577-586.
160. R. Pelton. *Adv Colloid Interface Sci* 85 (2000) 1-33.
161. H.G. Schild. *Prog Polym Sci* 17 (1992) 163-249.
162. M. Heskins, J.E. Guillet. *J Macromol Sci Chem A2* (1968) 1441-1455.
163. B. Jeong, S.W. Kim, Y.H. Bae. *Adv Drug Deliv Rev* 54 (2002) 37-51.
164. X. Huang, T.L. Lowe. *Biomacromolecules* 6 (2005) 2131-2139.
165. T. Mori, M. Maeda. *Langmuir* 20 (2004) 313-319.
166. C.A. Kavanagh, T.A. Gorelova, Selezneva, II, Y.A. Rochev, K.A. Dawson, W.M. Gallagher, A.V. Gorelov, A.K. Keenan. *J Biomed Mater Res A* 72 (2005) 25-35.

167. J.C. Leroux, E. Roux, D. Le Garrec, K.L. Hong, D.C. Drummond. *J Control Release* 72 (2001) 71-84.
168. K. Kono. *Adv Drug Deliv Rev* 53 (2001) 307-319.
169. H.G. Schild, D.A. Tirrell. *J Phys Chem* 94 (1990) 4352-4356.
170. S. Fujishige, K. Kubota, I. Ando. *J Phys Chem* 93 (1989) 3311-3313.
171. E.I. Tiktopulo, V.N. Uversky, V.B. Lushchik, S.I. Klenin, V.E. Bychkova, O.B. Ptitsyn. *Macromolecules* 28 (1995) 7519-7524.
172. M. Li, C. Wu. *Macromolecules* 32 (1999) 4311-4316.
173. H. Feil, Y.H. Bae, J. Feijen, S.W. Kim. *Macromolecules* 26 (1993) 2496-2500.
174. M. Shibayama, S. Mizutani, S. Nomura. *Macromolecules* 29 (1996) 2019-2024.
175. V. Chytrý, M. Netopilik, M. Bohdanecky, K. Ulbrich. *J Biomater Sci Polym Ed* 8 (1997) 817-824.
176. H.Y. Liu, X.X. Zhu. *Polymer* 40 (1999) 6985-6990.
177. F. Kohori, K. Sakai, T. Aoyagi, M. Yokoyama, M. Yamato, Y. Sakurai, T. Okano. *Colloids Surf B: Biointerfaces* 16 (1999) 195-205.
178. P.W. Zhu, D.H. Napper. *Langmuir* 16 (2000) 8543-8545.
179. X.P. Qiu, C. Wu. *Macromolecules* 30 (1997) 7921-7926.
180. D. Neradovic, O. Soga, C.F. van Nostrum, W.E. Hennink. *Biomaterials* 25 (2004) 2409-2418.
181. Y. Tachibana, M. Kurisawa, H. Uyama, T. Kakuchi, S. Kobayashi. *Chem Commun (Camb)* (2003) 106-107.
182. M.J. Hwang, J.M. Suh, Y.H. Bae, S.W. Kim, B. Jeong. *Biomacromolecules* 6 (2005) 885-890.
183. D. Neradovic, C.F. van Nostrum, W.E. Hennink. *Macromolecules* 34 (2001) 7589-7591.
184. D. Neradovic, M.J. van Steenbergen, L. Vansteelant, Y.J. Meijer, C.F. van Nostrum, W.E. Hennink. *Macromolecules* 36 (2003) 7491-7498.

Chapter 2

Poly(*N*-(2-hydroxypropyl) methacrylamide mono/di lactate): a new class of biodegradable polymers with tuneable thermosensitivity

Osamu Soga, Cornelus F. van Nostrum and Wim E. Hennink

Department of Pharmaceutics, Utrecht Institute for Pharmaceutical Sciences (UIPS),
Faculty of Pharmaceutical Sciences, Utrecht University, Utrecht, The Netherlands

Biomacromolecules 5 (2004) 818-821

Abstract

A novel class of thermosensitive and biodegradable polymers, poly(*N*-(2-hydroxypropyl) methacrylamide mono/di lactate) (poly(HPMAM-mono/di lactate)), was synthesized. The cloud points (CP) of poly(HPMAM-monolactate) and poly(HPMAM-dilactate) in water were 65 °C and 13 °C, respectively. The lower CP for poly(HPMAM-dilactate) is likely due to the greater hydrophobicity of the dilactate side group over the monolactate side group. The CP of poly(HPMAM-monolactate-*co*-HPMAM-dilactate) increased linearly with mol % of HPMA-monolactate, which demonstrates that the CP is tuneable by the copolymer composition.

1. Introduction

Thermosensitive polymers with a lower critical solution temperature (LCST) are presently under investigation for biomedical and pharmaceutical applications [1-5]. These polymers are soluble in aqueous solution below the cloud point (CP), but precipitate above this temperature due to the dehydration of the polymer chains. Poly(*N*-isopropylacrylamide) (PNIPAAm), which has its CP around 32 °C in water, is the most extensively studied polymer [6-10] and is used for the design of thermosensitive drug delivery systems such as polymeric micelles [11-14] and hydrogels [4,15]. This polymer has also been used to modify the surface properties of liposomes [16,17]. The CP of PNIPAAm can be modulated by copolymerizing with hydrophobic or hydrophilic comonomers: hydrophobic comonomers decrease the CP, whereas hydrophilic comonomers have the opposite effect [18,19].

For biomedical and pharmaceutical applications of thermosensitive polymers, it is important to have possibilities to control the CP around body temperature. Furthermore, polymers whose CP increase from below to above body temperature in time are very attractive materials, because e.g. the controlled release of drugs without thermal treatment is feasible using such polymers. We recently developed novel thermosensitive copolymers of NIPAAm and *N*-(2-hydroxypropyl) methacrylamide lactate (poly(NIPAAm-*co*-HPMAm-lactate)) and their block copolymers with poly(ethylene glycol) (poly(NIPAAm-*co*-HPMAm-lactate)-*b*-PEG) [20]. When ≥ 35 mol % HPMAm-lactate was copolymerized with NIPAAm, these polymers had their CP below body temperature, whereas after hydrolysis of the lactate side chain the CP increased above 37 °C. As a result, polymeric micelles formed with poly(NIPAAm-*co*-HPMAm-lactate)-*b*-PEG showed controlled instability at body temperature [20,21]. PNIPAAm, however, is a non-biodegradable polymer and its biocompatibility is not well known at present. Interestingly and as reported in this chapter, we found that poly(HPMAm-mono/di lactate) without NIPAAm also shows LCST behavior in aqueous solution. Importantly, due to the hydrolyzable lactic acid side groups, the CP will increase in time with lactic acid, an endogenous compound, and the water-soluble pHPMAm as degradation products. pHPMAm is a well-known non-toxic macromolecular carrier which is among others used for the development of polymeric prodrugs of cytostatic agents. The first generation of systems recently successfully entered into clinical trials already [22-25]. Therefore a good biocompatibility of poly(HPMAm-lactate) is expected.

2. Materials and methods

2.1. Materials

1,4-Dioxane 99±% (Fluka Chemie AG) was purified by distillation. α, α' -Azoisobutyronitrile (AIBN) was from Fluka Chemie AG (Buchs, Switzerland). HPMAM was synthesized as reported by Oupicky et al [26]. HPMAM esterified with mono-lactic acid or di-lactic acid (further abbreviated as HPMAM-monolactate and HPMAM-dilactate, respectively) was synthesized as described previously [21].

2.2. Synthesis of poly(HPMAM-monolactate), poly(HPMAM-dilactate) and their copolymers

HPMAM-monolactate and HPMAM-dilactate were dissolved at a concentration of 0.1 g/mL in 1,4-dioxane. The HPMAM-monolactate/HPMAM-dilactate ratios were 100/0, 75/25, 50/50, 25/75, and 0/100 (mol/mol). AIBN (total amount of monomers/AIBN is around 40/1 (mol/mol)) was added as radical initiator and the polymerization was conducted at 70 °C for 24 hours in a nitrogen atmosphere. The polymers were collected by centrifugation after precipitation in diethyl ether. The polymers were further purified by dissolving them in cold water, followed by filtration through a 0.22 μm filter. After freeze-drying, the products were characterized by ^1H NMR (solvent: CDCl_3) and gel permeation chromatography (GPC). ^1H NMR: $\delta = 6.6$ ppm (b, CO-NH-CH_2), 5.0 ppm (b, $\text{NH-CH}_2-\text{CH}(\text{CH}_3)-\text{O}$ and $\text{CO-CH}(\text{CH}_3)-\text{O}$, methine protons 1 and 2, Figure 1), 4.3 ppm (b, $\text{CO-CH}(\text{CH}_3)-\text{OH}$, methine protons 3, Figure 1), 3.2 ppm (b, $\text{NH-CH}_2-\text{CH}(\text{CH}_3)$), 2.2-0.6 ppm (the rest of the protons). GPC was done using Plgel 3 μm MIXED-D + Plgel 3 μm MIXED-E columns (Polymer Laboratories) and poly(ethylene glycol) standards. The eluent was DMF containing 10mM LiCl,

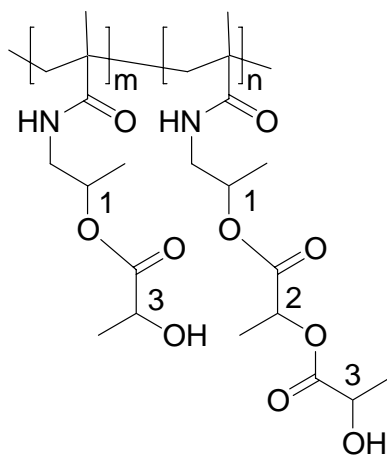


Figure 1. Structure of poly(HPMAM-monolactate) ($n = 0$), poly(HPMAM-dilactate) ($m = 0$), and poly(HPMAM-monolactate-*co*-HPMAM-dilactate) ($m, n \neq 0$). See Materials and methods for numbers (1-3) adjacent to the structure.

the elution rate was 0.7 mL/min, and the temperature was 40 °C. The copolymer composition of the polymers was determined by ¹H NMR from the ratio of the integral of the peak at 5.0 ppm ($I_{5.0}$, methine protons 1 and 2, Figure 1) to the integral of the peak at 4.3 ppm ($I_{4.3}$, methine protons 3, Figure 1) by the following formula: $I_{5.0}/I_{4.3} = 1 + x$, where x represents the molar fraction of HPMAM-dilactate in the copolymer.

2.3. Static light scattering (SLS)

The CP of the polymers was determined with static light scattering using a Horiba Fluorolog fluorometer (650 nm, at a 90° angle). The polymers were dissolved in water or in isotonic 120 mM ammonium acetate buffer (pH = 5.0) at 0 °C. The polymer concentration was varied between 0.1 mg/mL and 5 mg/mL. The scattering intensity was measured every 0.2 °C during heating and cooling (the heating/cooling rate was approximately 1 °C/min). Onsets on the X-axis, obtained by extrapolation of the intensity-temperature curves during heating to intensity zero were considered as the CP. The CP determinations were done at least two times and the deviations were smaller than 0.5 °C.

2.4. Differential scanning calorimetry (DSC)

The DSC measurements were carried out for poly(HPMAM-dilactate) solution in water (100 mg/mL) using a DSC Q1000 differential scanning calorimeter with a RCA cooling system (TA Instruments). Aluminium hermetic sealed pans containing 10 µL of the polymer solutions were heated at a scanning rate of 1 °C/min. Calibration was performed using indium as a standard.

3. Results and Discussion

Poly(HPMAM-monolactate), poly(HPMAM-dilactate) as well as their copolymers (Figure 1) were synthesized by radical polymerization. Five polymers with different monomer compositions were obtained in a yield between 50 and 70 % (Table 1). Figure 2 shows the ¹H NMR spectrum of poly(HPMAM-monolactate-*co*-HPMAM-dilactate) prepared at a monomer feed ratio of 1:1 (mol/mol). For all copolymers, the composition was close to the feed ratio of the monomers. Static light scattering measurements of these polymers in water and in isotonic 120 mM ammonium acetate buffer (pH = 5.0, to minimize hydrolysis of lactate ester side groups [21]) were performed. Interestingly, all polymers of Table 1 showed LCST behavior. Figure 3 shows a typical light scattering intensity-temperature curve for poly(HPMAM-monolactate-*co*-HPMAM-dilactate) in isotonic 120 mM ammonium acetate buffer (pH = 5.0).

Table 1. Characteristics of the polymers used in this study

	Feed ratio (mol/mol)	Ratio in polymer ^{a)} (mol/mol)	M_n ^{b)}	M_w ^{b)}	M_w/M_n	CP (°C) ^{c)}	CP (°C) ^{d)}
poly(HPMAm- monolactate)	100/0	-	11400	24400	2.14	65.0	63.0
poly(HPMAm- monolactate- <i>co</i> -HPMAm- dilactate)	75/25	75/25	7500	17600	2.35	50.5	47.5
	50/50	51/49	8100	16900	2.08	36.5	34.0
	25/75	26/74	6800	14000	2.06	25.0	23.0
poly(HPMAm- dilactate)	0/100	-	6300	10700	1.70	13.0	10.5

a) Determined by ^1H NMR.

b) M_n = number average molar weight and M_w = weight average molar weight determined by GPC.

c) Determined by SLS for 1 mg/mL solution in water.

d) Determined by SLS for 1 mg/mL solution in isotonic 120 mM ammonium acetate buffer (pH = 5.0).

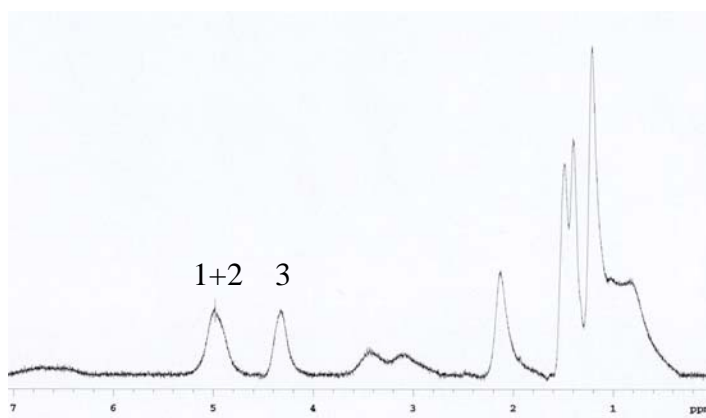


Figure 2. ^1H NMR spectrum of poly(HPMAm-monolactate-*co*-HPMAm-dilactate 51/49) in CDCl_3 . Numbers shown refer to the protons indicated in Figure 1. The polymer composition was determined as explained in Materials and methods.

Poly(HPMAm-monolactate) has a rather high CP (65 °C in water, Table 1) whereas poly(HPMAm-dilactate) has a relatively low CP (13 °C in water, Table 1). This can be explained by the greater hydrophobicity of the dilactate side group over the monolactate side group. Importantly, the CP of the copolymers linearly increased with mol % of HPMA-monolactate monomer (Figure 4), meaning that the CP of the copolymers can be tailored by the copolymer composition. Although the molecular weight of the polymers decreased as the

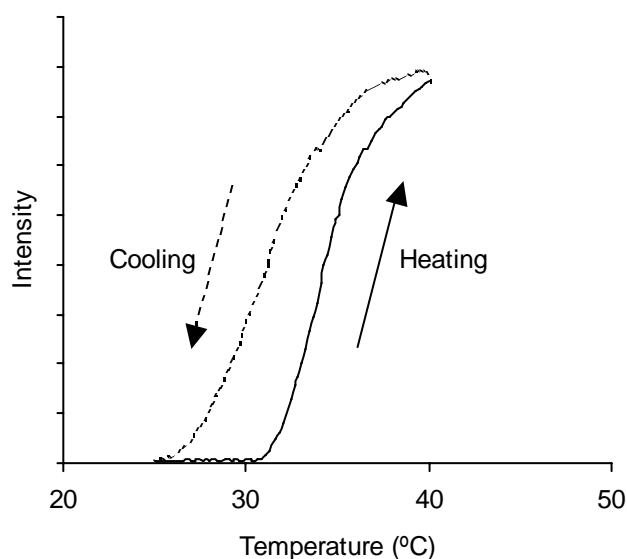


Figure 3. Light scattering intensity-temperature curve for poly(HPMAM-monolactate-*co*-HPMAM-dilactate) in isotonic 120 mM ammonium acetate buffer (pH = 5.0) at 5 mg/mL. The molar ratio of HPMAM-monolactate and HPMAM-dilactate is 51:49 (mol/mol).

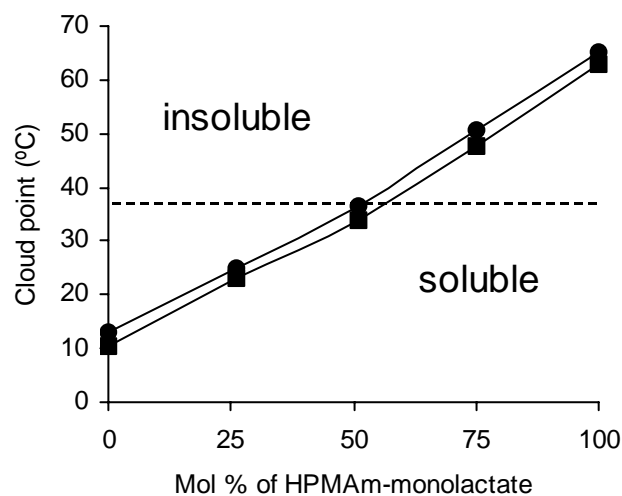


Figure 4. CP of poly(HPMAM-monolactate-*co*-HPMAM-dilactate) as a function of the mol % HPMAM-monolactate in the copolymer. ●: 1 mg/mL solution in water; ■: 1 mg/mL solution in isotonic 120 mM ammonium acetate buffer (pH = 5.0).

ratio of HPMAM-dilactate increased (Table 1), the decrease of molecular weight is not the reason for the decrease of the CP. We prepared poly(HPMAM-monolactate) with lower molecular weight and we observed that the CP slightly increased with the decrease of molecular weight (data not shown). The CP's in isotonic 120 mM ammonium acetate buffer (pH = 5.0) were approximately 2.5

°C lower than those in water (Table 1). This can be attributed to a salting-out effect of ions present in the buffer solution, and is an indication that the LCST behavior is due to dehydration of the polymer chain as demonstrated for PNIPAAm [8,27,28]. Figure 3 shows that thermohysteresis of around 5 °C is observed between the heating and cooling curve. It has been reported that PNIPAAm does not show LCST hysteresis [9]. In contrast, poly(*N*-isopropylmethacrylamide) shows hysteresis, which is ascribed to the α -methyl group in the polymer backbone resulting in a decreased chain flexibility [9,29]. Since the polymers of Table 1 also contain α -methyl groups in the polymer backbone, the hysteresis is likely due to the same phenomenon. Figure 5 shows the effect of the concentration of polymer on the CP. The CP decreased approximately 3 °C as the concentration increased 10-fold. The CP of PNIPAAm is hardly affected by its concentration [9,30], whereas other thermosensitive polymers also show an increase of CP with a decrease in concentration [2,31]. DSC analysis did not show a detectable endothermal peak around the CP for poly(HPMAm-dilactate) solution at 100 mg/mL (data not shown), whereas an aqueous PNIPAAm solution at 50 mg/mL displayed a clearly detectable endothermal peak around the CP (32 °C) with an enthalpy change of 43 J/g polymer [32,33]. This indicates that hardly any enthalpy change is involved in the phase transition of poly(HPMAm-dilactate). The mechanism of the phase transition will be investigated in Chapter 3.

In conclusion, this chapter reports on a novel class of polymers that are thermosensitive and hydrolytically sensitive. These features are attractive for materials in drug delivery and biomedical applications. The CP of the polymer can be tailored between 10 °C to 65 °C by the copolymer composition. In a previous paper we have shown that the lactic acid groups of poly(NIPAAm-*co*-HPMAm-lactate) as well as HPMAm-lactate monomer are hydrolytically

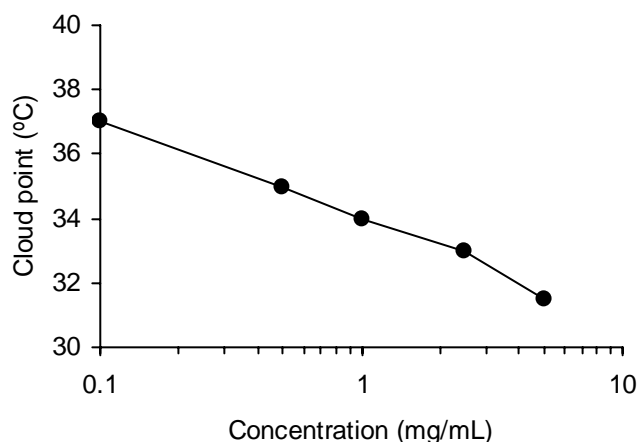


Figure 5. CP of poly(HPMAm-monolactate-*co*-HPMAm-dilactate 51/49) in isotonic 120 mM ammonium acetate buffer (pH = 5.0) as a function of the polymer concentration.

sensitive under physiological conditions (pH 7.4, 37 °C) [21]. It is obvious that this chemical hydrolysis also occurs in poly(HPMAM-lactate) consequently. Because of the removal of the lactic acid side groups in aqueous solution, poly(HPMAM-lactate) becomes more hydrophilic in time, which is associated with a gradual increase of the CP. Therefore, polymers can be designed which are initially associated but which start to dissolve once the CP increases beyond the incubation temperature. For example, Figure 4 shows that poly(HPMAM-dilactate) is above its CP at body temperature and thus is in its precipitated form, but when more than 50 % of HPMAM-dilactate are converted to HPMAM-monolactate, this polymer changes to a soluble state at body temperature. Such mechanism of controlled dissolution is unique, and not possible with other known biodegradable thermosensitive polymers, e.g. as recently described by Tachibana et al [34]. Further, it is expected that our polymers possess a good biocompatibility.

Thus, poly(HPMAM-lactate) is a valuable extension of thermosensitive polymeric materials and we anticipate that these systems have a great potential for biomedical and pharmaceutical applications.

Acknowledgement

The authors thank Mitsubishi Pharma Corporation (Japan) for their financial support.

References

1. B. Jeong, S.W. Kim, Y.H. Bae. *Adv Drug Deliv Rev* 54 (2002) 37-51.
2. A. Chilkoti, M.R. Dreher, D.E. Meyer, D. Raucher. *Adv Drug Deliv Rev* 54 (2002) 613-630.
3. A.V. Kabanov, E.V. Batrakova, V.Y. Alakhov. *J Control Release* 82 (2002) 189-212.
4. A. Kikuchi, T. Okano. *Adv Drug Deliv Rev* 54 (2002) 53-77.
5. B. Jeong, Y.H. Bae, D.S. Lee, S.W. Kim. *Nature* 388 (1997) 860-862.
6. R. Pelton. *Adv Colloid Interface Sci* 85 (2000) 1-33.
7. H.G. Schild. *Prog Polym Sci* 17 (1992) 163-249.
8. H.G. Schild, D.A. Tirrell. *J Phys Chem* 94 (1990) 4352-4356.
9. S. Fujishige, K. Kubota, I. Ando. *J Phys Chem* 93 (1989) 3311-3313.
10. C. Konak, D. Oupicky, V. Chytrý, K. Ulbrich, M. Helmstedt. *Macromolecules* 33 (2000) 5318-5320.
11. F. Kohori, K. Sakai, T. Aoyagi, M. Yokoyama, Y. Sakurai, T. Okano. *J Control Release* 55 (1998) 87-98.
12. M.D.C. Topp, P.J. Dijkstra, H. Talsma, J. Feijen. *Macromolecules* 30 (1997) 8518-8520.

13. J.E. Chung, M. Yokoyama, T. Okano. *J Control Release* 65 (2000) 93-103.
14. S. Cammas, K. Suzuki, C. Sone, Y. Sakurai, K. Kataoka, T. Okano. *J Control Release* 48 (1997) 157-164.
15. R. Yoshida, K. Uchida, Y. Kaneko, K. Sakai, A. Kikuchi, Y. Sakurai, T. Okano. *Nature* 374 (1995) 240-242.
16. K. Kono. *Adv Drug Deliv Rev* 53 (2001) 307-319.
17. J.C. Leroux, E. Roux, D. Le Garrec, K. Hong, D.C. Drummond. *J Control Release* 72 (2001) 71-84.
18. H. Feil, Y.H. Bae, J. Feijen, S.W. Kim. *Macromolecules* 26 (1993) 2496-2500.
19. M. Shibayama, S. Mizutani, S. Nomura. *Macromolecules* 29 (1996) 2019-2024.
20. D. Neradovic, C.F. van Nostrum, W.E. Hennink. *Macromolecules* 34 (2001) 7589-7591.
21. D. Neradovic, M.J. van Steenberg, L. Vansteelant, Y.J. Meijer, C.F. van Nostrum, W.E. Hennink. *Macromolecules* 36 (2003) 7491-7498.
22. P.A. Vasey, S.B. Kaye, R. Morrison, C. Twelves, P. Wilson, R. Duncan, A.H. Thomson, L.S. Murray, T.E. Hilditch, T. Murray, S. Burtles, D. Fraier, E. Frigerio, J. Cassidy. *Clin Cancer Res* 5 (1999) 83-94.
23. B. Rihova, J. Strohalm, J. Prausova, K. Kubackova, M. Jelinkova, L. Rozprimova, M. Sirova, D. Plocova, T. Etrych, V. Subr, T. Mrkvan, M. Kovar, K. Ulbrich. *J Control Release* 91 (2003) 1-16.
24. J. Kopecek, P. Kopeckova, T. Minko, Z. Lu. *Eur J Pharm Biopharm* 50 (2000) 61-81.
25. R. Duncan. *Nat Rev Drug Discov* 2 (2003) 347-360.
26. D. Oupicky, C. Konak, K. Ulbrich. *J Biomater Sci Polym Ed* 10 (1999) 573-590.
27. T.G. Park, A.S. Hoffman. *Macromolecules* 26 (1993) 5045-5048.
28. A. Durand, D. Hourdet. *Polymer* 41 (2000) 545-557.
29. M. Netopilik, M. Bohdanecky, V. Chytry, K. Ulbrich. *Macromol Rapid Commun* 18 (1997) 107-111.
30. Z. Tong, F. Zeng, X. Zheng, T. Sato. *Macromolecules* 32 (1999) 4488-4490.
31. H. Miyazaki, K. Kataoka. *Polymer* 37 (1996) 681-685.
32. F. Eeckman, A.J. Moes, K. Amighi. *Int J Pharm* 273 (2004) 109-119.
33. H.H. Lin, Y.L. Cheng. *Macromolecules* 34 (2001) 3710-3715.
34. Y. Tachibana, M. Kurisawa, H. Uyama, T. Kakuchi, S. Kobayashi. *Chem Commun (Camb)* (2003) 106-107.

Chapter 3

Physicochemical characterization of degradable thermosensitive polymeric micelles

Osamu Soga¹, Cornelus F. van Nostrum¹, Aissa Ramzi¹,
Tom Visser², Fouad Soulimani², Peter M. Frederik³, Paul H. H. Bomans³
and Wim E. Hennink¹

¹ Department of Pharmaceutics, Utrecht Institute for Pharmaceutical Sciences (UIPS),
Faculty of Pharmaceutical Sciences, Utrecht University, Utrecht, The Netherlands

² Department of Vibrational Spectroscopy, Faculty of Chemistry, Utrecht University,
Utrecht, The Netherlands

³ EM-unit, Department of Pathology, Medical Faculty, University Maastricht,
Maastricht, The Netherlands

Langmuir 20 (2004) 9388-9395

Abstract

Amphiphilic AB block copolymers consisting of thermosensitive poly(*N*-(2-hydroxypropyl) methacrylamide lactate) and poly(ethylene glycol), pHPMAmDL-*b*-PEG, were synthesized via a macroinitiator route. Dynamic light scattering measurements showed that these block copolymers form polymeric micelles in water with a size of around 50 nm by heating of an aqueous polymer solution from below to above the critical micelle temperature (CMT). The critical micelle concentration (CMC) as well as the CMT decreased with increasing pHPMAmDL block lengths, which can be attributed to the greater hydrophobicity of the thermosensitive block with increasing molecular weight. Cryo-transmission electron microscopy (cryo-TEM) analysis revealed that the micelles have a spherical shape with a narrow size distribution. ¹H NMR measurements in D₂O showed that the intensity of the peaks of the protons from pHPMAmDL block significantly decreased above the CMT, indicating that the thermosensitive blocks indeed form the solid-like core of the micelles. Static light scattering measurements demonstrated that pHPMAmDL-*b*-PEG micelles with relatively large pHPMAmDL blocks possess a highly packed core that is stabilized by a dense layer of swollen PEG chains. FT-IR analysis indicated that dehydration of amide bonds in the pHPMAmDL block occurs when the polymer dissolved in water is heated from below to above its CMT. The micelles were stable when an aqueous solution of micelles was incubated at 37 °C and at pH 5.0, where the hydrolysis rate of lactate side groups is minimized. On the other hand, at pH 9.0, where hydrolysis of the lactic acid side groups occurs, the micelles started to swell after 1.5 hours of incubation and complete dissolution of micelles was observed after 4 hours as a result of hydrophilization of the thermosensitive block. Fluorescence spectroscopy measurements with pyrene loaded in the hydrophobic core of the micelles showed that when these micelles were incubated at pH 8.6 and at 37 °C the microenvironment of pyrene became increasingly hydrated in time during this swelling phase. The results demonstrate the potential applicability of pHPMAmDL-*b*-PEG block copolymer micelles for the controlled delivery of hydrophobic drugs.

1. Introduction

Amphiphilic block copolymers consisting of a hydrophilic and a hydrophobic segment self-assemble into polymeric micelles in aqueous solution with a hydrophobic core stabilized by a hydrophilic shell [1,2]. Currently, polymeric micelles are extensively investigated for pharmaceutical applications [3-6] because of their attractive features as drug delivery vehicles. Hydrophobic drugs can be loaded into their hydrophobic core [7]. Moreover, the size of polymeric micelles is generally between 10 to 60 nm, which is relatively small compared to other colloidal drug carriers such as liposomes and emulsions. Due to their small size and hydrophilic surface, polymeric micelles are not easily recognized and captured by macrophages of the mononuclear phagocyte system (MPS). Therefore, polymeric micelles have a relatively long circulation time after intravenous administration, and as a result they accumulate in e.g. tumor and other inflammation tissues due to the so-called EPR (enhanced permeation and retention) effect [8]. Furthermore, the critical micelle concentration (CMC) of polymeric micelles is usually much lower than that of low molecular weight surfactant micelles, which ensures a good physical stability against dilution after injection into the bloodstream. Poly(ethylene glycol) (PEG) is most commonly used as the hydrophilic segment of the copolymers forming the micelles as well as for the coating of other colloidal drug carriers, because of its non-toxicity and good “stealth” properties [9,10]. On the other hand, a variety of polymers have been used as hydrophobic segment in polymeric micelles: poly(propylene glycol) (Pluronic®) [11], poly(aspartic acid) with chemically conjugated doxorubicin [12], poly(β -benzyl-L-aspartate) [7], and poly(ester)s such as poly(lactic acid) [13] and poly(ϵ -caprolactone) [14].

Recently, stimuli-sensitive polymers have been used in block copolymers for the preparation of intelligent drug carriers [15,16]. In particular, thermosensitive polymers, e.g. poly(*N*-isopropylacrylamide) (PNIPAAm) with its cloud point (around 32 °C in water) close to body temperature, have been investigated [17-19]. Block copolymers consisting of a thermosensitive PNIPAAm block and PEG indeed form micelles at 37 °C [20,21]. Destabilization of these micelles can be triggered by hypothermia or by the introduction of comonomers with hydrolyzable side groups [22,23].

Interestingly, it was reported in Chapter 2 that poly(*N*-(2-hydroxypropyl) methacrylamide lactate) (poly(HPMAm-lactate)) shows lower critical solution temperature (LCST) behavior in aqueous solution [24]. It is expected that due to hydrolysis of the lactic acid side groups the cloud point (CP) will increase in time with lactic acid, an endogenous compound, and pHPMAm as degradation products. pHPMAm is a water-soluble polymer and has shown to be non-toxic in clinical trials [25,26]. It was demonstrated that the CP of poly(HPMAm-lactate) can be well controlled by the length of the lactate acid side group (e.g.

monolactate or dilactate) and copolymer composition [24]. Among these polymers, in particular poly(HPMAM-dilactate) is an interesting polymer, because its CP (around 10 °C) is far below body temperature. It is expected that block copolymers of poly(HPMAM-dilactate) and PEG form polymeric micelles at 37 °C but gradually dissolve due to hydrolysis of the lactic acid side groups, by which a drug that is loaded in the hydrophobic core is released into the environment (Figure 1).

In this chapter, a number of block copolymers of poly(HPMAM-dilactate) and PEG (pHPMAMDL-*b*-PEG) were synthesized and the characteristics of polymeric micelles based on these block copolymers were investigated with cryo-transmission electron microscopy and light scattering techniques. The mechanism of the LCST behavior of poly(HPMAM-dilactate) was investigated with FT-IR and ^1H NMR spectroscopy. Finally, the destabilization behavior of the micelles was studied.

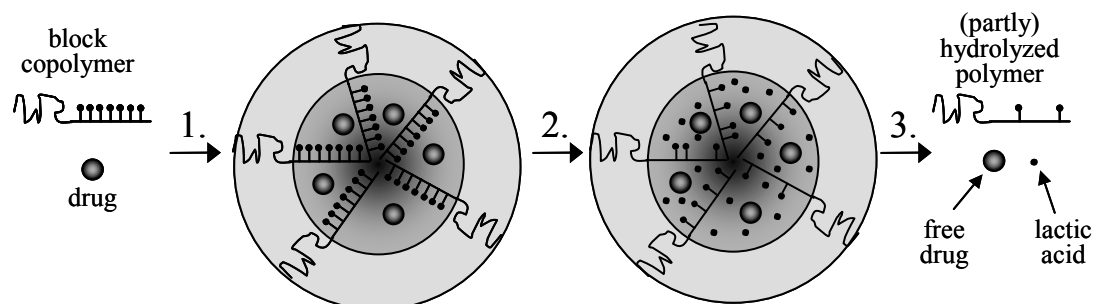


Figure 1. A schematic representation of the concept of polymeric micelles with controlled instability, formed from block copolymers with hydrolytically sensitive side groups. The numbered consecutive steps are the following: 1. Self-assembly and drug loading of polymeric micelles in water above the CMT. 2. Degradation and hydrophilization of the core. 3. Dissolution of the micelles and release of the drug.

2. Materials and methods

2.1. Materials

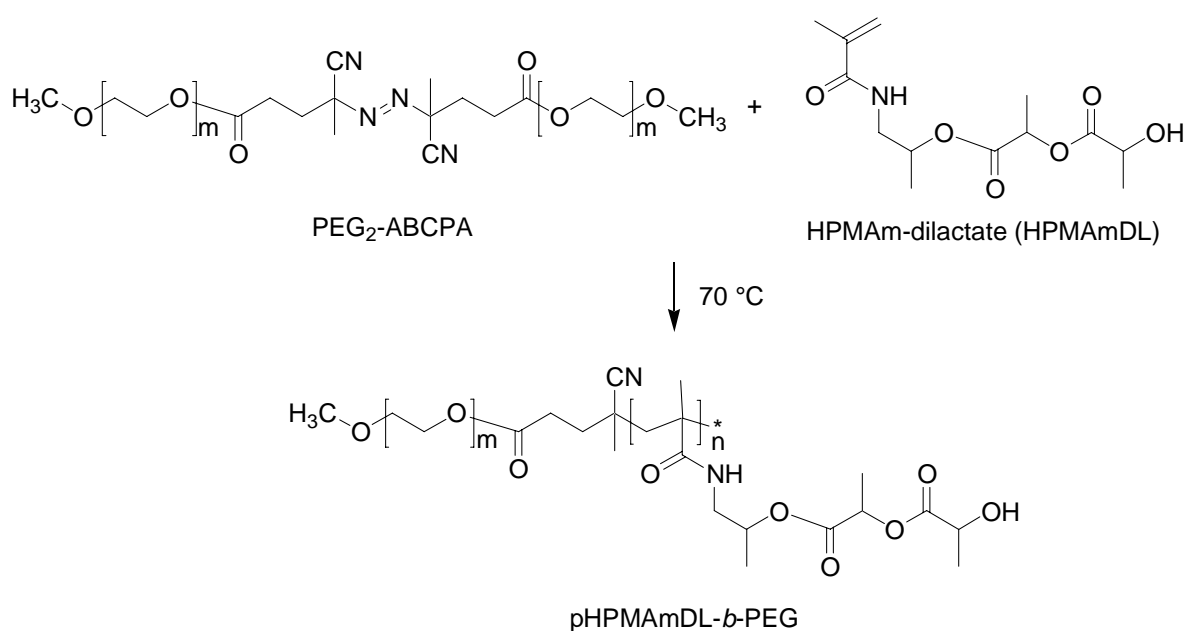
HPMAM esterified with optically pure di-*S*-lactic acid (further abbreviated as HPMAM-dilactate) was synthesized as described previously [23]. Monomethyl ether of poly(ethylene glycol) (mPEG), MW = 5,000 g/mol, was supplied by NEKTAR (San Carlos, CA, USA). 4,4-azobis(4-cyanopentanoic acid) (ABCPA) and pyrene were from Fluka, Chemie AG (Buchs, Switzerland). The PEG₂-ABCPA macroinitiator with PEG 5000 was prepared as described previously [22].

2.2. Synthesis of *p*(HPMAM-dilactate)-*b*-PEG block copolymers (*p*HPMAMDL-*b*-PEG)

*p*HPMAMDL-*b*-PEG block copolymers were synthesized by radical polymerization using HPMAM-dilactate as monomer and PEG₂-ABCPA as initiator. HPMAM-dilactate and PEG₂-ABCPA were dissolved at a total concentration of 0.3 g/mL in acetonitrile. To obtain block copolymers with different *p*HPMAMDL block lengths, the ratio of monomer to macroinitiator was varied between 35/1 to 140/1 (mol/mol). The polymerization was conducted at 70 °C for 24 hours in a nitrogen atmosphere. The polymers were collected by centrifugation after precipitation in diethyl ether. The polymers were purified by dissolving them in cold water, followed by filtration through a 0.22 μm filter and freeze-drying. The products were characterized by ¹H NMR with a Gemini 300 MHz spectrometer (Varian Associates Inc. NMR Instruments, Palo Alto, CA) and gel permeation chromatography (GPC). GPC was done using Plgel 3 μm MIXED-D + Plgel 3 μm MIXED-E columns (Polymer Laboratories) and poly(ethylene glycol) standards. The eluent was DMF containing 10 mM LiCl, the elution rate was 0.7 mL/min, and the temperature was 40 °C.

¹H NMR (solvent: CDCl₃) (see Scheme 1, all protons are from *p*HPMAMDL block except for methylene protons from PEG.): δ = 6.5 (b, CO-NH-CH₂), 5.0 (b, NH-CH₂-CH(CH₃)-O and CO-CH(CH₃)-O), 4.4 (b, CO-CH(CH₃)-OH), 3.6 (b, PEG methylene protons, O-CH₂-CH₂), 3.4 (b, NH-CH₂-CH(CH₃)), 2.0-0.6 (the rest of the protons from the *p*HPMAMDL block).

The number average molecular weight (M_n) of *p*HPMAMDL block was determined by ¹H NMR as follows: a) the value of the integral of the PEG protons divided by 454 (average number of protons per one PEG 5000 chain) gave the integral value for one PEG proton, and b) the number of HPMAMDL units in the polymers was determined from the ratio of the integral of the methine proton (CO-CH(CH₃)-OH) of HPMAMDL to the integral of one PEG proton. The number average molecular weight of the *p*HPMAMDL block was calculated from the resulting number of units.



Scheme 1. Synthesis route and structure of pHPMAmDL-*b*-PEG block copolymers.

2.3. Determination of the critical micelle temperature (CMT)

The CMT of the different block copolymers was determined with static light scattering using a Horiba Fluorolog fluorometer (650 nm, at a 90° angle). The polymers were dissolved at a concentration of 10 mg/mL in isotonic 120 mM ammonium acetate buffer (pH = 5.0) at 0 °C. The scattering intensity was measured every 0.2 °C during heating and cooling (the heating/cooling rate was approximately 1 °C/min). Onsets on the X-axis, obtained by extrapolation of the intensity-temperature curves during heating to intensity zero, were considered as the CMT. The CMT determinations were done at least two times and the deviations were smaller than 0.5 °C.

2.4. Formation of micelles

Micelles of the different block copolymers were formed by a quick heating of an aqueous polymer solution from below to above the CMT [27]. The polymers were dissolved at a concentration between 0.1 to 20 mg/mL in isotonic 120 mM ammonium acetate buffer (pH = 5.0) at 0 °C. Then the polymer solution (1 mL) was quickly heated from 0 °C to 50 °C and left at 50 °C for 1 minute. For DLS and other measurements, the micelle solution was incubated at 37 °C or at room temperature.

2.5. Dynamic light scattering (DLS)

DLS measurements were done to determine the size of the micelles, using a Malvern 4700 system (Malvern Ltd., Malvern, UK) consisting of an Autosizer 4700 spectrometer, a pump/filter unit, a Model 2013 air-cooler argon ion laser (75 mW, 488 nm, equipped with a model 2500 remote interface controller, Uniphase) and a computer with DLS software (PCS, version 3.15, Malvern). The measurement temperature was 37 °C and the measurement angle was 90°. The change in solvent viscosity with temperature was corrected by the software.

2.6. Determination of the critical micelle concentration (CMC)

The CMC of the block copolymers was determined using pyrene as a fluorescent probe [28]. Micelles of the different block copolymers were formed as described above in isotonic 120 mM ammonium acetate buffer (pH = 5.0) at a concentration of 2 mg/mL. The micellar solutions were cooled to room temperature and subsequently diluted with the same buffer yielding different polymer concentrations ranging from 1×10^{-5} to 1 mg/mL. Next, 15 μ L of pyrene dissolved in acetone (concentration, 1.8×10^{-4} M) was added to 4.5 mL of polymer solution. The polymer solutions with pyrene were incubated for 20 hours at room temperature in the dark to allow evaporation of acetone. Fluorescence excitation spectra of pyrene were obtained as a function of the polymer concentration using a Horiba Fluorolog fluorometer (at a 90° angle). The excitation spectra were recorded at 37 °C from 300 to 360 nm with the emission wavelength at 390 nm. The excitation and emission band slits were 4 nm and 2 nm, respectively. The intensity ratio of I_{338}/I_{333} was plotted against polymer concentration to determine the CMC.

2.7. Static light scattering (SLS)

The radius of gyration and weight average molecular weight of the different pHPMA $_{m}$ DL-*b*-PEG micelles were determined by SLS at 37 °C at a concentration of 10 mg/mL in 120 mM ammonium acetate buffer (pH = 5.0). SLS experiments were carried out using multi-angle laser light scattering DAWN-DSP-F (MALLS, Wyatt Technology Corp., Santa Barbara, CA) equipped with a 5 mW He-Ne laser source ($\lambda = 632.8$ nm), a K5 glass flow cell, thermostated by a Peltier control of the temperature (36.7 ± 0.2 °C). The HPLC-system was equipped with a column (15 \times 0.46 cm) packed with glass pearls (1.5 mm), placed in a column oven (Waters RCM-100/Column Heater), and was linked in series to the MALLS detector, a differential refractive index (RI) detector (ERMA ERC 7510) and a JASCO CD1595 UV detector. The MALLS instrument was calibrated to the scattering from HPLC-grade toluene, which has a high and accurately determined Rayleigh ratio, while the refractive index detector was calibrated using a saccharose solution in water. The injected

volume of micelle solution was 5 μL and the flow rate was 1.0 mL/min. During the chromatographic run, the MALLS detector measures simultaneously the degree of light scattering of the laser beam using detectors placed at 18 different angles ranging from 4.3° to 158.2° . For each sampling time of the elution pattern corresponding to one elution volume (V_i), the concentration (c_i) was calculated from the differential refractive index response. The data were analyzed for each individual slice “i” within the peak of interest using the algorithm from ASTRA software. Technically, the molar mass calculated for each slice from the fits, via Zimm, Debye, Berry or random coil plots, is weight averaged and the radius is z-averaged. These mass/radii can be used together with the concentration c_i , measured with the concentration sensitive detector, UV or RI, for each slice, to calculate the average mass for the entire peak. Following this determination, the intensity of the scattered light detected by the 15 Dawn-F photodiodes allows the determination of molecular weight (M_i) and radius of gyration ($R_i = \langle r_g^2 \rangle_i^{1/2}$, where $\langle r_g^2 \rangle_i$ is the mean square radius measured for the slice i) of the different micelles by ASTRA version 4.70.07 software, based on the equation:

$$\left(\frac{Kc}{R(\theta)} \right)_i = \frac{1}{M_i} \left(1 + \frac{16\pi^2}{3\lambda^2} \langle r_g^2 \rangle_i \sin^2(\theta/2) + 2A_2 M_i c_i \right)$$

where K is the optical constant defined as:

$$K = \frac{4\pi^2}{N_A \lambda^4} \frac{n_T^2}{R_T} \left(\frac{dn}{dc} \right)^2$$

n_T and R_T are the refractive index and Rayleigh ratio of toluene, respectively. N_A is Avogadro’s constant, and (dn/dc) is the specific refractive index increment of the dispersion. $R(\theta)$ is the excess Rayleigh ratio of the solute (excess intensity of scattered light at DAWN angle θ), λ is the wavelength of the incident laser beam, and c_i is calculated from the differential refractive index response. A_2 is the second virial coefficient, M_i and R_i are obtained from the “y” intercept to zero scattering angle and from the slope, respectively. The weight average molecular weights of the micelles ($M_{w(\text{mic})}$) is then calculated as

$$\overline{M}_w = \frac{\sum_i c_i M_i}{\sum_i c_i}$$

The root-mean-square z-average radius of gyration R_G^2 is

$$\overline{R_G^2} = \left\langle \overline{r_g^2} \right\rangle_z = \frac{\sum_i c_i M_i \left\langle r_g^2 \right\rangle_i}{\sum_i c_i M_i}$$

The density of the micelle was calculated by: $\rho_{\text{mic}} = M_{\text{w(mic)}}/N_a V$, where N_a is Avogadro's number and V is the average volume of the micelles. V was calculated based on the hydrodynamic radius (R_{hyd}) of micelles determined by DLS. The aggregation number of micelles (N_{agg}) was calculated by dividing $M_{\text{w(mic)}}$ by the number average molecular weight of block polymers determined by ^1H NMR (e.g. the M_n for pHPMAmDL(13600)-*b*-PEG(5000) is 18,600 g/mol). The surface area of the micelle's shell available per PEG chain (S/N_{agg}) was calculated by dividing S , the surface area of the shell of micelles calculated based on R_{hyd} , by N_{agg} [29].

2.8. Cryo-transmission electron microscopy (cryo-TEM)

Cryo-TEM measurements were performed on pHPMAmDL(13600)-*b*-PEG micelles prepared at a concentration of 10 mg/mL in 120 mM ammonium acetate buffer (pH = 5.0). Sample preparation for cryo-TEM was done in a temperature and humidity controlled chamber using a fully automated vitrification robot (FEI Company, Hillsboro, Oregon, USA) [30]. A thin aqueous film of micellar solution was formed on a Quantifoil R 2/2 grid (Quantifoil Micro Tools GmbH, Jena, Germany) at 22 °C and at 100 % relative humidity. The thin film was rapidly vitrified by shooting the grid into liquid ethane. The grids with the vitrified thin films were transferred into the microscope chamber using a Gatan 626 cryo-transfer/cryo-holder system (Gatan, Inc., Pleasanton, CA, USA). Micrographs were taken using a CM-12 transmission microscope (Philips, Eindhoven, The Netherlands) operating at 120 kV, with the specimen at -170 °C and using low-dose imaging conditions.

2.9. ^1H NMR measurements of block copolymers in D_2O

^1H NMR measurements were performed on pHPMAmDL(13600)-*b*-PEG block copolymer dissolved in D_2O (10 mg/mL) below the CMT (1 °C) and above the CMT (37 °C). The ^1H NMR spectra were recorded with an Inova 500 MHz spectrometer (Varian Associates Inc. NMR Instruments, Palo Alto, CA).

2.10. FT-IR measurements

FT-IR analysis was carried out with a Perkin-Elmer 2000 FT-IR instrument by accumulating 25 scans per spectrum at a data point resolution of 2 cm^{-1} . A spectrum of pHPMAmDL(13600)-*b*-PEG in KBr was recorded. Spectra of pHPMAmDL(13600)-*b*-PEG solutions (30 mg/mL in D_2O) were recorded by slowly heating a polymer solution in a 50 μm CaF_2 cell from below the CMT (2 °C) to above the CMT (50 °C) followed by cooling to 2 °C. Spectra were

recorded at different temperatures. A spectrum of D₂O recorded at 22 °C was subtracted from all spectra.

2.11. Micelle destabilization

The destabilization of micelles was monitored at two different pH's (5.0 and 9.0). For pH 5.0, micelles of pHPMAmDL(13600)-*b*-PEG block copolymer were formed as described in Section 2.4 in isotonic 120 mM ammonium acetate buffer at a concentration of 2 mg/mL. For pH 9.0, the polymer was first dissolved in water at 20 mg/mL at 0 °C and then diluted 10-fold with 300 mM NaHCO₃ buffer (pH = 9.0). Micelles were formed as described in Section 2.4. Both the size of the micelles and the intensity of the scattered light were measured by DLS at 37 °C as a function of time. Pyrene-loaded micelles were prepared as described in Section 2.6. The pyrene concentration was 6.0×10^{-7} M and the concentration of pHPMAmDL(13600)-*b*-PEG block copolymer was 2 mg/mL. Then, 0.2 mL of pyrene-loaded micelle solution was added to 0.8 mL of isotonic 120 mM ammonium acetate buffer (pH = 5.0) or 300 mM NaHCO₃ buffer (pH = 9.0). The latter dilution gave a final pH of 8.6. Fluorescence measurements were performed as described in the Section 2.6 and the change of the ratio of I₃₃₈/I₃₃₃ at 37 °C was monitored in time.

3. Results and Discussion

3.1. Synthesis and characterization of pHPMAmDL-*b*-PEG block copolymers

p(HPMAm-dilactate)-*b*-PEG block copolymers (pHPMAmDL-*b*-PEG) were synthesized by radical polymerization using HPMAm-dilactate as monomer and PEG₂-ABCPA as macroinitiator (Scheme 1). Table 1 summarizes the molecular characteristics of the synthesized copolymers. By changing the ratio of monomer to macroinitiator, three block copolymers with different pHPMAmDL block lengths (M_n from 3,000 to 13,600 g/mol, determined by ¹H NMR) and with a fixed PEG molecular weight ($M_n = 5,000$ g/mol) were obtained in yields between 75 and 80 %. In Chapter 2, it was shown that pHPMAmDL is a thermosensitive polymer with a cloud point (CP) around 10 °C in aqueous solution [24]. Consequently, it is expected that pHPMAmDL-*b*-PEG block copolymers can form micelles with hydrophilic PEG shells and hydrophobic pHPMAmDL cores above the CP of the pHPMAmDL blocks. The CMT of the block copolymers was determined by static light scattering. As shown in Table 1, the CMT decreased with increasing pHPMAmDL block lengths. A decreasing of CP with increasing molecular weight has also been observed for PNIPAAm [31] as well as for the homopolymer of HPMAmDL [24].

Table 1. Characteristics of pHPMAmDL-*b*-PEG block copolymers used in this study

Polymers	M_n ^{a)}	M_w ^{a)}	M_w/M_n	CMT (°C) ^{b)}	CMC (mg/mL) ^{c)}
pHPMAmDL(3000)- <i>b</i> -PEG ^{d)}	7400	10400	1.41	12.5	0.15
pHPMAmDL(6900)- <i>b</i> -PEG ^{d)}	11900	23300	1.95	7.5	0.03
pHPMAmDL(13600)- <i>b</i> -PEG ^{d)}	15000	32800	2.18	6.0	0.015

a) M_n = number average molar weight and M_w = weight average molar weight determined by GPC.

b) Determined by SLS at a concentration of 10 mg/mL in 120 mM ammonium acetate buffer (pH = 5.0).

c) Determined from pyrene excitation spectra for polymer solutions (Figure 2) in 120 mM ammonium acetate buffer (pH = 5.0) at 37 °C.

d) Number in brackets is M_n of pHPMAmDL block determined by ¹H NMR. M_n of PEG is 5,000 g/mol.

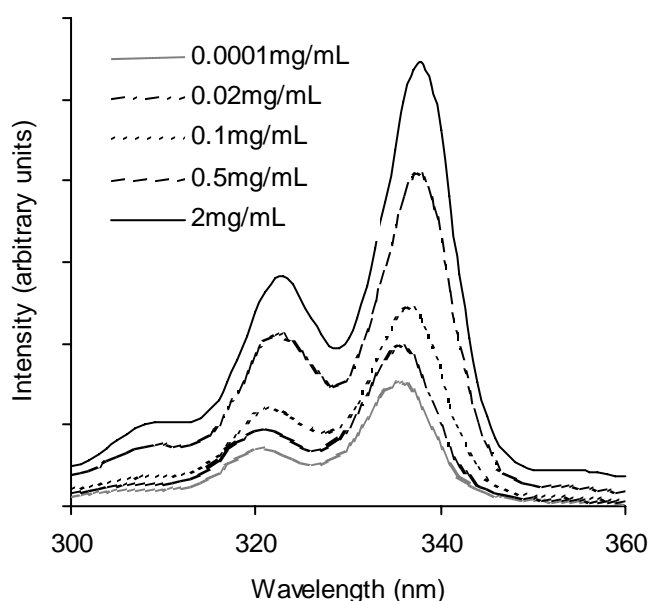


Figure 2. Fluorescence excitation spectra of pyrene (6.0×10^{-7} M) in 120 mM ammonium acetate buffer (pH = 5.0) containing pHPMAmDL(13600)-*b*-PEG at different concentrations. Emission wavelength = 390 nm.

The CMC of the block copolymers was determined using pyrene as a fluorescent probe. It is known that the fluorescent properties of pyrene largely depend on its microenvironment, and a red shift of the (0,0) band in its excitation spectra is observed when pyrene is partitioned from a hydrophilic to a more hydrophobic environment [28,32]. As shown in Figure 2, a red shift and intensity increase in the pyrene excitation spectra were observed with increasing

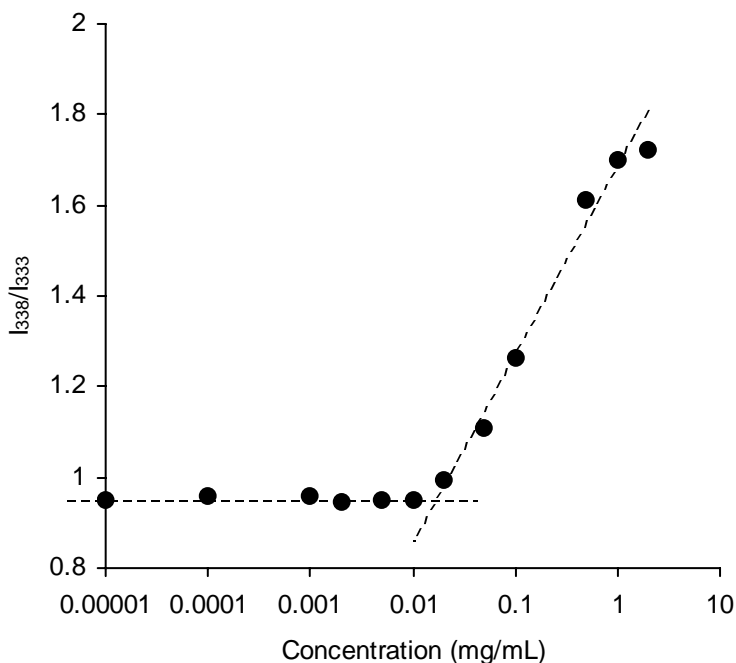


Figure 3. I_{338}/I_{333} ratio for pyrene as a function of the concentrations of pHPMAmDL(13600)-*b*-PEG. The CMC was taken from the intersection of the horizontal line at low polymer concentrations with the tangent of the curve at high polymer concentrations.

concentration of the pHPMAmDL-*b*-PEG block copolymer. The CMC could be accurately determined from the plot of the intensity ratio I_{338}/I_{333} as a function of the concentration of block copolymer (Figure 3). As expected, the CMC decreased with increasing pHPMAmDL block length (Table 1). The CMC values of pHPMAmDL(6900)-*b*-PEG and pHPMAmDL(13600)-*b*-PEG (0.03 and 0.015 mg/mL, respectively) are comparable to those of other amphiphilic block copolymers such as PBLA-*b*-PEG (0.005 to 0.018 mg/mL) [32,33] and PLA-*b*-PEG (0.0025 to 0.035 mg/mL) [34,35] which are appropriate for pharmaceutical applications. On the other hand, the CMC of pHPMAmDL(3000)-*b*-PEG is about 10-fold higher than those of the other two polymers, indicating an insufficient hydrophobicity of the pHPMAmDL(3000) block (containing ~10 monomer units of HPMAMDL) to form micelles at low concentration.

3.2. Characterization of micelles

It has been shown that the heating rate around the CMT is a critical parameter for the size of polymeric micelles based on thermosensitive polymers [27,36,37]. A rapid heating procedure favored the formation of small particles and was applied for the preparation of pHPMAmDL-*b*-PEG micelles. DLS

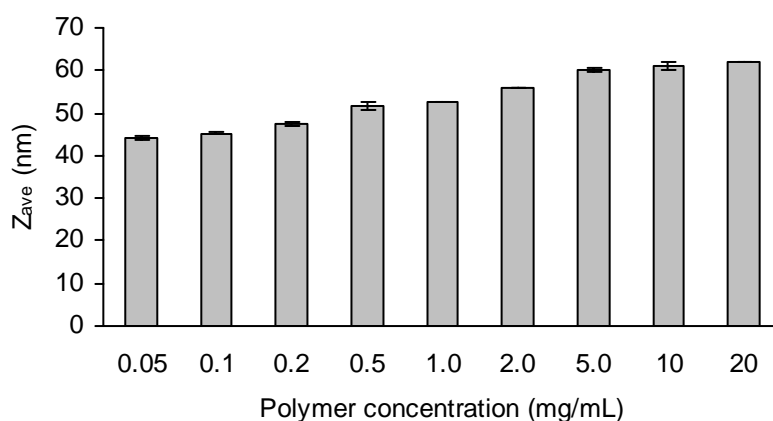


Figure 4. The effect of the polymer concentration on the size of pHPMAmDL(13600)-*b*-PEG micelles in isotonic 120 mM ammonium acetate buffer (pH = 5.0). The polydispersity index (PD) for the micelles was up to 10 mg/mL lower than 0.1; the PD for the micelles prepared at 20 mg/mL was 0.17. Data represent the mean and standard deviation of three independent experiments.

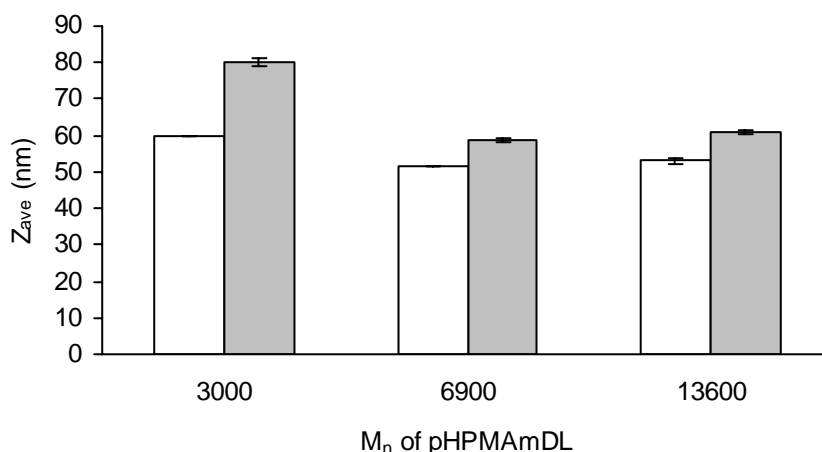


Figure 5. The effect of the pHPMAmDL block length on the size of pHPMAmDL-*b*-PEG micelles in isotonic 120 mM ammonium acetate buffer (pH = 5.0) at a concentration of 1 mg/mL (white bars) and 10 mg/mL (gray bars). Data represent the mean and standard deviation of three independent experiments.

measurements showed that micelles of pHPMAmDL(13600)-*b*-PEG with a size of 45 nm to 60 nm were obtained (Figure 4). During the formation of thermosensitive micelles upon heating, competition occurs between intrapolymer coil-to-globule transition (collapse) of the thermosensitive segments and interpolymer association. Smaller particles were formed with fast heating, owing to a rapid dehydration of the thermosensitive segments, and

therefore a collapse of these segments precedes the aggregation between polymers. As a result, micelles with well-defined core-shell structure are formed. In agreement with previous findings we found an increasing micelle size with increasing polymer concentration (Figure 4). This can be ascribed to higher probability of interpolymer aggregation at higher polymer concentration [27,36]. Figure 5 shows the effect of the pHPMAmDL block length on the size of micelles. pHPMAmDL(3000)-*b*-PEG formed, in particular at 10 mg/mL, larger micelles than the pHPMAmDL-*b*-PEG block copolymers with higher molecular weights of the thermosensitive segments. This observation is opposite to the results for PLA-*b*-PEG polymeric micelles, that showed a clear increase of their hydrodynamic diameter with increasing molecular weight of the PLA block [29]. As evidenced from static light scattering measurements (*vide infra*; Table 2), pHPMAmDL(3000)-*b*-PEG copolymers forms micelles with a rather low density likely due to relatively weak hydrophobic interactions of the low molecular weight pHPMAmDL, as also indicated by the high CMT and CMC values (Table 1).

The radius of gyration (R_g), and the weight average molecular weight ($M_{w(mic)}$) of the micelles composed of different block copolymers were determined by static light scattering (SLS) measurements at 37 °C (Table 2). The R_g/R_{hyd} ratio of pHPMAmDL-*b*-PEG micelles is between 0.59 and 0.80 and is in the same range as reported for other core-shell polymeric micelles [38-42]. Static light scattering measurements revealed that the aggregation number (N_{agg}) of pHPMAmDL(3000)-*b*-PEG micelles is 2-4 times lower than the N_{agg} of the other micelles. Despite this lower N_{agg} , DLS showed that pHPMAmDL(3000)-*b*-PEG micelles had the highest hydrodynamic radius (Figure 5 and Table 2). This indeed proves that the pHPMAmDL(3000) block is insufficiently hydrophobic to create a highly packed core structure and is reflected by a 10-20 fold lower ρ_{mic} value for the pHPMAmDL(3000)-*b*-PEG micelles than for the other systems. pHPMAmDL(6900/13600)-*b*-PEG micelles showed substantially higher ρ_{mic} and lower S/N_{agg} as compared to PLA-*b*-PEG with comparable molecular weights of both blocks and R_{hyd} . For example, PLA-*b*-PEG with M_n of PLA = 15,000 g/mol and M_n of PEG = 5,000 g/mol showed R_{hyd} = 25.3 nm, N_{agg} = 278, S/N_{agg} = 29 nm² and ρ_{mic} = 0.136 g/cm³ [29]. This indicates that pHPMAmDL(6900/13600)-*b*-PEG forms micelles with a quite dense core. Furthermore, the very low value of S/N_{agg} (7-13 nm²) for the pHPMAmDL(6900/13600)-*b*-PEG micelles demonstrates that their surfaces have a high PEG grafting density. This is a favorable property for drug delivery purposes, as it has been reported that colloidal particles showed increasing blood circulation times with increasing PEG surface grafting [35,43]. The low surface area for a PEG chain (S/N_{agg}) also indicates that PEG at the surface of pHPMAmDL(6900/13600)-*b*-PEG micelles exists in a highly stretched “brush” form.

Table 2. Characteristics of pHPMAmDL-*b*-PEG polymeric micelles at 10 mg/mL

Polymers	R_g ^{a)} (nm)	R_{hyd} ^{b)} (nm)	R_g/R_{hyd}	$M_{w(mic)}$ ^{a)} ($\times 10^6$ Da)	ρ_{mic} ^{c)} (g/cm ³)	N_{agg} ^{d)}	S/N_{agg} ^{e)} (nm ²)
pHPMAmDL(3000)- <i>b</i> -PEG	27 ± 1	40 ± 1	0.67 ± 0.04	3.3 ± 0.1	0.020	410	49.5
pHPMAmDL(6900)- <i>b</i> -PEG	17 ± 2	29 ± 1	0.59 ± 0.08	9.9 ± 0.2	0.16	830	12.7
pHPMAmDL(13600)- <i>b</i> -PEG	24 ± 2	30 ± 1	0.80 ± 0.08	32 ± 1	0.47	1720	6.6

a) R_g = radius of gyration of micelles, $M_{w(mic)}$ = weight average molecular weight of micelles determined by SLS.

b) R_{hyd} = hydrodynamic radius ($Z_{ave}/2$) of micelles determined by DLS.

c) ρ_{mic} = density of the micelles.

d) N_{agg} = aggregation number of the micelles.

e) S/N_{agg} = surface area per PEG chain.

See Materials and methods for the calculation of ρ_{mic} , N_{agg} and S/N_{agg} .

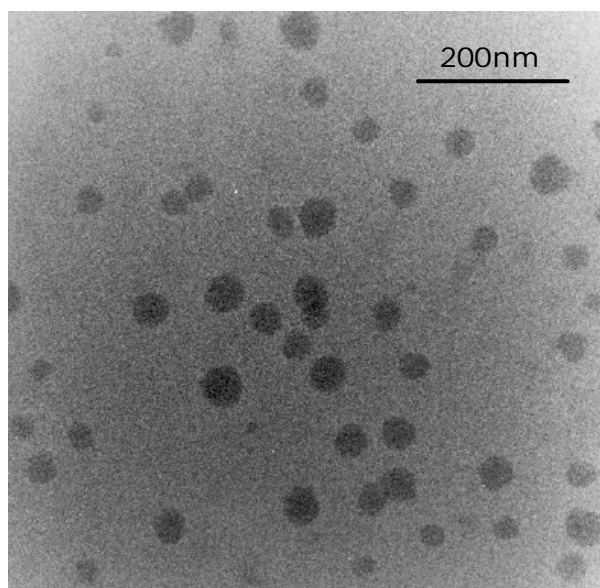


Figure 6. Cryo-TEM image of pHPMAmDL(13600)-*b*-PEG micelles. The polymer concentration was 10 mg/mL in 120 mM ammonium acetate buffer (pH = 5.0).

The morphology of pHPMAmDL(13600)-*b*-PEG micelles formed at 10 mg/mL was visualized by cryo-TEM. As shown in Figure 6, spherical structures with a narrow size distribution were observed. It should be noted that the outer PEG shells can not be seen with this technique because PEG is not electron-dense enough to be visualized without chemical staining. So, the observed spheres are the cores of the micelles that consist mainly of the pHPMAmDL block. The core size is between 25 nm and 50 nm and the average size is approximately 40 nm. The length of a PEG 5000 brush is 11.2 nm [44], suggesting that the average overall size of pHPMAmDL(13600)-*b*-PEG micelles is approximately 60 nm, which is in good agreement with the size as determined by DLS (Figure 4).

¹H NMR measurements were performed for pHPMAmDL(13600)-*b*-PEG in D₂O (10 mg/mL) below and above the CMT (Figure 7). This technique provides information on the mobility of polymer chains in aqueous solutions [29,45-47]. Below the CMT (1 °C), the intensity ratio of the peaks from pHPMAmDL block to the peak from PEG in D₂O was identical to that in CDCl₃, indicating that the pHPMAmDL chain is fully hydrated. On the other hand, above the CMT (37 °C), the peaks of the pHPMAmDL block almost completely disappeared while the intensity of signal of the PEG hydrogen atoms did not alter significantly (Figure 7). This indicates that the pHPMAmDL core of the micelles has a solid-like character. Around 20 % of the protons from the pHPMAmDL block can be still detected at 37 °C. Likely, pHPMAmDL segments adjacent to PEG and therefore located in the interfacial region of the core-shell structure of the micelles possess some flexibility and are therefore detectable with NMR [47].

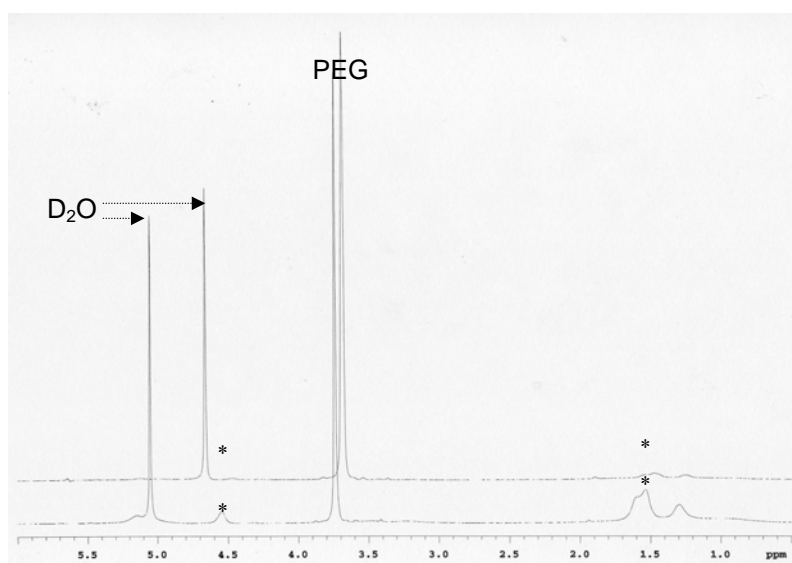


Figure 7. ^1H NMR spectra of pHPMAmDL(13600)-*b*-PEG in D_2O (10 mg/mL) at 1 °C (bottom) and at 37 °C (top). Asterisks represent peaks from pHPMAmDL blocks.

3.3. Mechanism of micelle formation

The mechanism of the micelle formation of pHPMAmDL(13600)-*b*-PEG block copolymer in aqueous solution was studied by FT-IR. Measurements were carried out for pHPMAmDL(13600)-*b*-PEG solutions at 30 mg/mL in D_2O at different temperatures below and above the CMT. The CMT of pHPMAmDL(13600)-*b*-PEG in D_2O at 30 mg/mL determined by SLS was 8.5 °C, while the CP in 120 mM ammonium acetate buffer was slightly lower (6.0 °C, Table 1), likely due to salting-out effects. Figure 8a shows the FT-IR spectra of the polymer in D_2O as a function of the temperature. As can be seen, some of the peaks are unaffected by changes in temperature, but the bands around 3400 cm^{-1} (N-H stretching vibration), 1735 cm^{-1} (C=O stretching), 1640 cm^{-1} (amide-I) and 1540 cm^{-1} (amide-II) shifted with temperature. Most striking are the changes of the amide-I and amide-II bands, showing from 2 to 50 °C a blue ($\Delta\nu = 5\text{ cm}^{-1}$) and a red ($\Delta\nu = 12\text{ cm}^{-1}$) shift, respectively (Figure 8b). A blue and red shift for the amide-I and amide-II vibrations has also been observed for PNIPAAm-*b*-PEG [21] and was explained by a change from hydrogen bonding of the amide groups with D_2O to intramolecular hydrogen bonding between amide groups above the CMT. The amide-I band exhibits the appearance of a shoulder at the low wavenumber side (1618 cm^{-1} ; marked with an asterisk in Figure 8a) at low temperatures, which disappears at high temperatures. A possible explanation is that below the CMT, the amide group of pHPMAmDL has rotational freedom and may occur in both the *cis* and *trans* conformation, whereas above the CMT the mobility of the polymer chain is restricted by which the amide group is essentially in the more stable *trans* conformation.

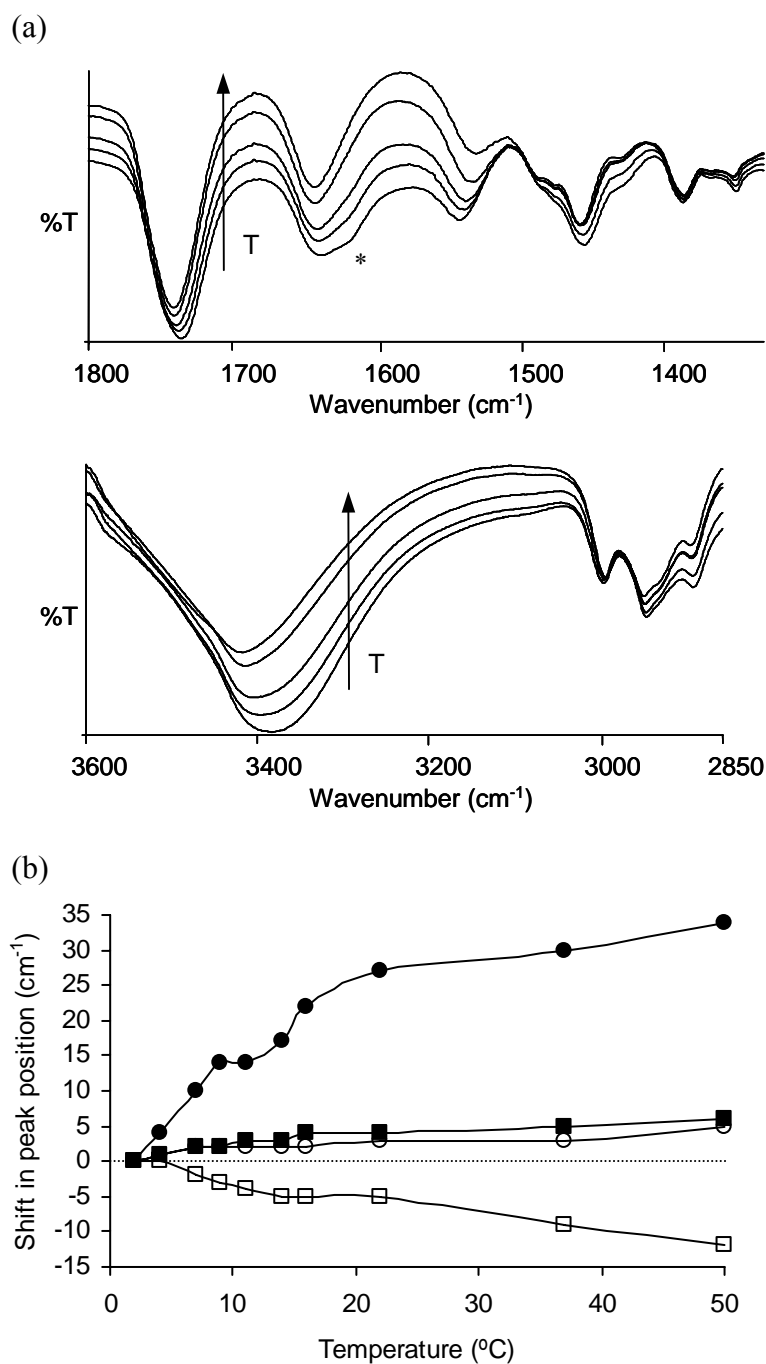


Figure 8. (a) FT-IR spectra of pHPMAmDL(13600)-*b*-PEG at 30 mg/mL in D₂O at different temperatures (50 °C, 37 °C, 16 °C, 9 °C and 2 °C from top to bottom, respectively). (b) The shift in peak position in FT-IR spectra as a function of temperature. The values are expressed as the difference of wavenumber compared to the peak position at 2 °C. Closed circles: N-H stretching (3382 cm⁻¹ at 2 °C); Closed squares: C=O stretching (1734 cm⁻¹ at 2 °C); Open circles: amide-I (1637 cm⁻¹ at 2 °C); Open squares: amide-II (1541 cm⁻¹ at 2 °C).

The observed peak position of the C=O stretching band of the lactic acid side groups (1734 to 1740 cm^{-1}) for pHPMAmDL(13600)-*b*-PEG in D_2O (above and below the CMT) is close to that for pHPMAmDL(13600)-*b*-PEG in the solid state (1744 cm^{-1}), but considerably higher than that of carbonyl groups that are subject to hydrogen bonding e.g. with D_2O (1710 to 1720 cm^{-1}) [48]. This indicates that even below the CMT the carbonyl groups of the lactic acid side groups in pHPMAmDL(13600)-*b*-PEG give no hydrogen bonding with D_2O . The peak around 3400 cm^{-1} , corresponding to the N-H stretching vibrations, is blue-shifted (34 cm^{-1} ; Figure 8b) by heating. This again points to a dehydration of the amide bond with temperature. When the polymer dissolved in D_2O solution was heated from 2 to 50 °C and subsequently cooled to 2 °C, its IR spectrum was identical to that of the non-heated polymer solution. This demonstrates that the temperature induced phase transition of pHPMAmDL-*b*-PEG is completely reversible.

*3.4. Destabilization of pHPMAmDL-*b*-PEG micelles*

As suggested in Chapter 2 [24], one of the attractive features of pHPMAmDL is that its CP increases in time because of hydrolysis of the lactate side groups of pHPMAmDL in aqueous medium, as observed for the copolymer of HPMAmDL and NIPAAm [23]. As a result, pHPMAmDL is converted to the more hydrophilic poly(HPMAm-monolactate) (pHPMAmML), which has its CP around 65 °C [24], and finally to the water-soluble pHPMAm. Accordingly, polymeric micelles of pHPMAmDL-*b*-PEG are expected to gradually destabilize when incubated at physiological conditions (pH 7.4, 37 °C). At pH 5, where the hydrolysis of lactic acid side group is minimized [23], the micelles were very stable over 60 hours (Figure 9). On the other hand, at pH 9, where the hydrolysis is enhanced by hydroxyl ions [23], the size of the micelles and the scattering intensity started to increase after 1.5 hour of incubation, probably due to hydrophilization and subsequent swelling of the core. The micelles started to dissociate after 4 hours, as indicated by the disappearance of scattering, and finally a clear solution was obtained. Obviously the lactic acid side groups were hydrolyzed to such an extent that the CP of the thermosensitive block passed 37 °C. Previously it was shown that the hydrolysis of lactic acid side groups is a first order reaction in hydroxyl ion concentration [23], which means that 1 hour at pH 9.0 corresponds to 40 hours at pH 7.4 (physiological pH). Thus, at physiological condition, the swelling of micelles is supposed to start at 60 hours, and the dissolution of micelles occurs in 160 hours.

Pyrene-loaded pHPMAmDL(13600)-*b*-PEG micelles were incubated at 37 °C and at pH 5.0 and 8.6. As shown in Figure 10, the I_{338}/I_{333} ratio of pyrene loaded into the micelles was constant at pH 5.0 over 12 hours at 37 °C, indicating that the polarity of the microenvironment of pyrene (the hydrophobic core of the

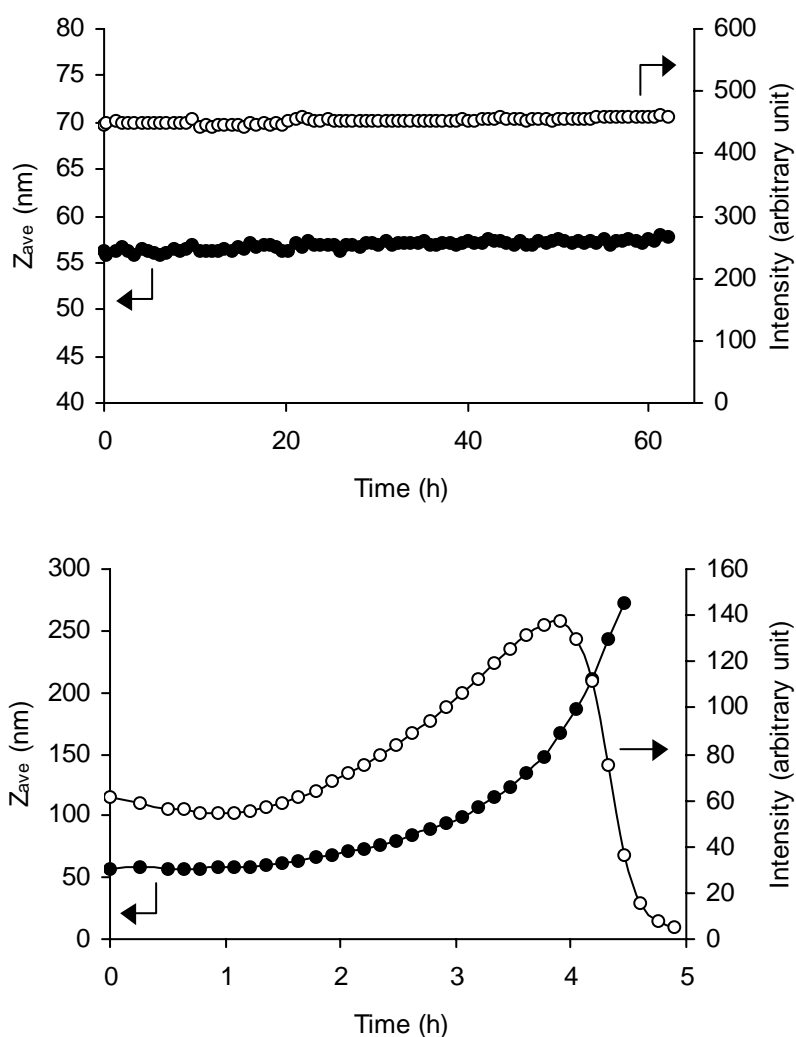


Figure 9. Stability of pHPMAmDL(13600)-*b*-PEG micelles at 37 °C and at pH 5.0 (top) and pH 9.0 (bottom), as determined by dynamic light scattering.

micelle) did not change in time. In contrast, the I_{338}/I_{333} ratio of pyrene in the micelles incubated at pH 8.6 decreased in time, indicating that the microenvironment of pyrene increased in polarity due to the ongoing hydrolysis of the lactic acid side groups and the resulting hydrophilization of the micellar core.

4. Conclusions

In this study, novel thermosensitive and biodegradable block copolymers, pHPMAmDL-*b*-PEG, were synthesized. Stable polymeric micelles with a size around 50 nm were obtained when aqueous solutions of pHPMAmDL(6900/13600)-*b*-PEG were heated above the CMT. ^1H NMR and static light scattering measurements demonstrate that the micelles have solid-

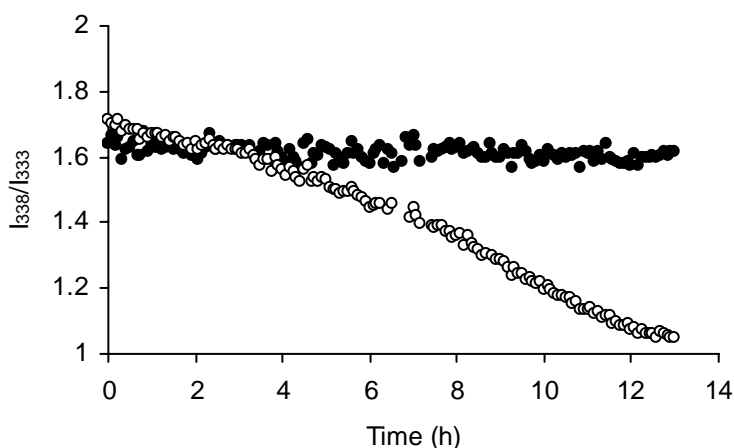


Figure 10. Change in emission spectra (I_{338}/I_{333} ratio) of pyrene solubilized in pHPMAmDL(13600)-*b*-PEG micelles at 37 °C and at pH 5.0 (closed circles) and pH 8.6 (open circles).

like and dense core structures and that the hydrophobic core is stabilized with a hydrophilic PEG corona. Importantly, it was found that pHPMAmDL-*b*-PEG micelles showed a controlled instability due to hydrolysis of the lactic acid side chains in the thermosensitive block. Furthermore, the dense and stable core of the micelles should allow the loading of hydrophobic drugs. These features, together with the simple preparation method, avoiding the use of organic solvents, make these micelles very suitable as delivery vehicles for hydrophobic drugs.

Acknowledgements

The authors thank Mitsubishi Pharma Corporation (Japan) for their financial support. The authors thank Dr Johan Kemmink for his assistance with the ^1H NMR measurements and Professor Kees de Kruif, Mr. Kees Olie man and Mr. Jan Klok from Nizo food research, Ede, The Netherlands, for their help in performing the light scattering measurements.

References

1. S. Forster, T. Plantenberg. *Angew Chem Int Ed Engl* 41 (2002) 689-714.
2. G. Riess. *Prog Polym Sci* 28 (2003) 1107-1170.
3. C. Allen, D. Maysinger, A. Eisenberg. *Colloids Surf B: Biointerfaces* 16 (1999) 3-27.
4. M.C. Jones, J.C. Leroux. *Eur J Pharm Biopharm* 48 (1999) 101-111.
5. K. Kataoka, A. Harada, Y. Nagasaki. *Adv Drug Deliv Rev* 47 (2001) 113-131.

6. G.S. Kwon. *Crit Rev Ther Drug Carrier Syst* 20 (2003) 357-403.
7. G.S. Kwon, M. Naito, M. Yokoyama, T. Okano, Y. Sakurai, K. Kataoka. *Pharm Res* 12 (1995) 192-195.
8. H. Maeda, J. Wu, T. Sawa, Y. Matsumura, K. Hori. *J Control Release* 65 (2000) 271-284.
9. G. Molineux. *Cancer Treat Rev* 28 (2002) 13-16.
10. M.C. Woodle, D.D. Lasic. *Biochim Biophys Acta* 1113 (1992) 171-199.
11. A.V. Kabanov, E.V. Batrakova, V.Y. Alakhov. *J Control Release* 82 (2002) 189-212.
12. M. Yokoyama, S. Fukushima, R. Uehara, K. Okamoto, K. Kataoka, Y. Sakurai, T. Okano. *J Control Release* 50 (1998) 79-92.
13. R.T. Liggins, H.M. Burt. *Adv Drug Deliv Rev* 54 (2002) 191-202.
14. R. Savic, L. Luo, A. Eisenberg, D. Maysinger. *Science* 300 (2003) 615-618.
15. Y.H. Bae, S. Fukushima, A. Harada, K. Kataoka. *Angew Chem Int Ed Engl* 42 (2003) 4640-4643.
16. J. Taillefer, M.C. Jones, N. Brasseur, J.E. van Lier, J.C. Leroux. *J Pharm Sci* 89 (2000) 52-62.
17. H.G. Schild. *Progress in Polymer Science* 17 (1992) 163-249.
18. R. Pelton. *Adv Colloid Interface Sci* 85 (2000) 1-33.
19. S. Fujishige, K. Kubota, I. Ando. *J Phys Chem* 93 (1989) 3311-3313.
20. M.D.C. Topp, P.J. Dijkstra, H. Talsma, J. Feijen. *Macromolecules* 30 (1997) 8518-8520.
21. Y. Maeda, N. Taniguchi, I. Ikeda. *Macromol Rapid Commun* 22 (2001) 1390-1393.
22. D. Neradovic, C.F. van Nostrum, W.E. Hennink. *Macromolecules* 34 (2001) 7589-7591.
23. D. Neradovic, M.J. van Steenberg, L. Vansteelant, Y.J. Meijer, C.F. van Nostrum, W.E. Hennink. *Macromolecules* 36 (2003) 7491-7498.
24. O. Soga, C.F. van Nostrum, W.E. Hennink. *Biomacromolecules* 5 (2004) 818-821.
25. J. Kopecek, P. Kopeckova, T. Minko, Z. Lu. *Eur J Pharm Biopharm* 50 (2000) 61-81.
26. R. Duncan. *Nat Rev Drug Discov* 2 (2003) 347-360.
27. D. Neradovic, O. Soga, C.F. van Nostrum, W.E. Hennink. *Biomaterials* 25 (2004) 2409-2418.
28. M. Wilhelm, C.L. Zhao, Y.C. Wang, R.L. Xu, M.A. Winnik, J.L. Mura, G. Riess, M.D. Croucher. *Macromolecules* 24 (1991) 1033-1040.
29. T. Riley, S. Stolnik, C.R. Heald, C.D. Xiong, M.C. Garnett, L. Illum, S.S. Davis, S.C. Purkiss, R.J. Barlow, P.R. Gellert. *Langmuir* 17 (2001) 3168-3174.
30. A. Moschetta, P.M. Frederik, P. Portincasa, G.P. vanBerge-Henegouwen, K.J. van Erpecum. *J Lipid Res* 43 (2002) 1046-1053.
31. E.I. Tiktopulo, V.N. Uversky, V.B. Lushchik, S.I. Klenin, V.E. Bychkova, O.B. Ptitsyn. *Macromolecules* 28 (1995) 7519-7524.
32. G. Kwon, M. Naito, M. Yokoyama, T. Okano, Y. Sakurai, K. Kataoka. *Langmuir* 9 (1993) 945-949.

33. S.B. La, T. Okano, K. Kataoka. *J Pharm Sci* 85 (1996) 85-90.
34. K. Yasugi, Y. Nagasaki, M. Kato, K. Kataoka. *J Control Release* 62 (1999) 89-100.
35. S.A. Hagan, A.G.A. Coombes, M.C. Garnett, S.E. Dunn, M.C. Davis, L. Illum, S.S. Davis, S.E. Harding, S. Purkiss, P.R. Gellert. *Langmuir* 12 (1996) 2153-2161.
36. P.W. Zhu, D.H. Napper. *Langmuir* 16 (2000) 8543-8545.
37. X.P. Qiu, C. Wu. *Macromolecules* 30 (1997) 7921-7926.
38. M.R. Talingting, P. Munk, S.E. Webber, Z. Tuzar. *Macromolecules* 32 (1999) 1593-1601.
39. H. Schuch, J. Klingler, P. Rossmanith, T. Frechen, M. Gerst, J. Feldthusen, A.H. Muller. *Macromolecules* 33 (2000) 1734-1740.
40. S. Dai, P. Ravi, C.Y. Leong, K.C. Tam, L.H. Gan. *Langmuir* 20 (2004) 1597-1604.
41. P. Ravi, C. Wang, K.C. Tam, L.H. Gan. *Macromolecules* 36 (2003) 173-179.
42. S. Pispas, N. Hadjichristidis, I. Potemkin, A. Khokhlov. *Macromolecules* 33 (2000) 1741-1746.
43. S. Stolnik, B. Daudali, A. Arien, J. Whetstone, C.R. Heald, M.C. Garnett, S.S. Davis, L. Illum. *Biochim Biophys Acta* 1514 (2001) 261-279.
44. D. Marsh, R. Bartucci, L. Sportelli. *Biochim Biophys Acta* 1615 (2003) 33-59.
45. J.S. Hrkach, M.T. Peracchia, A. Domb, N. Lotan, R. Langer. *Biomaterials* 18 (1997) 27-30.
46. Y. Yamamoto, K. Yasugi, A. Harada, Y. Nagasaki, K. Kataoka. *J Control Release* 82 (2002) 359-371.
47. C.R. Heald, S. Stolnik, K.S. Kujawinski, C. De Matteis, M.C. Garnett, L. Illum, S.S. Davis, S.C. Purkiss, R.J. Barlow, P.R. Gellert. *Langmuir* 18 (2002) 3669-3675.
48. L.J. Bellamy. *Advances in Infrared Group Frequencies*, Methuen, London (1968).

Chapter

4

Thermosensitive and biodegradable polymeric micelles for paclitaxel delivery

Osamu Soga, Cornelus F. van Nostrum, Marcel H.A.M. Fens,
Cristianne J.F. Rijcken, Raymond M. Schiffelers, Gert Storm
and Wim E. Hennink

Department of Pharmaceutics, Utrecht Institute for Pharmaceutical Sciences (UIPS),
Faculty of Pharmaceutical Sciences, Utrecht University, Utrecht, The Netherlands

Journal of Controlled Release 103 (2005) 341-353

Abstract

The preparation, release and *in vitro* cytotoxicity of a novel polymeric micellar formulation of paclitaxel (PTX) were investigated. The micelles consisted of an AB block copolymer of poly(*N*-(2-hydroxypropyl) methacrylamide lactate) and poly(ethylene glycol) (pHPMAmDL-*b*-PEG). Taking advantage of the thermosensitivity of pHPMAmDL-*b*-PEG, the loading was done by simple mixing of a small volume of a concentrated PTX solution in ethanol and an aqueous polymer solution and subsequent heating of the resulting solution above the critical micelle temperature of the polymer. PTX could be almost quantitatively loaded in the micelles up to 2 mg/mL. By dynamic light scattering and cryo-transmission electron microscopy, it was shown that PTX-loaded micelles have a mean size around 60 nm with narrow size distribution. At pH 8.8 and 37 °C, PTX-loaded micelles destabilized within 10 hours due to the hydrolysis of the lactic acid side group of the pHPMAmDL. Because the hydrolysis of the lactic acid side groups is first order in hydroxyl ion concentration, the micelles were stable for about 200 hours at physiological conditions. The presence of serum proteins did not have an adverse effect on the stability of the micelles during at least 15 hours. Interestingly, the dissolution kinetics of pHPMAmDL-*b*-PEG micelles was retarded by incorporation of PTX, indicating a strong interaction between PTX and the pHPMAmDL block. The PTX-loaded micelles showed a release of the incorporated 70 % of PTX during 20 hours at 37 °C and at pH 7.4. PTX-loaded pHPMAmDL-*b*-PEG micelles showed comparable *in vitro* cytotoxicity against B16F10 cells compared to the Taxol standard formulation containing Cremophor EL, while pHPMAmDL-*b*-PEG micelles without PTX were far less toxic than the Cremophor EL vehicle. Confocal laser-scanning microscopy (CLSM) and fluorescence activated cell sorting (FACS) analysis of fluorescently labeled micelles showed that pHPMAmDL-*b*-PEG micelles were internalized by the B16F10 cells. The present results suggest that pHPMAmDL-*b*-PEG block copolymer micelles are a promising delivery system for the parenteral administration of PTX.

1. Introduction

Polymeric micelles composed of amphiphilic block copolymers are currently extensively investigated as a novel type of drug carrier [1-5]. Polymeric micelles have a core-shell structure with a size typically between 10 and 60 nm in aqueous solution. The hydrophobic core has a large capacity to accommodate hydrophobic drugs in particular whereas the hydrophilic shell stabilizes the micelle structure. Their small size and hydrophilic surface enable polymeric micelles to oppose the recognition by macrophages of the mononuclear phagocyte system (MPS) after intravenous administration, which allows accumulation in e.g. tumor and other pathological areas due to the so-called EPR (enhanced permeation and retention) effect [6]. Furthermore, by use of stimuli-sensitive polymers (e.g. temperature, pH) as a segment of block copolymers, it is possible to achieve a controlled release of encapsulated drugs from micelles in response to environmental changes [7-10].

In Chapter 2, we reported on a novel class of biodegradable and thermosensitive polymers, poly(*N*-(2-hydroxypropyl) methacrylamide lactate) (poly(HPMAM-lactate)). Poly(HPMAM-lactate) showed a lower critical solution temperature (LCST) in aqueous solution and the cloud point (CP) can be well controlled between 10 to 65 °C by the length of the lactate side group (e.g. monolactate or dilactate) and copolymer composition [11]. In Chapter 3, it was shown that AB block copolymers of poly(HPMAM-dilactate) and poly(ethylene glycol) (pHPMAMDL-*b*-PEG) form polymeric micelles of around 50 nm with a dense core and a hydrophilic shell. It was further demonstrated that these polymeric micelles gradually dissolve due to hydrolysis of the lactic acid side groups [12]. This unique destabilization property may provide for a controlled release mechanism of drugs from pHPMAMDL-*b*-PEG polymeric micelles.

Paclitaxel (PTX) is an important anticancer drug used in clinical practice and exhibits strong cytotoxic activity against a variety of cancer types, especially breast and ovarian cancer [13]. Its cytotoxic activity is due to a stabilizing effect on the microtubule cytoskeleton by which cancer cells are arrested in its G2/M phase. PTX is a hydrophobic compound and therefore poorly soluble in water. To enhance its solubility, PTX is currently formulated as a 50:50 mixture of Cremophor EL (a polyethoxylated castor oil) and ethanol (Taxol®). However, the amount of Cremophor EL required to solubilize PTX is considerably high (26 mL of Cremophor EL for an average patient for a single intravenous administration dose [14]), which results in significant side effects such as hypersensitivity and hampers the clinical use of PTX. Therefore, alternatives for Cremophor EL to solubilize PTX are under current investigation and include polymeric micelles [15-24], emulsions [25-27], nanoparticles [28-30], dendrimers [31], hydrogels [32,33] and liposomes [34-36]. These carriers do not only solubilize PTX but also may give targeted delivery after intravenous administration due to the EPR effect [6].

In this study, we investigated PTX-loaded pHPMAmDL-*b*-PEG micelles regarding loading efficiency, morphology, release, stability, and *in vitro* cytotoxicity. To get insight into the mechanism of the cytotoxicity of the PTX-loaded micelles, CLSM and FACS studies with fluorescently labeled micelles were performed.

2. Materials and methods

2.1. Materials

N-(3-aminopropyl) methacrylamide hydrochloride (AMA) was from Polysciences, Inc. (Brunswick chemie, Warrington, PA). Rhodamine B isothiocyanate (RITC), Cremophor EL and sodium 3'-[1-(phenylaminocarbonyl)-3,4-tetrazolium]-bis(4-methoxy-6-nitro)benzene sulfonic acid hydrate (XTT) were from Sigma-Aldrich (St. Louis, MO, USA). HPMAm-dilactate was synthesized as described before [37]. Monomethyl ether of poly(ethylene glycol), MW 5,000 g/mol (PEG 5000) was from NEKTAR (San Carlos, CA, USA). The PEG₂-ABCPA macroinitiator with PEG 5000 was prepared as described previously [38]. A p(HPMAm-dilactate)-*b*-PEG block copolymer, (number average molar weight of p(HPMAm-dilactate) and PEG are 13600 and 5000 g/mol, respectively) was synthesized and characterized as described in Chapter 3 [12]. Paclitaxel (PTX) was purchased from MP Biomedicals, Inc. (Ohio, USA). Phosphate buffered saline (PBS, pH 7.4) was from B. Brawn Melsungen AG (Melsungen, Germany). Dulbecco's modification of Eagle's Medium (DMEM) was from Gibco BRL (Breda, The Netherlands). Fetal calf serum (FCS) was purchased from Integro B. V. (Dieren, The Netherlands) and was used after inactivation by heating at 56 °C for 30 minutes.

2.2. Paclitaxel (PTX) loading into pHPMAmDL-*b*-PEG micelles

PTX was dissolved in ethanol at concentrations of 5, 10, 20 and 40 mg/mL. pHPMAmDL-*b*-PEG was dissolved in isotonic 120 mM ammonium acetate buffer (pH = 5.0) at a concentration of 10 mg/mL at 0 °C (below the CMT of the polymer, which is 6.0 °C [12]). 0.2 mL of PTX dissolved in ethanol was added to 1.8 mL of the polymer solution (or PEG 5000 solution at 10 mg/mL or buffer as a control) at 0 °C. The resulting solutions contained 0.5, 1, 2 or 4 mg/mL PTX, 9 mg/mL pHPMAmDL-*b*-PEG (or 9 mg/mL PEG 5000) and 10 % (v/v) ethanol. The mixtures were immediately brought to 50 °C by soaking into a water bath to form micelles and to simultaneously load PTX into the hydrophobic core of the micelles. After 1 minute of incubation at 50 °C, the mixture was slowly cooled down to room temperature and the non-entrapped,

precipitated PTX was removed by filtration through a 0.45 μm filter (Schleicher & Schuell MicroScience GmbH, Dassel, Germany). The amount of PTX in the filtrate was determined by isocratic reverse-phase HPLC (Waters system, Waters Associates Inc., Milford, MA, USA) using a LiChroCART 125-4 RP-18 column (5 μm , 125 \times 4 mm i.d.). The mobile phase consisted of acetonitrile/water (50/50 w/w). The flow rate was 1.0 mL/min and the detection wavelength was 227 nm. The PTX samples were 1:1 diluted with acetonitrile and 100 μL was injected. A calibration curve was prepared for PTX dissolved in acetonitrile/water (50/50 w/w). The size of PTX-loaded micelles was measured by dynamic light scattering (DLS) at 25 $^{\circ}\text{C}$ as described in Chapter 3 [12].

2.3. Cryo-transmission electron microscopy (cryo-TEM)

PTX-loaded micelles (PTX = 1 mg/mL, polymer = 9 mg/mL) were prepared as described in Section 2.2. Sample preparation for cryo-TEM and microphotography were carried out as described in Chapter 3 [12].

2.4. Stability of PTX-loaded micelles

The stability of PTX-loaded micelles was monitored at two different pH's (7.4 and 8.8). For pH 7.4, PTX-loaded micelles (PTX = 1 mg/mL, polymer = 9 mg/mL) were prepared as described in Section 2.2 except that phosphate buffered saline (PBS, pH 7.4) instead of 120 mM ammonium acetate buffer (pH 5.0) was used, and then diluted 10-fold with PBS. For comparison, 10 μL of PTX at 1 mg/mL in ethanol was added to 1 mL PBS or water (concentration of PTX after dilution was 10 $\mu\text{g}/\text{mL}$). For pH 8.8, PTX-loaded micelles (PTX = 1 mg/mL, polymer = 9 mg/mL) were prepared with 120 mM ammonium acetate buffer (pH 5.0) and then diluted 10-fold with 300 mM NaHCO_3 buffer (pH 9.0). For comparison, non-loaded micelles were prepared by adding ethanol to the polymer solution. Both the size of micelles and the intensity of scattered light were measured at 37 $^{\circ}\text{C}$ as a function of time using DLS.

The stability of the micelles in the presence of serum was also studied. Non-loaded pHPMAmDL-*b*-PEG micelles were formed as described in Section 2.2. To 0.4 mL of this micellar solution, 0.4 mL PBS and 0.2 mL FCS were added. The concentration of polymer and serum in the resulting solution were 0.4 mg/mL and 20 % (v/v), respectively. The size of micelles and the intensity of scattered light were measured at 37 $^{\circ}\text{C}$ as a function of time by DLS.

2.5. In vitro release of PTX from PTX-loaded micelles

The *in vitro* release of PTX from PTX-loaded pHPMAmDL-*b*-PEG micelles was evaluated by a dialysis method. PTX-loaded micelles (PTX = 1 mg/mL, polymer = 9 mg/mL) were prepared with 120 mM ammonium acetate buffer (pH 5.0) and were diluted 10-fold with PBS. Then 1.5 mL of the diluted solution

was placed into a pre-swollen dialysis bag with a 3,500 g/mol molecular weight cut-off (Spectra/Por® 3 dialysis membrane, Spectrum Laboratories, Inc.) and immersed into 500 mL PBS at 37 °C. When 100 % of PTX is released into the medium, the concentration of PTX is 0.3 µg/mL, which is equal to the solubility of PTX in water at 25 °C. Dialysis was performed at 37 °C for 20 hours with gentle stirring and the amount of PTX released into medium was measured after 0, 1, 2, 3, 5 and 20 hours. After 20 hours, the amount of PTX remaining in the dialysis bag was also measured. The PTX concentration in the different samples was determined by HPLC as described in Section 2.2.

2.6. Synthesis of rhodamine B isothiocyanate (RITC)-labeled pHPMAmDL-*b*-PEG

pHPMAmDL-*b*-PEG labeled with a fluorescent compound (RITC) was synthesized as follows. First, pHPMAmDL-*b*-PEG containing 1 mol % AMA with respect to HPMAm-dilactate (further abbreviated as p(HPMAmDL-*co*-AMA)-*b*-PEG) was synthesized by radical polymerization using HPMAm-dilactate and AMA as monomers (HPMAm-dilactate/AMA = 100:1 (mol/mol)) and PEG₂-ABCPA as initiator. In detail, HPMAm-dilactate and PEG₂-ABCPA were dissolved at a total concentration of 0.3 g/mL (total volume 3.6 mL) in acetonitrile. An aqueous solution of AMA (0.36 mL, concentration 14.9 mg/mL) was added and the copolymerization was conducted at 70 °C for 20 hours in a nitrogen atmosphere. The polymer was collected by centrifugation after precipitation in diethyl ether. After dissolving the polymer in cold water, low molecular weight impurities were removed by dialysis (Spectra/Por® 3 dialysis membrane with a 3,500 g/mol molecular weight cut-off, Spectrum Laboratories, Inc.) against 5 mM ammonium acetate buffer (pH 5.0) for 40 hours and then against water for 10 hours at 4 °C. The purified polymer was filtrated through a 0.22 µm filter and freeze-dried. The number average molecular weight of the p(HPMAmDL-*co*-AMA) block, as determined by ¹H NMR [12], was 7,800 g/mol.

To couple the fluorescent probe RITC to p(HPMAmDL-*co*-AMA)-*b*-PEG, the polymer was dissolved in PBS. Next, RITC (one equivalent with respect to AMA) dissolved in the same buffer was added (final polymer concentration was 50 mg/mL). The reaction was conducted at 0 °C for 20 hours. Free RITC was removed by dialysis (Slide-A-Lyzer dialysis membrane with a 10,000 g/mol molecular weight cut-off, Pierce, Rockford, IL, USA) against water for 4 days at 4 °C. The purified polymer was filtrated through a 0.22 µm filter and frozen until use. This polymer is further abbreviated as p(HPMAmDL-*co*-AMA-RITC)-*b*-PEG.

2.7. Confocal laser-scanning microscopy (CLSM) analysis

Polymeric micelles were formed from p(HPMAmDL-*co*-AMA-RITC)-*b*-PEG at 10 mg/mL in water in the same way as described in Section 2.2 for pHPMAmDL-*b*-PEG micelles. Then, the micelles were diluted with PBS to 1, 0.1, 0.01 and 0.001 mg/mL. Beside the fluorescent labeled micelles, non-labeled micelles (pHPMAmDL-*b*-PEG at 1 mg/mL) and a PBS control were evaluated. 2×10^4 B16F10 (melanoma carcinoma) cells/well were seeded in a 16-well confocal slide, 24 hours before adding samples. 100 μ L of the samples and 100 μ L culture medium (DMEM + 10 % FCS) were added per well and the cells were incubated at 37 °C and in 5 % CO₂ for 1 or 24 hours. After aspiration of the samples, the wells were washed twice with PBS. Finally the cells were fixed with formalin (2 %)/glutaraldehyde (0.1 %) for 30 minutes, washed again with PBS and mounted with Fluorsave™ at room temperature. The fixed cells were analyzed on a Leica TCS-SP confocal laser scanning microscope equipped with a 488 nm argon, 568 nm krypton and 647 nm HeNe laser.

2.8. Fluorescence activated cell sorting (FACS) analysis

B16F10 cells were seeded in a 24-well plate (5×10^4 cells per well) 24 hour prior to the experiment. Solutions of p(HPMAmDL-*co*-AMA-RITC)-*b*-PEG micelles in PBS were prepared at 1, 0.1, 0.01 and 0.001 mg/mL as described in Section 2.7. 1 mL of each sample was added to the cells and 1 mL of culture medium was added. As controls, cells incubated with 1 mL PBS plus 1 mL culture medium and cells incubated with 2 mL culture medium were measured. 1, 4 and 24 hours after incubation at 37 °C and 5 % CO₂, the sample and culture medium were aspirated and the cells were washed with cold 1 % BSA in PBS to remove extracellular/non-associated micelles and subsequently with PBS. Next, a trypsin/EDTA solution (0.05 % (w/v)) was added to bring the adherent cells into suspension. After 10 minutes at 37 °C, 1 mL 1 % BSA in PBS was added. After centrifugation (5 min, $300 \times g$), the supernatant was removed and the cell-pellet was resuspended in 0.4 mL 1 % BSA in PBS (4 °C) and put on ice. Fluorescence activated cell sorting (FACS) analysis was performed on a FACS Calibur (Becton Dickinson). 10,000 cells per sample were counted and WinMDI (version 2.8) was used for data analysis.

2.9. In vitro cytotoxicity studies

B16F10 cells were seeded in a 96-well plate at a density of 5×10^3 cells per well, 24 hours before the *in vitro* cytotoxicity studies started. PTX-loaded micelles (PTX = 1 mg/mL, polymer = 9 mg/mL) and non-loaded micelles (polymer = 9 mg/mL) were prepared with PBS as described in Section 2.2. For comparison, PTX solubilized in Cremophor EL (Taxol) was prepared according to Lee et al [19]. In detail, 12 mg of PTX was dissolved in 1.0 mL ethanol and to this

solution 1.0 mL Cremophor EL was added. Then this mixture was sonicated for 30 minutes. The obtained Taxol formulation (PTX = 6 mg/mL) was diluted 6-fold with PBS. A control formulation without PTX was prepared using ethanol instead of PTX/ethanol. The four stock solutions were further stepwise diluted with PBS to give PTX concentrations ranging from 0.0001 to 100 $\mu\text{g/mL}$. To evaluate their cytotoxic effects, 100 μL of the different PTX formulations and 100 μL culture medium (DMEM + 10 % FCS) were added to the cells. As a reference, 100 μL PBS and 100 μL culture medium (DMEM + 10 % FCS) were added. The cells were incubated for 72 hours at 37 $^{\circ}\text{C}$ in a humidified atmosphere with 5% CO_2 . After incubation, the number of viable cells was determined using a XTT colorimetric assay [39].

3. Results and Discussion

3.1. Loading of PTX into pHPMAmDL-*b*-PEG micelles

In Chapter 3 it was shown that pHPMAmDL-*b*-PEG (Figure 1) forms polymeric micelles in aqueous solution above its critical micelle temperature (CMT) and that the physical characteristics of the micelles (size, core density, CMC, CMT etc.) depend on the length of the hydrophobic pHPMAmDL block [12]. Among the three investigated block copolymers with different pHPMAmDL molecular weight, the one with the largest pHPMAmDL block (number average molar weight of pHPMAmDL and PEG are 13,600 and 5,000 g/mol, respectively) is the best candidate for drug loading and further *in vivo* application for the following reasons. Firstly, this polymer had the lowest CMC value (0.015 mg/mL) [12]. Secondly, polymeric micelles composed of this polymer had the highest density of PEG chains at their surface [12], which is favourable for prolonged circulation in the bloodstream after intravenous administration [40,41]. Thirdly, a large hydrophobic block is generally associated with a good loading capacity of hydrophobic drugs [19,42]. To prepare PTX-loaded pHPMAmDL-*b*-PEG micelles, PTX dissolved in ethanol was added to an aqueous polymer solution below the CMT and then quickly heated above the CMT (50 $^{\circ}\text{C}$). An opalescent and homogenous solution was obtained (Figure 2).

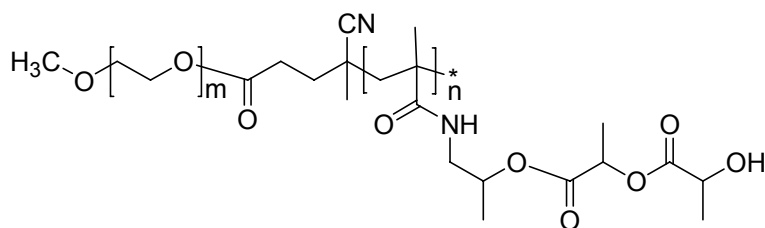


Figure 1. Chemical structure of pHPMAmDL-*b*-PEG block copolymer.

However, when PTX dissolved in ethanol was added to either a PEG 5000 solution or buffer and the resulting solutions were heated to 50 °C, large precipitates were observed. After filtration through a 0.45 µm filter (to remove possible PTX precipitates), HPLC analysis showed that PTX was almost quantitatively retained in the pHPMAmDL-*b*-PEG micellar solution (Table 1). On the other hand, only a trace amount of PTX remained in the PEG 5000 solution and buffer after filtration. The concentration of PTX for the latter samples (1.2 and 1.5 µg/mL) is slightly higher than the solubility of PTX in water (0.3 µg/mL) [43], which is probably due to the presence of 10 % (v/v) ethanol. The average size of the PTX-loaded micelles was 60 nm with a low polydispersity according to DLS, similar to the size of empty micelles [12]. These results demonstrate that pHPMAmDL-*b*-PEG micelles efficiently solubilize PTX. Moreover, the loading of the micelles can easily be done by heating an aqueous solution of the thermosensitive pHPMAmDL-*b*-PEG to which a small volume PTX in ethanol is added. This loading method is simple as compared to the loading of e.g. micelles/nanoparticles based on PDLLA-*b*-PEG where large amounts of organic solvents are used, which have to be removed by dialysis or evaporation [15,16,28].

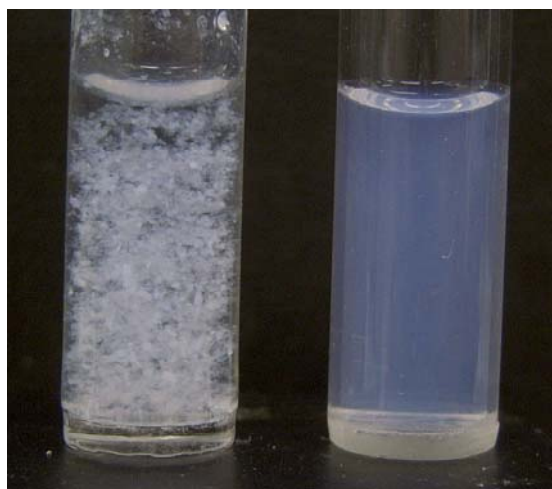


Figure 2. PTX dissolved in ethanol and added to a solution of PEG 5000 (left) and pHPMAmDL-*b*-PEG micelles (right). The concentrations of PTX and polymer are 1 mg/mL and 9 mg/mL, respectively. The mixtures were incubated at 50 °C for 1 minute and then were cooled down to room temperature.

Table 1. Paclitaxel (PTX) loading into pHPMAmDL-*b*-PEG micelles

	PTX + buffer	PTX + PEG 5000	PTX + pHPMAmDL- <i>b</i> -PEG
PTX feed (mg/mL)	1.0	1.0	1.0
Polymer (mg/mL)	-	9.0	9.0
PTX solubilized (mg/mL)	0.0015	0.0012	0.96
% solubilized	0.15%	0.12%	96%
Z_{ave} (PD)	-	-	60 nm (0.04)

Figure 3 shows the relationship between the amount of PTX initially added to the block copolymer solution and the solubilized amount of PTX. Nearly 100 % of PTX was solubilized up to 2 mg/mL, which was associated with a slight increase in the size of the micelles (64 nm as compared to 60 nm for the non-loaded micelles). At 4 mg/mL the loading efficiency was very low (10 % of the initially added PTX amount). Likely, at this high PTX concentration, not enough polymer was added to solubilize the PTX resulting in the formation of PTX aggregates. The solubilized PTX concentration of 2 mg/mL is considerably higher than achieved with other polymeric micellar systems [18,21-24], whereas the loading capacity (22 % (w/w)) of the pHPMAmDL-*b*-PEG micelles is comparable with that found for methoxy poly(ethylene glycol)-*b*-poly(D,L-lactide) (25 % (w/w)), which is the most successful alternative formulation for PTX in terms of solubilization efficiency [15]. Besides hydrophobic interactions between hydrophobic lactate groups of pHPMAmDL block and apolar portions

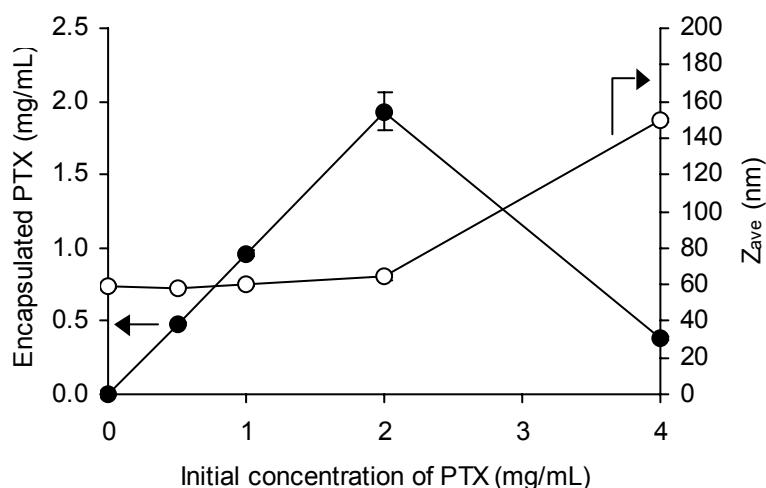


Figure 3. The effect of the initial concentration of PTX on the encapsulated PTX into pHPMAmDL-*b*-PEG micelles (closed circles) and the size of PTX-loaded micelles (open circles). Data represent the mean and standard deviation of two to three independent experiments.

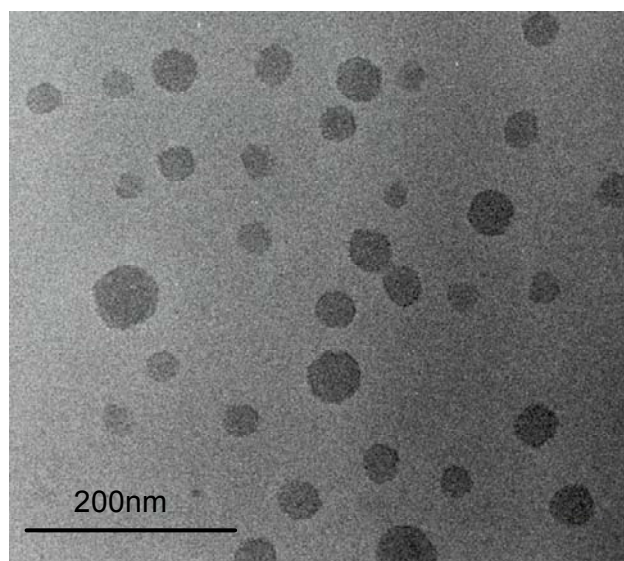


Figure 4. Cryo-TEM image of PTX-loaded pHPMAmDL-*b*-PEG micelles. The concentration of PTX and polymer were 1 mg/mL and 9 mg/mL, respectively.

of PTX, the formation of hydrogen bonds between OH groups of the lactate side chain of pHPMAmDL block and the polar segments of PTX might be an important factor contributing to the good solubilization capacity of the pHPMAmDL-*b*-PEG micelles, as reported by Lee et al. for the solubilization of papaverine by poly(lactide)-*b*-PEG block copolymer containing carboxylic acid groups [44].

The morphology of PTX-loaded micelles (PTX = 1 mg/mL, polymer = 9 mg/mL) was evaluated by cryo-TEM. As shown in Figure 4, PTX-loaded micelles have a spherical shape with a relatively narrow size distribution between 25 and 60 nm, which is consistent with the size as determined with DLS (Table 1). It should be noted that the PEG shell can not be seen in this image because of its low electron density. The size and morphology of the PTX-loaded pHPMAmDL-*b*-PEG micelles is almost identical to that of non-loaded micelles [12]. Furthermore, no large aggregates (e.g. larger than 200 nm) were observed, indicating that the dispersion of PTX-loaded micelles does not contain any (micro) precipitates of PTX.

3.2. Stability of PTX-loaded pHPMAmDL-b-PEG micelles

In Chapter 3, it was shown that pHPMAmDL-*b*-PEG micelles have a pH dependent stability [12]. At physiological conditions (pH 7.4, 37 °C), the micelles were stable for more than 60 hours, whereas at pH 9.0 almost quantitative hydrolysis of lactic acid side groups occurred within 1.5 hours. Hydrolysis of the lactic acid side groups was associated with a hydrophobic to hydrophilic conversion of the pHPMAmDL core in time yielding the water-

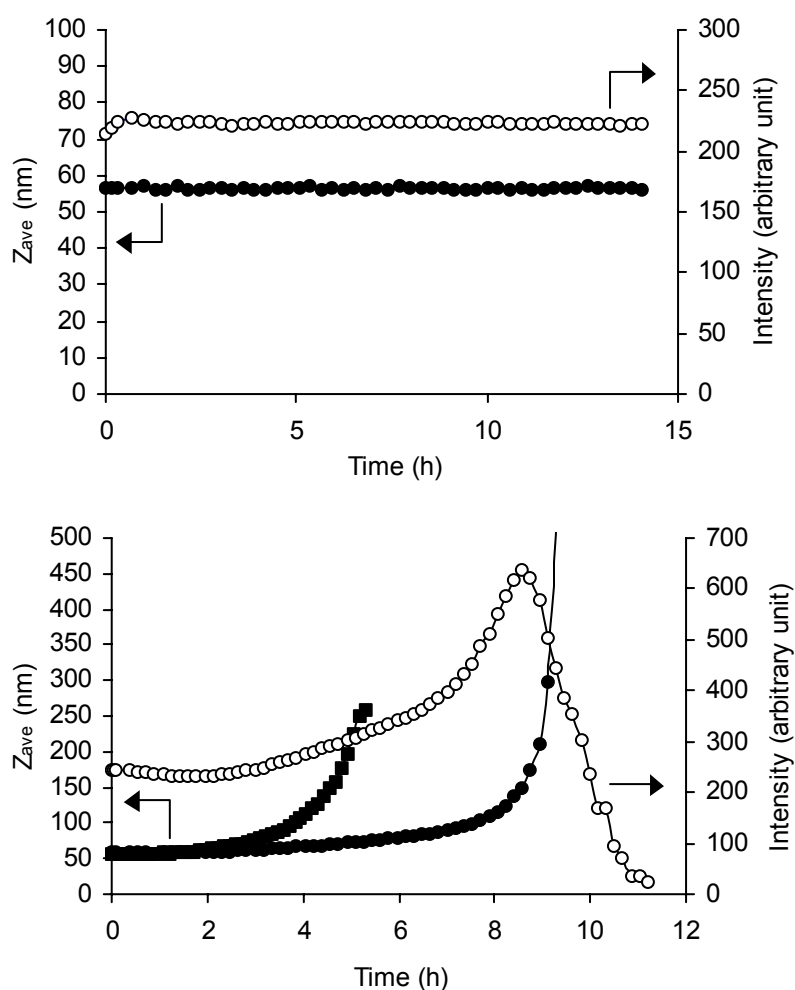


Figure 5. Size (Z_{ave}) and scattering intensity as a function of time of PTX-loaded and empty pHPMAmDL-*b*-PEG micelles at 37 °C and at pH 7.4 (top) and pH 8.8 (bottom), as measured by DLS. Closed circles: Z_{ave} of PTX-loaded pHPMAmDL-*b*-PEG micelles; Open circles: scattering intensity of PTX-loaded pHPMAmDL-*b*-PEG micelles; Closed squares: Z_{ave} of non-loaded pHPMAmDL-*b*-PEG micelles.

soluble pHPMAm-*b*-PEG block copolymer [12,37]. Therefore, it was studied whether pH-induced destabilization of the micelles is associated with release of PTX. Figure 5 shows that, at pH 7.4 and 37 °C, the size of PTX-loaded micelles and the intensity of the scattered light were stable over 14 hours at 37 °C while formation of PTX precipitates was not observed. When 10 μ L of PTX at 1 mg/mL in ethanol was added to 1 mL PBS or water, significant precipitation of PTX was observed. Therefore it can be concluded that PTX is stably incorporated in the micelles at 37 °C and at pH 7.4. Figure 5 also shows that, if PTX micelles were subjected to accelerated degradation conditions (pH 8.8, 37 °C), the intensity of scattered light started to gradually increase after approximately 4 hours of incubation, to reach a maximum at 9 hours, and

thereafter the signal dropped to almost zero. Simultaneously, the size substantially increased after 8 hours of incubation. This behavior points to swelling and dissolution of the micelles due to hydrolysis of the lactic acid side groups as observed in Chapter 3 for empty and pyrene-loaded micelles [12]. After 14 hours fluffy precipitate particles were observed at the bottom of the cuvette. Empty micelles completely dissolved after 6 hours with no precipitate formation, which means that the precipitates observed after dissolution of the PTX-loaded micelles were due to PTX. This means that the decrease of the intensity of scattered light after 8 hours is a result of sedimentation of PTX aggregates. The hydrolysis of lactic acid side groups is a first order reaction in hydroxyl ion concentration [37]. Therefore, at physiological conditions (pH 7.4, 37 °C), the destabilization of the PTX-loaded micelles is expected after 200 hours of incubation. Indeed, we observed that incubation of PTX-loaded micelles at pH 7.4 and 37 °C resulted in a drastic increase of size after 210 hours, which is in very good agreement with the predicted time (results not shown). Due to hydrolysis of the lactic acid side groups, pHPMAM-*b*-PEG is formed. Since the blocks are connected via a hydrolysable ester bond, this will result in the formation of pHPMAM and PEG. pHPMAM as such is non-degradable, but elimination via the kidneys is expected once applied *in vivo* because its molecular weight is below the renal threshold ($M < 45,000$ g/mol [45]).

Figure 5 also shows that the swelling and dissolution of the micelles was significantly delayed in case of the PTX-loaded micelles as compared to the empty micelles. This indicates that the core of micelles is stabilized by PTX and can be explained by a decrease of the dielectric constant of the microenvironment in the core due to the presence of PTX and/or a decreased accessibility of water to the core. Indeed, it was demonstrated previously that the hydrolysis of lactic acid ester slows down with decreasing dielectric constant of the environment [46]. Alternatively, the core of the micelle is held together by hydrophobic interactions between the (partly hydrolyzed) pHPMAMDL and PTX.

For *in vivo* application, it is important that polymeric micelles have low interactions with blood components to slow down rapid uptake by the macrophages in the MPS in liver and spleen. Also, the CLSM, FACS and *in vitro* cytotoxicity studies performed with pHPMAMDL-*b*-PEG micelles were carried out in the presence of serum proteins (see Sections 2.7, 2.8 and 2.9). Therefore, the stability of the micelles was also studied in the presence of serum. It was shown that, at a polymer concentration of 4 mg/mL and in the presence of serum (20 % (v/v)), the average size of the micelles was the same as in buffer (60 nm). Moreover, the size of the micelles and the intensity of scattered light were stable at 37 °C for 15 hours, indicating that neither aggregation nor destabilization induced by serum proteins occurred (data not shown).

pHPMA_{DL}-*b*-PEG micelles have a rather high density of PEG chains (the surface area per PEG chain is 6.6 nm²) [12]. Thus, the size stability of the micelles in serum is likely to be attributed to their highly hydrophilic surface, which protects them from non-specific adsorption of serum components.

3.3. *In vitro* release of PTX from PTX-loaded micelles

In the previous section, it was shown that PTX was stably encapsulated in the micelles at relatively high concentrations at physiological temperature and pH. However, *in vivo* administration will result in sink conditions, which may result in the release of the drug from the micelles. Therefore, *in vitro* release of PTX from micelles at 37 °C in PBS (pH 7.4) was evaluated by a dialysis method. The total volume of the aqueous phase was chosen such that when PTX was released quantitatively its concentration was below its solubility in water (0.3 µg/mL). As shown in Figure 6, 40 % and 70 % of PTX was released after 5 hours and 20 hours, respectively. After 20 hours 5 % of the initial PTX was found to remain inside the dialysis bag. Therefore, some adsorption of PTX onto the glass wall or the dialysis bag could have occurred. The release of PTX from micelles upon dilution is probably controlled by diffusion as a result of partitioning between the core and the aqueous phase rather than by the destabilization of the micelles. It can be calculated that the volume ratio of micellar phase/aqueous phase during dialysis is 5.7×10^{-6} , based on the hydrodynamic radius (30 nm) and molecular weight (3.2×10^7 Da) of pHPMA_{*b*}-PEG micelles [12].

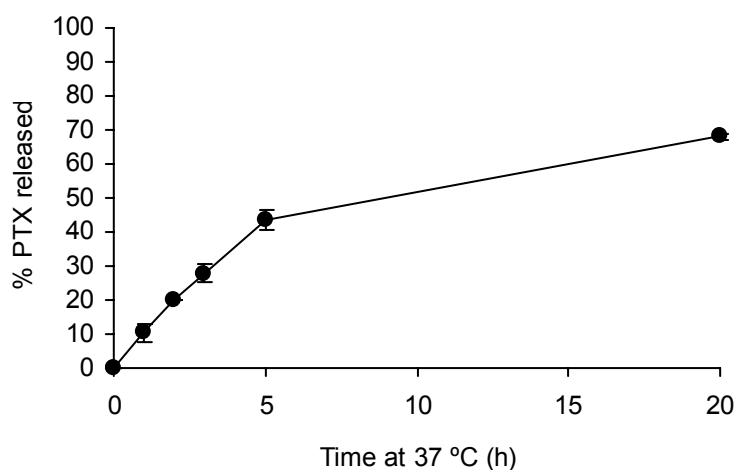


Figure 6. *In vitro* release of PTX from pHPMA_{DL}-*b*-PEG micelles. Data represent the mean and standard deviation of three independent experiments.

*3.4. Cellular internalization of pHPMAmDL-*b*-PEG micelles*

The internalization of polymeric micelles into cells was recently reported [47-49]. In this study, the internalization of pHPMAmDL-*b*-PEG labeled with rhodamine B isothiocyanate (p(HPMAmDL-*co*-AMA-RITC)-*b*-PEG) into B16F10 cells was evaluated by CLSM and FACS analysis. CLSM analysis showed strong fluorescent signals inside the cells after incubation with the labeled micelles at 37 °C for 1 hour (Figure 7). The fluorescence was localized in the cytoplasm and not in the nucleus. Cytoplasmic localization was also observed by Savic et al. for poly(caprolactone)-*b*-PEG micelles [47] and is different from cell membrane localization of Pluronic P-105 micelles [49]. These results indicate that pHPMAmDL-*b*-PEG micelles are internalized by cells. FACS analysis showed that this cellular uptake is time- and concentration-dependent (Figure 8). The internalization of pHPMAmDL-*b*-PEG micelles may occur via fluid state endocytosis rather than via interaction with the outer cell membrane, since the PEG shell of the pHPMAmDL-*b*-PEG micelles is expected to shield them from binding to the negatively charged cell surface.

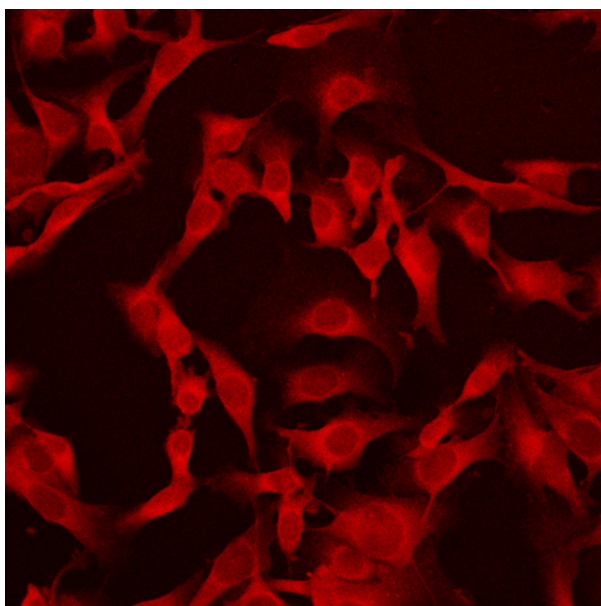


Figure 7. CLSM-imaged B16f10 cellular internalization of p(HPMAmDL-*co*-AMA-RITC)-*b*-PEG micelles after incubation at 37 °C for 1 hour. The polymer concentration in the incubation medium was 1 mg/mL.

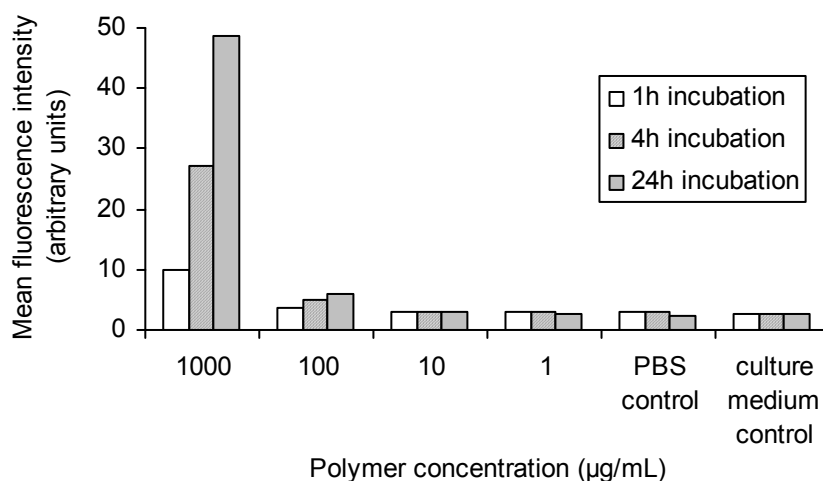


Figure 8. Effect of incubation time and polymer concentration on cell-associated p(HPMAmDL-*co*-AMA-RITC)-*b*-PEG micelles.

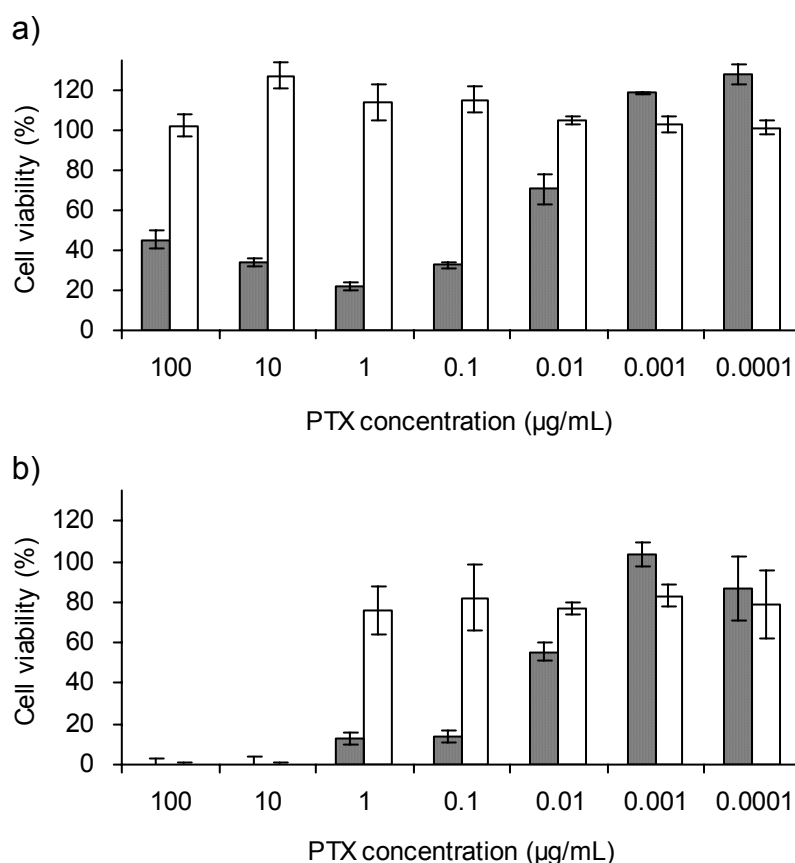


Figure 9. *In vitro* cytotoxicity of PTX-loaded pHPMAmDL-*b*-PEG micelles (a) and Taxol (b) on B16F10 cells after 72 hours of incubation. Left (gray) bars: formulation with PTX. Right (white) bars: control formulation without PTX. Data represent the mean and standard deviation of three independent experiments.

3.5. In vitro cytotoxic effect of PTX-loaded micelles

The cytotoxicity of PTX-loaded micelles was studied *in vitro* with cultured B16F10 melanoma cells. For comparison, the cytotoxicity of empty micelles, Taxol and its vehicle (Cremophor EL/ethanol = 50/50 (v/v), further abbreviated as Taxol vehicle) was also evaluated. As shown in Figure 9, empty micelles did not show any toxicity even at the highest concentration tested, while the Taxol vehicle showed strong cytotoxicity, in agreement with previous observations [19,30]. Therefore, it can be expected that also *in vivo* pHPMAmDL-*b*-PEG micelles are far less toxic than the Taxol vehicle, which may allow the administration of PTX-loaded micelles at higher drug dose than PTX formulated in the Taxol vehicle. The PTX-loaded micelles showed comparable cytotoxic activity as PTX formulated with Cremophor EL/ethanol, indicating that PTX remains biologically active after incorporation into pHPMAmDL-*b*-PEG micelles. Taxol showed a strong cytotoxicity at 10 and 100 $\mu\text{g/mL}$, but this is apparently due to the Cremophor EL vehicle rather than PTX. In contrast, for PTX-loaded micelles, it is obvious that the cytotoxicity is solely due to PTX. The polymer concentration for pHPMAmDL-*b*-PEG micelles at 1 $\mu\text{g/mL}$ of PTX was 0.009 mg/mL, which is lower than its CMC (0.015 mg/mL) [12]. Therefore, at and below this concentration, the cytotoxicity is likely due to the PTX, which was taken up by cells in its free form. At higher concentrations above the CMC of the polymer, PTX can be taken up by cells either after its extracellular release from the micelles or in its micellar form, as suggested by the results shown in Section 3.4. At present it is not clear which mechanism is responsible for the observed cytotoxicity.

4. Conclusions

This study demonstrates that PTX can be loaded into pHPMAmDL-*b*-PEG micelles up to 2 mg/mL by a simple mixing of a PTX solution in ethanol with an aqueous polymer solution, followed by a heating step. Release of PTX was induced by the pH-dependent destabilization of the micelles at relatively high concentration of PTX, while dialysis against a large volume of water induced the release of PTX by diffusion. PTX-loaded micelles showed comparable cytotoxicity as Taxol against B16F10 cells. On the other hand, the empty micelles were far less toxic than the Cremophor EL vehicle, which is beneficial for *in vivo* applications. pHPMAmDL-*b*-PEG were stable in the presence of serum protein. These features (large solubilization capacity of PTX, a simple preparation method, small size around 60 nm and size stability) make pHPMAmDL-*b*-PEG micelles an attractive vehicle for parenteral PTX delivery.

Acknowledgements

The authors thank Dr. Peter M. Frederik and Mr. Paul H.H. Bomans at University Maastricht for cryo-TEM measurements and Mitsubishi Pharma Corporation (Japan) for their financial support.

References

1. C. Allen, D. Maysinger, A. Eisenberg. *Colloids Surf B: Biointerfaces* 16 (1999) 3-27.
2. M.C. Jones, J.C. Leroux. *Eur J Pharm Biopharm* 48 (1999) 101-111.
3. K. Kataoka, A. Harada, Y. Nagasaki. *Adv Drug Deliv Rev* 47 (2001) 113-131.
4. G.S. Kwon. *Crit Rev Ther Drug Carrier Syst* 20 (2003) 357-403.
5. C.F. van Nostrum. *Adv Drug Deliv Rev* 56 (2004) 9-16.
6. H. Maeda, J. Wu, T. Sawa, Y. Matsumura, K. Hori. *J Control Release* 65 (2000) 271-284.
7. Y. Bae, S. Fukushima, A. Harada, K. Kataoka. *Angew Chem Int Ed Engl* 42 (2003) 4640-4643.
8. J. Taillefer, M.C. Jones, N. Brasseur, J.E. van Lier, J.C. Leroux. *J Pharm Sci* 89 (2000) 52-62.
9. J.E. Chung, M. Yokoyama, T. Okano. *J Control Release* 65 (2000) 93-103.
10. F. Kohori, K. Sakai, T. Aoyagi, M. Yokoyama, M. Yamato, Y. Sakurai, T. Okano. *Colloids Surf B: Biointerfaces* 16 (1999) 195-205.
11. O. Soga, C.F. van Nostrum, W.E. Hennink. *Biomacromolecules* 5 (2004) 818-821.
12. O. Soga, C.F. van Nostrum, A. Ramzi, T. Visser, F. Soulimani, P.M. Frederik, P.H. Bomans, W.E. Hennink. *Langmuir* 20 (2004) 9388-9395.
13. E.K. Rowinsky, R.C. Donehower. *N Engl J Med* 332 (1995) 1004-1014.
14. H. Gelderblom, J. Verweij, K. Nooter, A. Sparreboom. *Eur J Cancer* 37 (2001) 1590-1598.
15. R.T. Liggins, H.M. Burt. *Adv Drug Deliv Rev* 54 (2002) 191-202.
16. S.C. Kim, D.W. Kim, Y.H. Shim, J.S. Bang, H.S. Oh, S.W. Kim, M.H. Seo. *J Control Release* 72 (2001) 191-202.
17. V.P. Torchilin, A.N. Lukyanov, Z. Gao, B. Papahadjopoulos-Sternberg. *Proc Natl Acad Sci U S A* 100 (2003) 6039-6044.
18. Z. Gao, A.N. Lukyanov, A.R. Chakilam, V.P. Torchilin. *J Drug Target* 11 (2003) 87-92.
19. S.C. Lee, C. Kim, I.C. Kwon, H. Chung, S.Y. Jeong. *J Control Release* 89 (2003) 437-446.
20. A. Miwa, A. Ishibe, M. Nakano, T. Yamahira, S. Itai, S. Jinno, H. Kawahara. *Pharm Res* 15 (1998) 1844-1850.
21. G. Cavallaro, M. Licciardi, G. Giammona, P. Caliceti, A. Semenzato, S. Salmaso. *J Control Release* 89 (2003) 285-295.
22. A. Krishnadas, I. Rubinstein, H. Onyuksel. *Pharm Res* 20 (2003) 297-302.

23. J.H. Kim, K. Emoto, M. Iijima, Y. Nagasaki, T. Aoyagi, T. Okano, Y. Sakurai, K. Kataoka. *Polym Adv Technol* 10 (1999) 647-654.
24. H. Alkan-Onyuksel, S. Ramakrishnan, H.B. Chai, J.M. Pezzuto. *Pharm Res* 11 (1994) 206-212.
25. L. He, G.L. Wang, Q. Zhang. *Int J Pharm* 250 (2003) 45-50.
26. P.P. Constantinides, K.J. Lambert, A.K. Tustian, B. Schneider, S. Lalji, W. Ma, B. Wentzel, D. Kessler, D. Worah, S.C. Quay. *Pharm Res* 17 (2000) 175-182.
27. B.B. Lundberg. *J Pharm Pharmacol* 49 (1997) 16-21.
28. Y. Dong, S.S. Feng. *Biomaterials* 25 (2004) 2843-2849.
29. L. Mu, S.S. Feng. *J Control Release* 86 (2003) 33-48.
30. C. Fonseca, S. Simoes, R. Gaspar. *J Control Release* 83 (2002) 273-286.
31. T. Ooya, J. Lee, K. Park. *J Control Release* 93 (2003) 121-127.
32. G.M. Zentner, R. Rathi, C. Shih, J.C. McRea, M.H. Seo, H. Oh, B.G. Rhee, J. Mestecky, Z. Moldoveanu, M. Morgan, S. Weitman. *J Control Release* 72 (2001) 203-215.
33. E. Ruel-Gariepy, M. Shive, A. Bichara, M. Berrada, D. Le Garrec, A. Chenite, J.C. Leroux. *Eur J Pharm Biopharm* 57 (2004) 53-63.
34. A. Sharma, R.M. Straubinger. *Pharm Res* 11 (1994) 889-896.
35. M. Schmitt-Sody, S. Strieth, S. Krasnici, B. Sauer, B. Schulze, M. Teifel, U. Michaelis, K. Naujoks, M. Dellian. *Clin Cancer Res* 9 (2003) 2335-2341.
36. P. Crosasso, M. Ceruti, P. Brusa, S. Arpicco, F. Dosio, L. Cattel. *J Control Release* 63 (2000) 19-30.
37. D. Neradovic, M.J. van Steenberg, L. Vansteelant, Y.J. Meijer, C.F. van Nostrum, W.E. Hennink. *Macromolecules* 36 (2003) 7491-7498.
38. D. Neradovic, C.F. van Nostrum, W.E. Hennink. *Macromolecules* 34 (2001) 7589-7591.
39. D.A. Scudiero, R.H. Shoemaker, K.D. Paull, A. Monks, S. Tierney, T.H. Nofziger, M.J. Currens, D. Seniff, M.R. Boyd. *Cancer Res* 48 (1988) 4827-4833.
40. S.A. Hagan, A.G.A. Coombes, M.C. Garnett, S.E. Dunn, M.C. Davis, L. Illum, S.S. Davis, S.E. Harding, S. Purkiss, P.R. Gellert. *Langmuir* 12 (1996) 2153-2161.
41. S. Stolnik, B. Daudali, A. Arien, J. Whetstone, C.R. Heald, M.C. Garnett, S.S. Davis, L. Illum. *Biochim Biophys Acta* 1514 (2001) 261-279.
42. B.S. Lele, J.C. Leroux. *Polymer* 43 (2002) 5595-5606.
43. J. Lee, S.C. Lee, G. Acharya, C.J. Chang, K. Park. *Pharm Res* 20 (2003) 1022-1030.
44. J. Lee, E.C. Cho, K. Cho. *J Control Release* 94 (2004) 323-335.
45. L.W. Seymour, R. Duncan, J. Strohmalm, J. Kopecek. *J Biomed Mater Res* 21 (1987) 1341-1358.
46. S.J. de Jong, E.R. Arias, D.T.S. Rijkers, C.F. van Nostrum, J.J. Kettenes-van den Bosch, W.E. Hennink. *Polymer* 42 (2001) 2795-2802.
47. R. Savic, L. Luo, A. Eisenberg, D. Maysinger. *Science* 300 (2003) 615-618.
48. X. Shuai, T. Merdan, A.K. Schaper, F. Xi, T. Kissel. *Bioconjug Chem* 15 (2004) 441-448.

49. N. Rapoport. *Int J Pharm* 277 (2004) 155-162.

Chapter 5

In vivo efficacy of paclitaxel-loaded
thermosensitive biodegradable polymeric micelles

Osamu Soga, Cornelus F. van Nostrum, Cor J. Snel, Marcel H.A.M. Fens,
Raymond M. Schiffelers, Gert Storm and Wim E. Hennink

Department of Pharmaceutics, Utrecht Institute for Pharmaceutical Sciences (UIPS),
Faculty of Pharmaceutical Sciences, Utrecht University, Utrecht, The Netherlands

Manuscript in preparation

Abstract

The *in vivo* biodistribution and therapeutic efficacy of novel thermosensitive and biodegradable polymeric micelles loaded with paclitaxel (PTX) were investigated. The micelles are composed of an AB block copolymer of poly(*N*-(2-hydroxypropyl)methacrylamide dilactate) and poly(ethylene glycol) (pHPMAmDL-*b*-PEG). These block copolymers self-assemble into micellar structures above the cloud point temperature (around 10 °C) of the thermosensitive pHPMAmDL block. The hydrophobic core of the micelles was loaded with the hydrophobic drug PTX by adding a small volume of a concentrated PTX solution in ethanol to a cold polymer solution, followed by heating of the resulting solution. When administered intravenously into rats, empty pHPMAmDL-*b*-PEG micelles showed prolonged blood circulation time with 20 % of the injected dose in the bloodstream after 24 hours. Liver was the major organ involved in the clearance of pHPMAmDL-*b*-PEG micelles (36 % of the injected dose after 24 hours). The uptake of the micelles by spleen and lung was low (3.7 % and 0.8 % of the injected dose after 24 hours, respectively). These characteristics are likely due to their small size of approximately 60 nm and their hydrophilic PEG corona. In contrast to empty micelles, PTX that was loaded into pHPMAmDL-*b*-PEG micelles was cleared quite rapidly after intravenous administration in mice (0.9 % of the injected PTX remained in the circulation after 1 hour). This suggests that PTX was not stably associated with the micelles, but was e.g. extracted from the micelles by plasma proteins such as albumin. The therapeutic efficacy of PTX-loaded pHPMAmDL-*b*-PEG micelles was evaluated in mice with B16F10 melanoma carcinoma after intravenous administration and in mice with OVCAR-3 human ovarian carcinoma after intraperitoneal administration. PTX-loaded pHPMAmDL-*b*-PEG micelles showed comparable *in vivo* antitumor efficacy as the standard Cremophor EL formulation of paclitaxel (Taxol®) both after intravenous and intraperitoneal administration. The results indicate that pHPMAmDL-*b*-PEG block copolymer micelles are interesting candidates as a delivery system for the parenteral administration of PTX and other hydrophobic cytostatics.

1. Introduction

Paclitaxel (PTX) is an anticancer drug with a unique mechanism of action. It stabilizes the microtubule cytoskeleton by promoting the assembly of tubulin dimers and therefore arrests cancer cells in their G2/M phase [1]. PTX is known to be highly effective against various types of cancers and has been used for the treatment of ovarian, breast and non-small cell lung cancers [2,3]. Because of its extremely low solubility in water, the commercially available formulation of PTX (Taxol®) consists of a non-aqueous 50:50 mixture of Cremophor EL (a polyethoxylated castor oil) and ethanol to solubilize PTX. However, Cremophor EL causes adverse side effects such as hypersensitivity reactions and it therefore limits the clinical use of PTX [4,5]. To overcome these unwanted side effects and to enhance the therapeutic effect of PTX, a number of new formulations have been developed and some of them such as CT-2103 (a PTX-polyglutamate conjugate [6]) and ABI-007 (an albumin-stabilized PTX nanoparticle [7]) are clinically evaluated at present.

In recent years, polymeric micelles have been extensively investigated as formulation vehicles for PTX [8-12]. Polymeric micelles are self-assembled nanostructures consisting of amphiphilic block copolymers which in aqueous solution form a core-shell structure. The hydrophobic core has a large capacity to solubilize hydrophobic drugs, while the hydrophilic shell stabilizes the micelle structure. Their relatively small size (typically between 10 to 60 nm) and hydrophilic surface allow polymeric micelles prolonged circulation in the bloodstream after intravenous administration by opposing the recognition by macrophages of the mononuclear phagocyte system (MPS), which results in the accumulation of polymeric micelles in e.g. tumor and other pathological areas due to the so-called EPR (enhanced permeation and retention) effect [13]. These features make polymeric micelles promising carriers for hydrophobic drugs [14-17]. Clinical results of polymeric micellar formulations of PTX and doxorubicin have been reported recently [18,19].

In Chapter 3 we reported on a novel class of biodegradable and thermosensitive polymeric micelles, which consists of an AB block copolymer of poly(*N*-(2-hydroxypropyl) methacrylamide dilactate) and poly(ethylene glycol) (pHPMAmDL-*b*-PEG, structure see Figure 1). It was demonstrated that these polymeric micelles gradually destabilize due to hydrolysis of the lactic acid side groups [20]. In Chapter 4 it was shown that PTX-loaded micelles could be obtained using a simple process (mixing a polymer solution and a concentrated PTX in ethanol and subsequent heating [21]) by taking advantage of the thermosensitivity of the pHPMAmDL block. The loading capacity for PTX was high (22 % (w/w)) and the loading was quantitative. Furthermore, we demonstrated that the empty micelles were not toxic to B16F10 cells and that

the micellar PTX formulation was equally effective *in vitro* as compared to Taxol [21].

In this study, we investigated the *in vivo* biodistribution and antitumor efficacy of PTX-loaded pHPMAmDL-*b*-PEG micelles in comparison with Taxol to evaluate the utility of this novel micelle type to deliver a hydrophobic anticancer drug.

2. Materials and methods

2.1. Materials

Two pHPMAmDL-*b*-PEG polymers with different number average molecular weights of the pHPMAmDL block, pHPMAmDL(6900)-*b*-PEG and pHPMAmDL(13600)-*b*-PEG, and a fixed molecular weight of PEG (5,000 g/mol) were synthesized as described in Chapter 3 [20]. pHPMAmDL-*b*-PEG containing 1 mol % *N*-(3-aminopropyl) methacrylamide hydrochloride (AMA) with respect to HPMAm-dilactate, (p(HPMAmDL-*co*-AMA)-*b*-PEG, number average molecular weight of p(HPMAmDL-*co*-AMA) block and PEG were 7,800 and 5,000 g/mol, respectively) was synthesized by a radical polymerization of HPMAm-dilactate and AMA using PEG macroinitiator [21]. Paclitaxel (PTX) was purchased from MP Biomedicals, Inc. (Ohio, USA). Taxol® was from Bristol-Myers Squibb (Princeton, NJ, USA). Cremophor EL was obtained from Sigma-Aldrich Co. (St. Louis, MO, USA). *N*-succinimidyl[2,3-³H]-propionate ([³H]-NSP) solution in toluene, activity 1 mCi/mL, was from Amersham Biosciences (USA). Phosphate buffered saline (PBS, pH 7.4) was from B. Brawn Melsungen AG (Melsungen, Germany). [¹⁴C]-labeled paclitaxel was purchased from Campro Sci. BV (Veenendaal, The Netherlands).

2.2. Paclitaxel (PTX) loading into pHPMAmDL-*b*-PEG micelles

The formation of pHPMAmDL-*b*-PEG micelles with and without PTX loading was performed as described in Chapter 4 [21]. Briefly, PTX was dissolved in ethanol at a concentration of 20 mg/mL. pHPMAmDL-*b*-PEG was dissolved in cooled (0 °C) PBS at a concentration of 10 mg/mL. Then, 0.2 mL of the PTX solution was added to 1.8 mL of the polymer solution. The resulting solution contained 2 mg/mL PTX, 9 mg/mL pHPMAmDL-*b*-PEG and 10 % (v/v) ethanol. Next, the solution was rapidly heated to 50 °C to form the PTX-loaded micelles. This quick heating procedure gives micelles with small size [22]. After 1 minute of incubation at 50 °C, the mixture was slowly cooled down to room temperature and the non-entrapped precipitated PTX was removed by filtration through a 0.45 µm filter (Schleicher & Schuell MicroScience GmbH, Dassel,

Germany). The amount of PTX in the filtrate was determined by isocratic reverse-phase HPLC [21]. The size of PTX-loaded micelles was measured by dynamic light scattering (DLS) at 25 °C.

2.3. Labeling of p(HPMAmDL-co-AMA)-b-PEG block copolymer with [³H]-NSP
The labeling of polymer with [³H]-NSP was performed essentially as described for proteins [23]. In detail, p(HPMAmDL-co-AMA)-b-PEG was dissolved in 0.1 M sodium borate buffer (pH 8.0) at 0 °C and at a concentration of 1.0 mg/mL. Next, 200 µL [³H]-NSP in toluene (approximately 7 to 8 MBq) was pipetted into an Eppendorf vial. Toluene was evaporated under a nitrogen stream at room temperature during 30-60 minutes and 200 µL of the polymer solution was added. The mixture was stirred for 1 hour at 0 °C and thereafter dialyzed at 4 °C against 150 mL PBS, using a dialysis cassette with a 10,000 g/mol molecular weight cut-off membrane (Slide-A-Lyzer® dialysis cassette, Pierce). The dialysate was checked for radioactivity and refreshed after 1, 3, 5 and 24 hours. The radioactivity of the different samples was determined using a liquid scintillation counter (Philips PW 4700, The Netherlands) and Ultima Gold scintillation cocktail (Packard BioScience B.V., Groningen, The Netherlands).

2.4. Biodistribution studies of empty pHPMAmDL-b-PEG micelles in rats
The formulation was prepared by mixing tritium labeled p(HPMAmDL-co-AMA)-b-PEG in PBS with non-labeled pHPMAmDL(6900)-b-PEG which was dissolved in PBS at a concentration of 20 mg/mL at 0 °C. In detail, tritium labeled p(HPMAmDL-co-AMA)-b-PEG in PBS was added to the pHPMAmDL(6900)-b-PEG solution so that the radioactivity and the polymer concentration of the final solution were 250 to 500 KBq/mL and 10 mg/mL, respectively. The micelles were formed by quickly heating this solution from 0 °C to 50 °C after which the solution was cooled down to room temperature [20]. Male rats (Wistar HsdCpb:wu, Harlan, The Netherlands) weighing 220-240 g were used for the biodistribution studies. Five hundred µL of radioactively labeled micelles (concentration of 10 mg/mL, corresponding to a dose of 5 mg/rat) was intravenously administered into the tail vein of the rats. Each formulation was injected into four rats. Under slight ether anesthesia, 150 µL blood samples were taken at 5 min, 1 hour, 2 hours, 4 hours, 8 hours and 24 hours after injection and a trace amount of heparin was added to prevent coagulation. After 24 hours the rats were euthanized, and the major organs (liver, spleen, kidneys, lungs) were collected. The blood samples (100 µL) were mixed with 100 µL Solvable tissue sollubilizer (Perkin Elmer, The Netherlands) and were incubated at 50 °C for 24 hours. Subsequently, 0.2 mL 0.5 M EDTA and 0.25 mL 35 % hydrogen peroxide aqueous solution were added to decolorize the samples. The excess of hydrogen peroxide was inactivated by heating the

samples at 50 °C overnight. After mixing with 10 mL of Ultima Gold scintillation cocktail, the radioactivity was measured. The organs were dissolved in 0.5 mL (lung, kidney and spleen) or 1.0 mL (liver) Solvable tissue solubilizer at 50 °C for 1 to 3 days. Then, the solution was decolorized with 0.1 to 0.5 mL 35 % hydrogen peroxide until the solution turned to pale yellow. The inactivation of hydrogen peroxide and the measurement of the radioactivity were performed in the same way as described above for the blood samples.

2.5. Biodistribution studies of PTX-loaded pHPMAmDL-b-PEG micelles in tumor bearing mice

A radioactive polymer solution was prepared by mixing ³H-labeled p(HPMAmDL-co-AMA)-b-PEG with non-labeled pHPMAmDL(13600)-b-PEG as described in Section 2.4. A radioactive PTX solution was prepared as follows. Ten µL of [¹⁴C]- PTX (500 KBq) in ethyl acetate was pipetted into a glass scintillation vial and the solvent was evaporated under a nitrogen stream at room temperature. Next, 0.5 mL non-labeled PTX (20 mg/mL) in ethanol was added to dissolve the [¹⁴C]- PTX. Double labeled (¹⁴C-drug and ³H-polymer) PTX-loaded pHPMAmDL-b-PEG micelles were prepared as described in Section 2.2. Taxol containing radioactive PTX was prepared as follows. Ten µL of [¹⁴C]-PTX (500 KBq) in ethyl acetate was pipetted into a glass scintillation vial and the solvent was evaporated under a nitrogen stream at room temperature. Then, 2 mL Taxol was added to dissolve [¹⁴C]- PTX and 4 mL PBS was added to yield a final PTX concentration of 2 mg/mL.

The biodistribution studies were carried out in male mice (C57bl/6JOlaHsd, Harlan, The Netherlands) bearing B16F10 melanoma cells. 100 µL B16F10 cells (1×10^6 cells per mouse) were inoculated into mice subcutaneously in the left flank at day 0. At day 11, the mice received tail vein injections with labeled PTX-loaded pHPMAmDL-b-PEG micelles or labeled Taxol at a PTX dose of 20 mg/kg. For both formulations the concentration of PTX was 2 mg/mL and the volume was around 200 µL, depending on the weight of the mice. Blood samples and the major tissues (liver, spleen, kidneys, lungs and tumor) were collected after 1 hour and 24 hours and the radioactivity was measured as described in Section 2.4.

2.6. Antitumor efficacy of PTX-loaded pHPMAmDL-b-PEG micelles after i.v. injection

PTX-loaded pHPMAmDL(13600)-b-PEG micelles were prepared as described in Section 2.2. Non-loaded pHPMAmDL(13600)-b-PEG micelles (empty micelles) were prepared by adding ethanol to the polymer solution instead of PTX dissolved in ethanol. Taxol was diluted three times with PBS to give a final PTX concentration of 2 mg/mL. The antitumor efficacy of *i.v.* administered

formulations was evaluated in male mice (C57bl/6JOlaHsd, Harlan, The Netherlands) inoculated with B16F10 melanoma cells (1×10^7 cells per mouse) in the left flank. The treatment started at day 7 at the time that the tumor became palpable. PTX-loaded micelles and Taxol were injected at two different PTX doses and schedules: 20 mg/kg at day 7, 9, 11, 13 and 15 (high dose schedule) and 5 mg/kg at day 7, 11 and 15 (low dose schedule). Empty micelles were injected at an equivalent polymer concentration as for the PTX-micelles at the high dose schedule. As a control, 200 μ L PBS was injected at day 7, 9, 11, 13 and 15. Each formulation was injected into the tail vein of the tumor bearing mice ($n = 3$ to 5 per group). At day 7, 9, 11, 13, 15 and 17 the volume of the tumor was calculated from the length and the width of the tumor. The volume of spheroid tumor was calculated as $0.5 \times (\text{length}) \times (\text{width})^2$.

2.7. Antitumor efficacy of PTX-loaded pHPMAmDL-b-PEG micelles after i.p. injection

The formulations (Taxol and the PTX-loaded pHPMAmDL(13600)-b-PEG micelles) were prepared as described in Section 2.6. As control, the Taxol vehicle (a 50:50 mixture of Cremophor EL and ethanol), which was prepared by mixing equal volumes of Cremophor EL and ethanol, and empty pHPMAmDL(13600)-b-PEG micelles in PBS (9 mg/mL) were also evaluated.

The antitumor efficacy of the PTX formulations was evaluated in male mice (Atymic Balb/c, Harlan, The Netherlands) bearing human ovarian carcinoma cells (OVCAR-3). Therefore, 150 μ L OVCAR-3 cells (1×10^7 cells per mouse) were inoculated into the peritoneal cavity of mice at day 0 and the treatment started at day 4. PTX-loaded micelles and Taxol were injected intraperitoneally ($n = 4$ to 6 per group) at a dose of 20 mg/kg and at two different schedules: at day 4, 5, 6, 7 and 8 (high dose) and at day 4, 6 and 8 (low dose). As a negative control, empty micelles in PBS (concentration = 9 mg/mL, polymer dose = 90 mg/kg) and 200 μ L Taxol vehicle and PBS were injected at day 4, 5, 6, 7 and 8. At day 10 the mice were euthanized. Tumor tissue was collected by washing the peritoneal cavity twice with 5 mL cold PBS and subsequent centrifugation at 2,000 rpm for 5 minutes. The weight of the pellets was measured.

3. Results and Discussion

3.1. Biodistribution of pHPMAmDL-*b*-PEG micelles in rats after i.v. administration

In Chapter 3 we reported on a novel class of biodegradable and thermosensitive polymeric micelles consisting of pHPMAmDL-*b*-PEG block copolymers (Figure 1). In that Chapter it was reported that pHPMAmDL(6900/13600)-*b*-PEG self-assembled upon heating from 0 to 50 °C in an aqueous solution into polymeric micelles with a size around 50 nm. It was shown that these micelles have a highly packed solid-like core that is stabilized by a dense layer of PEG [20]. It was demonstrated that pHPMAmDL(13600)-*b*-PEG micelles can solubilize PTX up to 2 mg/mL by a simple mixing method utilizing the thermosensitivity of pHPMAmDL-*b*-PEG. Further, it was demonstrated *in vitro* that PTX-loaded pHPMAmDL-*b*-PEG micelles destabilized after approximately one week at physiological pH and temperature due to the hydrolysis of the lactic acid side group of the pHPMAmDL, resulting in concomitant release of PTX [21]. The empty micelles were not toxic to B16F10 cells and the micellar PTX formulation showed equally effective cell killing *in vitro* as compared to Taxol [21].

In this Chapter, investigations of the circulation kinetics and the tissue distribution of pHPMAmDL-*b*-PEG micelles in rats are reported. Tritium labeled pHPMAmDL(6900)-*b*-PEG micelles with a mean size of 60 nm, as determined by dynamic light scattering, were injected intravenously into healthy male rats at a polymer dose of 5 mg/rat. The concentration in the circulation after immediate distribution over the blood compartment is approximately 0.25 mg/mL (assuming 20 mL blood/rat), which is 8 times higher than the critical micelle concentration of pHPMAmDL(6900)-*b*-PEG (0.03 mg/mL) [20]. Figure 2 shows that around 20 % and 60 % of the injected dose is cleared in 5 minutes and in 1 hour after injection, respectively. This initial clearance during the first hour is in line with the circulation kinetics of other polymeric micelle systems [24,25]. As shown in Figure 3, liver uptake is one of the major factors involved in the initial clearance. The uptake by the other organs investigated (spleen, lung and kidneys) is rather low (< 5 %).

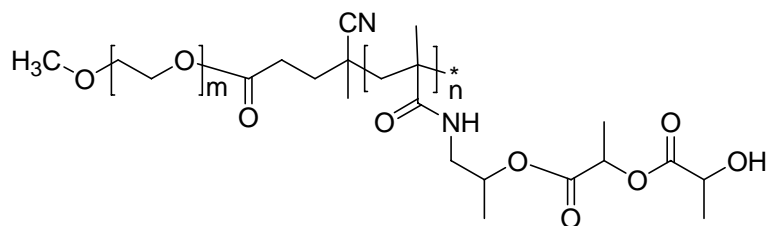


Figure 1. Chemical structure of the pHPMAmDL-*b*-PEG block copolymer.

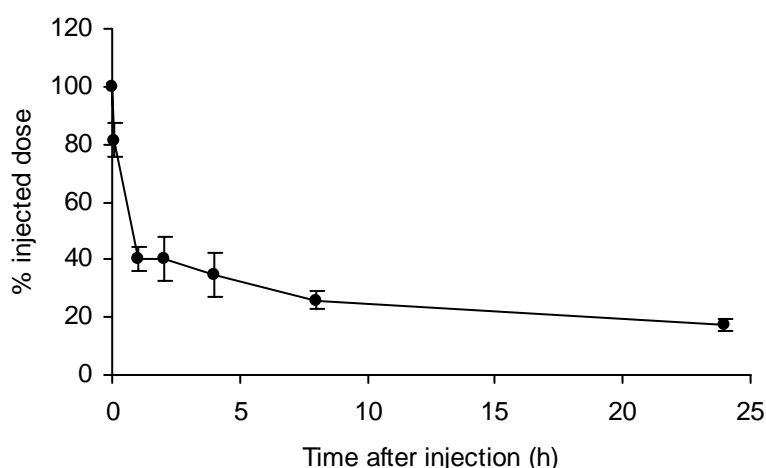


Figure 2. Blood circulation profiles of pHPMAmDL(6900)-*b*-PEG micelles after intravenous administration at a dose of 5 mg/rat. Each point represents the mean \pm standard deviation of four rats. % Injected dose refers to the percentage of the initially injected amount of radioactivity (estimated blood volume is 20 mL/rat).

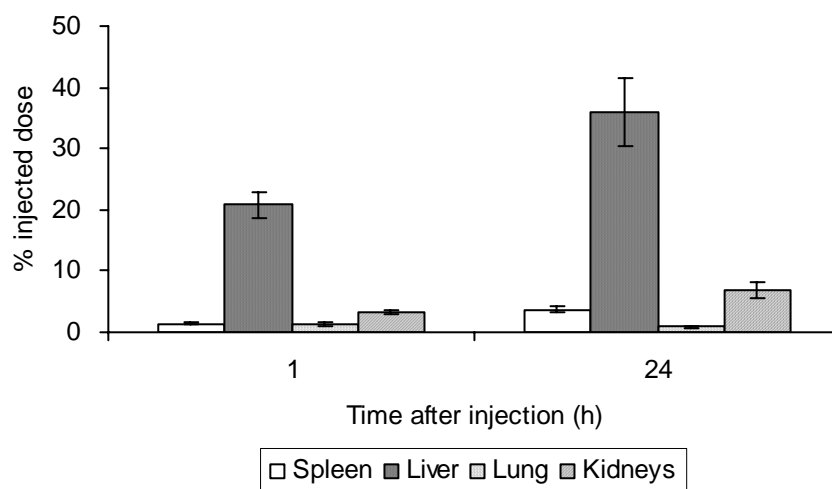


Figure 3. Organ distribution profiles for pHPMAmDL(6900)-*b*-PEG micelles at 1 and 24 hours after intravenous administration in rats at a dose of 5 mg/rat. The presented data are the mean \pm standard deviation of four rats per time point. % Injected dose refers to the percentage of the initially injected amount of radioactivity (estimated blood volume 20 mL/rat).

It has been reported that liposomes and polymeric micelles with a size smaller than 70 nm show a relatively high accumulation in the liver presumably due to uptake by Kupffer cells but also to their ability to penetrate through the fenestrate in the endothelial lining of the liver (about 100 nm in rat [26])

allowing them to reach the parenchymal cells [27,28]. Indeed liver perfusion studies have demonstrated that liposomes (around 100 nm or more) were restricted entirely to the sinusoidal lumen [29], while lipid nanospheres (25 to 50 nm) went through liver fenestrae and were distributed into the space of Disse (the space between the fenestrated endothelium and the parenchyma of the liver) [30]. The size of pHPMAmDL(6900)-*b*-PEG micelles is 50 to 60 nm [20], and therefore it is likely that the micelles were not only taken up by cells of the mononuclear phagocyte system (MPS) in the liver, but also entered the space of Disse. In line herewith is the observation that the uptake of the micelles by the spleen, another MPS-rich organ, is relatively low, suggesting that the uptake of intact micelles by splenic macrophages is not a major process [31]. Further, it is important to note that the uptake of the micelles by the lung is very low as well (< 0.8 % after 24 hours), suggesting that the PEG corona prevented serum protein-induced aggregation of the micelles in the bloodstream. Figure 2 also shows that after the initial clearance, the micelles were relatively slowly cleared leaving approximately 20 % of the injected dose in the bloodstream 24 hours post injection, which is considered sufficient to deliver therapeutics to e.g. tumor and other pathological sites by exploiting the EPR effect [13]. Overall, the observed circulation kinetics of pHPMAmDL-*b*-PEG micelles is rather comparable to that of other polymeric micellar systems [25,32].

Table 1. Organ distribution profiles for PTX-loaded pHPMAmDL(13600)-*b*-PEG micelles and Taxol at 1 and 24 hours after intravenous administration in tumor-bearing mice

	^3H -pHPMAmDL- <i>b</i> -PEG		^{14}C -PTX in pHPMAmDL- <i>b</i> -PEG		^{14}C -PTX in Taxol	
	1 hr	24 hr	1 hr	24 hr	1 hr	24 hr
Blood	24.6 ± 7.8	4.6 ± 0.7	0.9 ± 0.3	0.1 ± 0.1	4.3 ± 1.0	0.1 ± 0.0
Tumor	0.9 ± 0.2	1.4 ± 0.4	1.0 ± 0.6	0.4 ± 0.1	0.7 ± 0.3	0.2 ± 0.2
Liver	1.2 ± 0.2	1.7 ± 1.1	17.2 ± 3.3	0.6 ± 0.1	17.3 ± 2.9	0.3 ± 0.2
Spleen	0.3 ± 0.0	0.4 ± 0.0	0.5 ± 0.3	0.0 ± 0.0	0.3 ± 0.1	0.0 ± 0.0
Kidneys	0.6 ± 0.1	0.2 ± 0.0	0.4 ± 0.1	0.0 ± 0.0	0.7 ± 0.0	0.0 ± 0.0
Lungs	3.8 ± 0.5	5.6 ± 0.4	1.3 ± 0.2	0.2 ± 0.2	1.7 ± 0.3	0.0 ± 0.0

The data are expressed as the percentage of the initially injected dose of radioactivity (estimated blood volume is 2 mL/mouse). The presented data are the mean ± standard deviation of four mice per time point.

*3.2. Biodistribution studies of PTX-loaded pHPMAmDL-*b*-PEG micelles in tumor bearing mice*

The biodistribution of PTX-loaded pHPMAmDL-*b*-PEG micelles in tumor bearing mice was investigated using a double labeling procedure based on [¹⁴C]-labeled PTX and [³H]-labeled polymer. For comparison, the biodistribution of [¹⁴C]-PTX formulated with Cremophor EL/ethanol was also evaluated. The formulations were injected intravenously into mice bearing B16F10 melanoma cells at exponential tumor growth phase and at a PTX dose of 20 mg/kg mice. In these studies, a polymer with a higher molecular weight of the thermosensitive pHPMAmDL block (13,600 g/mol versus 6,900 g/mol for the biodistribution studies in rats, Section 3.1) was used because this polymer has a higher loading capacity for PTX [21].

Table 1 reports the biodistribution of PTX and the pHPMAmDL(13600)-*b*-PEG block copolymer micelles 1 and 24 hours post injection. The table shows that the micelles show some tumor accumulation (0.9 and 1.4 % of the injected dose, 1 and 24 hours post injection respectively). One hour post injection 25 % of the injected dose of micelles was in the circulation, whereas, remarkably less than 1 % of the injected dose of PTX was in the circulation. This indicates that most of PTX was released from pHPMAmDL(13600)-*b*-PEG micelles within the first hour after injection. We have shown in Chapter 4 that the *in vitro* release of PTX from pHPMAmDL-*b*-PEG micelles is much slower (only ~10 % of the contents was released during the first hour [21]). It is known that PTX has strong affinity for blood proteins e.g. albumin [33] and therefore it may be possible that PTX is extracted from the micelles by blood proteins after intravenous injection. In line herewith, Liu et al. reported accelerated release of ellipticine from poly(5-benzyloxy-trimethylene carbonate)-*b*-PEG micelles in the presence of albumin, although there were no significant interactions between the micelles and albumin [34]. The biodistribution of PTX-loaded PDLLA-*b*-PEG micelles in rats has been investigated by Burt et al. in the same way as we performed [35]. They reported that the blood level of PTX was lower than that of the micelles at 5 minutes after injection and suggested a rapid release of PTX from the micelles, which is in agreement with our data. Table 1 also shows that the blood level of PTX formulated in pHPMAmDL(13600)-*b*-PEG micelles at 1 hour after administration (0.9 %) was significantly lower than that of PTX formulated in Taxol (4.3 %). A similar phenomenon has been observed also for PTX-loaded PDLLA-*b*-PVP micelles by Le Garrec et al [11]. It was known that PTX formulated in Cremophor EL had a higher AUC (= area under the curve) than formulated in other surfactants such as Tween 80, likely due to relatively high affinity of PTX for Cremophor EL [4]. Except the blood level, the tissue distribution profiles of PTX was similar for pHPMAmDL(13600)-*b*-PEG micelles and Taxol. At 1 hour post injection the liver was the major organ of distribution and the total amount of [¹⁴C]-PTX recovered was around 20 %.

Hepatobiliary excretion into faeces is the major pathway of elimination of PTX [36]. The above-mentioned double labeling experiment by Burt et al. revealed that 5 min after injection PTX almost evenly distributed in the tissues such as the kidneys, thyroid, lungs, submaxillary glands, brown fat, heart, pituitary gland, liver and pancreas [35]. It might be possible that PTX which was not completely recovered in our study at 1 hour after injection, distributed to other organs than those studied (see Table 1).

Table 1 and Figure 2 show that the micelles are more rapidly cleared from the blood in mice than in rats (e.g. dose remaining in the circulation after 24 hours is 5 % in mice and 20 % in rats, respectively). Moreover, as shown in Table 1 and Figure 2, the liver uptake in mice is much lower than in rats (1.7 % in mice and 35 % in rats at 24 hours, respectively). The reason for the discrepancy between the observed differences in circulation kinetics of pHPMAmDL-*b*-PEG micelles in rats and mice is not fully understood yet. Firstly it might be related to species differences. Secondly, another possibility could be the difference of the length of the thermosensitive pHPMAmDL block: the block in non-labeled polymers had a number average molecular weight of 13,600 g/mol (Section 3.2), and the block in the tritium labeled polymers had a number average molecular weight of 7,800 g/mol. Due to the lower molecular weight, the labeled polymer might have been preferentially extracted from pHPMAmDL(13600)-*b*-PEG micelles.

3.3. Antitumor efficacy of PTX-loaded pHPMAmDL-*b*-PEG micelles after *i.v.* injection

The *in vivo* antitumor efficacy of intravenously injected PTX-loaded pHPMAmDL-*b*-PEG micelles and Taxol was evaluated in mice bearing a subcutaneous B16F10 tumor. Both formulations were injected either at a PTX dose of 20 mg/kg (maximum tolerance dose of PTX formulated with Cremophor EL/ethanol after *i.v.* administration [9]) every two days (high dose schedule), or at 5 mg/kg every four days (low dose schedule). Figure 4 shows that the PTX-loaded pHPMAmDL-*b*-PEG micelles showed comparable therapeutic efficacy as Taxol at the same dose. This result is reasonable because the tumor accumulation of PTX for these two formulations is similar (Table 1). One important observation is that mice which were injected with Taxol showed local inflammation at the site of injection after repeated administrations (featured by local erythema and pain, and vocal signs of discomfort), whereas mice injected with PTX-loaded pHPMAmDL-*b*-PEG micelles did not show any sign of inflammation. Therefore, the pHPMAmDL-*b*-PEG micellar system is superior in terms of preventing local toxicity *in vivo*, which is in line with *in vitro* experiments [21].

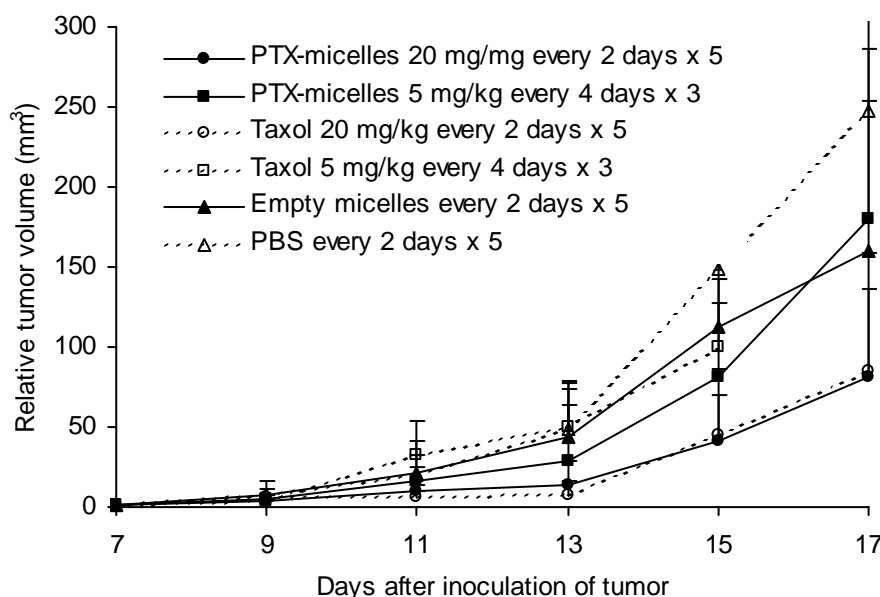


Figure 4. Antitumor efficacy of PTX-loaded pHPMAmDL(13600)-*b*-PEG micelles and Taxol in B16f10 melanoma bearing mice.

3.4. Antitumor efficacy of PTX-loaded pHPMAmDL-*b*-PEG micelles after *i.p.* injection

The *in vivo* antitumor efficacy of PTX-loaded pHPMAmDL-*b*-PEG micelles and Taxol after intraperitoneal administration was evaluated in mice bearing OVCAR-3 tumor cells in their peritoneal cavity. Both formulations were injected at a PTX dose of 20 mg/kg, which equals the maximum tolerated dose of intraperitoneally administered PTX formulated with Cremophor EL/ethanol [37]. As shown in Figure 5, both formulations showed a strong antitumor effect. The therapeutic efficacy of PTX-loaded PDLLA-*b*-PEG micelles after intraperitoneal administration has been investigated by Zhang et al. Their formulation showed, at a PTX dose of 50 mg/kg, comparable same survival rate as Taxol at 20 mg/kg in P388 tumor-inoculated mice [37]. Remarkably, our PTX-loaded pHPMAmDL-*b*-PEG micelles show comparable antitumor efficacy as Taxol at the same PTX dose of 20 mg/kg.

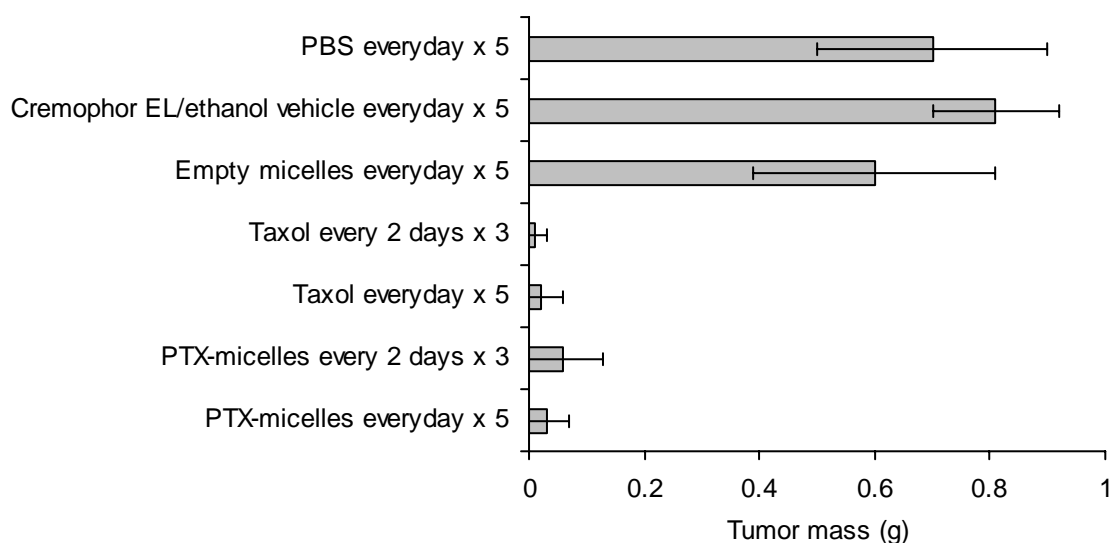


Figure 5. Antitumor efficacy of PTX-loaded pHPMAmDL(13600)-*b*-PEG micelles and Taxol in OVCAR-3 bearing mice.

4. Conclusions

This study demonstrates that PTX-loaded pHPMAmDL-*b*-PEG micelles do not enhance the tumor concentration of PTX when compared to Taxol but are as effective as Taxol in terms of antitumor activity. Due to the avoidance of the use of Cremophor EL/ethanol vehicle, lower toxicity of pHPMAmDL-*b*-PEG micelles is expected. This may allow an increase of the dose for pHPMAmDL-*b*-PEG micelles with a resulting superior therapeutic effect. Further studies are necessary to support this hypothesis.

Acknowledgement

The authors thank Mitsubishi Pharma Corporation (Japan) for their financial support.

References

1. P.B. Schiff, J. Fant, S.B. Horwitz. *Nature* 277 (1979) 665-667.
2. J. Crown, M. O'Leary. *Lancet* 355 (2000) 1176-1178.
3. E.K. Rowinsky, R.C. Donehower. *N Engl J Med* 332 (1995) 1004-1014.
4. H. Gelderblom, J. Verweij, K. Nooter, A. Sparreboom. *Eur J Cancer* 37 (2001) 1590-1598.
5. A.K. Singla, A. Garg, D. Aggarwal. *Int J Pharm* 235 (2002) 179-192.

6. C.J. Langer. *Expert Opin Investig Drugs* 13 (2004) 1501-1508.
7. N.K. Ibrahim, N. Desai, S. Legha, P. Soon-Shiong, R.L. Theriault, E. Rivera, B. Esmali, S.E. Ring, A. Bedikian, G.N. Hortobagyi, J.A. Ellerhorst. *Clin Cancer Res* 8 (2002) 1038-1044.
8. R.T. Liggins, H.M. Burt. *Adv Drug Deliv Rev* 54 (2002) 191-202.
9. S.C. Kim, D.W. Kim, Y.H. Shim, J.S. Bang, H.S. Oh, S.W. Kim, M.H. Seo. *J Control Release* 72 (2001) 191-202.
10. V.P. Torchilin, A.N. Lukyanov, Z. Gao, B. Papahadjopoulos-Sternberg. *Proc Natl Acad Sci U S A* 100 (2003) 6039-6044.
11. D. Le Garrec, S. Gori, L. Luo, D. Lessard, D.C. Smith, M.-A. Yessine, M. Ranger, J.C. Leroux. *J Control Release* 99 (2004) 83-101.
12. K.M. Huh, S.C. Lee, Y.W. Cho, J. Lee, J.H. Jeong, K. Park. *J Control Release* 101 (2005) 59-68.
13. H. Maeda, J. Wu, T. Sawa, Y. Matsumura, K. Hori. *J Control Release* 65 (2000) 271-284.
14. K. Kataoka, A. Harada, Y. Nagasaki. *Adv Drug Deliv Rev* 47 (2001) 113-131.
15. M.C. Jones, J.C. Leroux. *Eur J Pharm Biopharm* 48 (1999) 101-111.
16. G.S. Kwon. *Crit Rev Ther Drug Carrier Syst* 20 (2003) 357-403.
17. C.F. van Nostrum. *Adv Drug Deliv Rev* 56 (2004) 9-16.
18. Y. Matsumura, T. Hamaguchi, T. Ura, K. Muro, Y. Yamada, Y. Shimada, K. Shirao, T. Okusaka, H. Ueno, M. Ikeda, N. Watanabe. *Br J Cancer* 91 (2004) 1775-1781.
19. T.Y. Kim, D.W. Kim, J.Y. Chung, S.G. Shin, S.C. Kim, D.S. Heo, N.K. Kim, Y.J. Bang. *Clin Cancer Res* 10 (2004) 3708-3716.
20. O. Soga, C.F. van Nostrum, A. Ramzi, T. Visser, F. Soulimani, P.M. Frederik, P.H. Bomans, W.E. Hennink. *Langmuir* 20 (2004) 9388-9395.
21. O. Soga, C.F. van Nostrum, M.H.A.M. Fens, C.J.F. Rijcken, R.M. Schiffelers, G. Storm, W.E. Hennink. *J Control Release* 103 (2005) 341-353.
22. D. Neradovic, O. Soga, C.F. van Nostrum, W.E. Hennink. *Biomaterials* 25 (2004) 2409-2418.
23. G.H. Muller. *J Cell Sci* 43 (1980) 319-328.
24. S.A. Hagan, A.G.A. Coombes, M.C. Garnett, S.E. Dunn, M.C. Davis, L. Illum, S.S. Davis, S.E. Harding, S. Purkiss, P.R. Gellert. *Langmuir* 12 (1996) 2153-2161.
25. Y. Yamamoto, Y. Nagasaki, Y. Kato, Y. Sugiyama, K. Kataoka. *J Control Release* 77 (2001) 27-38.
26. F. Braet, E. Wisse. *Comp Hepatol* 1 (2002) 1.
27. D. Liu, A. Mori, L. Huang. *Biochim Biophys Acta* 1104 (1992) 95-101.
28. S. Stolnik, C.R. Heald, J. Neal, M.C. Garnett, S.S. Davis, L. Illum, S.C. Purkis, R.J. Barlow, P.R. Gellert. *J Drug Target* 9 (2001) 361-378.
29. S.N. Hilmer, V.C. Cogger, M. Muller, D.G. Le Couteur. *Drug Metab Dispos* 32 (2004) 794-799.
30. J. Seki, S. Sonoke, A. Saheki, H. Fukui, H. Sasaki, T. Mayumi. *Int J Pharm* 273 (2004) 75-83.

31. J.M. Metselaar, P. Bruin, L.W. de Boer, T. de Vringer, C.J. Snel, C. Oussoren, M.H. Wauben, D.J.A. Crommelin, G. Storm, W.E. Hennink. *Bioconjug Chem* 14 (2003) 1156-1164.
32. G. Kwon, S. Suwa, M. Yokoyama, T. Okano, Y. Sakurai, K. Kataoka. *J Control Release* 29 (1994) 17-23.
33. K. Paal, J. Muller, L. Hegedus. *Eur J Biochem* 268 (2001) 2187-2191.
34. J. Liu, F. Zeng, C. Allen. *J Control Release* 103 (2005) 481-497.
35. H.M. Burt, X.C. Zhang, P. Toleikis, L. Embree, W.L. Hunter. *Colloids Surf B: Biointerfaces* 16 (1999) 161-171.
36. A. Sparreboom, O. van Tellingen, W.J. Nooijen, J.H. Beijnen. *Anticancer Drugs* 9 (1998) 1-17.
37. X. Zhang, H.M. Burt, D. Von Hoff, D. Dexter, G. Mangold, D. Degen, A.M. Oktaba, W.L. Hunter. *Cancer Chemother Pharmacol* 40 (1997) 81-86.

Chapter 6

Summary and perspectives

Summary

Amphiphilic block copolymers consisting of a hydrophilic and a hydrophobic segment form core-shell nanostructures, so-called polymeric micelles, in aqueous solution [1,2]. The hydrophilic segment of a block copolymer forms the shell and stabilizes the micellar structure, while the hydrophobic segment forms the core of the micelles. The hydrophobic core can accommodate a great variety of in particular hydrophobic drugs. The size of polymeric micelles depends on the molecular weight of the hydrophobic and hydrophilic segments in the block copolymer and is generally between 10 to 60 nm, which is relatively small as compared to other colloidal drug carriers such as liposomes and emulsions. Due to their small size and hydrophilic surface, polymeric micelles are not easily recognized and captured by macrophages of the mononuclear phagocyte system (MPS) after intravenous administration, allowing their accumulation in e.g. tumor tissue and other pathological sites due to the so-called EPR (enhanced permeation and retention) effect [3]. Because of these attractive features as drug delivery vehicles, polymeric micelles are currently emerging as a novel type of drug carrier and some polymeric micellar drug delivery systems are presently undergoing clinical evaluation [4-6].

It is of great importance for the therapeutic efficacy of drug-loaded polymeric micelles to retain their payloads in the bloodstream after intravenous administration and to release the drugs after reaching the pathological site. The release of the drugs from polymeric micelles can occur either by passive means, indicating that the drug diffuses out of the core, or by active means, by application of a certain trigger, e.g. ultrasound [7] or hyper/hypothermia [8]. The release can also be triggered by differences in e.g. pH [9], redox-potential [10] or enzymatic activity [11] between healthy and pathological tissues. A mixed active-passive approach to achieve release of the drug of interest from polymeric micelles is the gradual conversion of a hydrophobic micellar core to a more hydrophilic state within the body, which eventually results in the dissolution of the micelles and the concomitant release of the entrapped drugs [12]. In this approach, there should be a balance between the time needed for the drug-loaded micelle to reach its target site and the destabilization kinetics.

Block copolymers consisting of a hydrophilic block and a temperature sensitive block with a lower critical solution temperature (LCST) can be utilized for the design of such polymeric micelles. These polymers are soluble in aqueous solution below the cloud point (CP) of the temperature sensitive block, but self-assemble into micellar structures when heated to above the CP. Here, the polymeric micelles consist of the hydrophobic core of the temperature sensitive block and the shell of the hydrophilic block. When the CP of the temperature sensitive block is below 37 °C, these polymers form micelles in aqueous solution at body temperature. As pointed out above, the hydrophobic core can be

loaded with a hydrophobic drug and the drug can be released once the drug-loaded micelles have reached their site of action (e.g. a tumor) by hypothermia. However, such an approach is not always feasible and therefore other approaches are under investigation to release the drug from such micellar systems. We therefore hypothesized that if we are able to design degradable thermosensitive polymers whose CP increase from below to above body temperature in time, such polymers should be very attractive tools for “hydrophobic to hydrophilic” conversion of polymeric micelles.

Based on this idea, our group had previously developed thermosensitive copolymers of *N*-isopropylacrylamide and *N*-(2-hydroxypropyl) methacrylamide lactate (poly(NIPAAm-*co*-HPMAm-lactate)) and their block copolymers with poly(ethylene glycol) (poly(NIPAAm-*co*-HPMAm-lactate)-*b*-PEG) [13]. When 35 mol % HPMAm-lactate was copolymerised with NIPAAm, poly(NIPAAm-*co*-HPMAm-lactate) had its CP below body temperature, whereas after hydrolysis of the lactate side groups the CP increased above 37 °C [13]. Owing to this unique LCST behavior of poly(NIPAAm-*co*-HPMAm-lactate), polymeric micelles formed with poly(NIPAAm-*co*-HPMAm-lactate)-*b*-PEG block copolymers showed a controlled dissolution profile at body temperature as a result of “hydrophobic to hydrophilic” conversion of the poly(NIPAAm-*co*-HPMAm-lactate) core [14]. The aim of the study described in this Thesis is to further develop this novel polymeric micellar system and demonstrate its utility as a drug delivery vehicle. Since PNIPAAm is not biodegradable and its biocompatibility is not well understood at present, we are interested in designing novel, NIPAAm-free, thermosensitive polymers that can be expected to show good biocompatibility and low toxicity.

Chapter 1 gives an introduction on polymeric micelles emerging as novel drug delivery systems. The physicochemical aspect of polymeric micelles and the design of polymeric micellar systems with controlled instability are discussed in detail. The aim and outline of this Thesis are presented.

In **Chapter 2** the synthesis and characteristics of a novel class of thermosensitive and biodegradable polymers, poly(*N*-(2-hydroxypropyl) methacrylamide mono/di lactate) (poly(HPMAm-mono/di lactate)), are reported. Polymers with different monomer compositions were synthesized by radical polymerization of HPMAm-monolactate and HPMAm-dilactate at different feed ratios. Interestingly, all these polymers showed LCST behavior in aqueous solution. The CP's of poly(HPMAm-monolactate) and poly(HPMAm-dilactate) in water were 65 °C and 13 °C, respectively. The lower CP for poly(HPMAm-dilactate) is attributed to the greater hydrophobicity of the dilactate side group over the monolactate side group. The CP of the copolymers increased linearly with mol % of HPMA-monolactate, demonstrating that the CP can be tailored by the copolymer composition. Importantly, due to the hydrolyzable ester bond,

it is expected that the lactate side chains of poly(HPMAm-mono/di lactate) will be gradually removed from the polymers in aqueous solution, resulting in the increase of their CP. Finally, by hydrolysis of the lactate side groups, these polymers are converted into the water-soluble pHPMAm with lactic acid, an endogenous compound, as a degradation product. pHPMAm is a well-known non-toxic macromolecular drug carrier. Therefore, a good biocompatibility and low toxicity of poly(HPMAm-mono/di lactate) is expected. Among the polymers described in this chapter, poly(HPMAm-dilactate) is supposed to be suitable for “hydrophobic to hydrophilic” conversion at body temperature, since its CP (13 °C in water) is far below 37 °C and this polymer will be converted in time into poly(HPMAm-monolactate) (CP = 65 °C in water) and eventually into hydrophilic pHPMAm.

In **Chapter 3**, amphiphilic AB block copolymers of poly(HPMAm-dilactate) and PEG (pHPMAmDL-*b*-PEG) are described. Three pHPMAmDL-*b*-PEG block copolymers with different pHPMAmDL block lengths (M_n from 3,000 to 13,600 g/mol) and with a fixed PEG molecular weight ($M_n = 5,000$ g/mol) were synthesized via a macroinitiator route. As expected, these block copolymers formed polymeric micelles in water with a size of around 50 nm by rapidly heating an aqueous polymer solution from below to above the critical micelle temperature (CMT). By cryo-transmission electron microscopy (cryo-TEM) analysis, it was shown that pHPMAmDL-*b*-PEG micelles have a spherical shape with a narrow size distribution. The critical micelle concentration (CMC), determined using pyrene as a fluorescent probe, as well as the CMT decreased with increasing pHPMAmDL block lengths, which can be attributed to the greater hydrophobicity of the thermosensitive block with increasing molecular weight. The CMC values of pHPMAmDL(6900)-*b*-PEG and pHPMAmDL(13600)-*b*-PEG were sufficiently low (0.03 and 0.015 mg/mL, respectively) to maintain their micellar form upon dilution after e.g. intravenous administration. ^1H NMR measurements in D_2O and static light scattering (SLS) measurements demonstrated that pHPMAmDL(6900)-*b*-PEG micelles and pHPMAmDL(13600)-*b*-PEG micelles possess a highly packed solid-like core and a dense layer of swollen PEG chains. The former property should allow efficient and stable entrapment of hydrophobic drugs, and the latter likely contributes to the stabilization of the micelles in the bloodstream. FT-IR analysis was performed to understand the mechanism of the micelle formation and showed that dehydration of the amide bonds in the pHPMAmDL block occurs when the block copolymer dissolved in water is heated from below to above its CMT. To access our key concept of controlled instability, the destabilization of pHPMAmDL(13600)-*b*-PEG micelles at 37 °C and at different pH's was monitored by dynamic and static light scattering (DLS/SLS). At pH 5.0, where the hydrolysis rate of lactate side groups is minimized, the micelles were stable

over 60 hours. On the other hand, at pH 9.0, where the hydrolysis is enhanced by hydroxyl ions, the micelles started to swell after 1.5 hours of incubation and complete dissolution of micelles was observed after 4 hours, as a result of hydrophilization of the thermosensitive block so that the CMT of the block copolymer passed 37 °C. It was calculated that under physiological conditions (pH 7.4 and 37 °C) the dissolution of the micelles occurs in 160 hours. These results demonstrate that our concept of controlled instability can be achieved with pHPMAmDL-*b*-PEG micelles. Furthermore, fluorescence spectroscopy measurements with pyrene loaded in the hydrophobic core of the micelles showed that when these micelles were incubated at pH 8.6 and at 37 °C the microenvironment of pyrene increased in polarity due to hydrophilization of the micellar core. These physicochemical features revealed in this Chapter, together with the simple preparation method avoiding the use of organic solvents, make pHPMAmDL-*b*-PEG micelles very suitable as delivery vehicles for hydrophobic drugs.

In **Chapter 4** the loading of paclitaxel (PTX), a very hydrophobic cytostatic drug, into pHPMAmDL-*b*-PEG micelles is studied to assess the potential of pHPMAmDL-*b*-PEG micelles as drug delivery vehicles. A simple loading method taking advantage of the thermosensitivity of pHPMAmDL-*b*-PEG was used. A pHPMAmDL-*b*-PEG aqueous solution below its CMT was mixed with a small volume of a concentrated PTX solution in ethanol, and the mixture was subsequently rapidly heated above the CMT. Using this method, PTX was almost quantitatively loaded in the micelles up to a concentration of 2 mg/mL. This is more than 6,000-times the solubility of PTX in water (0.3 µg/mL). DLS and cryo-TEM analysis revealed that the PTX-loaded micelles are spherical and have a mean size around 60 nm with narrow size distribution; almost the same morphology as non-loaded pHPMAmDL-*b*-PEG micelles. To evaluate if the release of PTX from pHPMAmDL-*b*-PEG micelles occurred when the micelles dissolved, the stability of PTX-loaded pHPMAmDL-*b*-PEG micelles at 37 °C and at different pH's was monitored by DLS and SLS as performed for non-loaded micelles in Chapter 3. At pH 7.4, no precipitation of PTX was observed over 14 hours and the scattering intensity of the micellar solution remained constant, indicating that PTX is stably incorporated in pHPMAmDL-*b*-PEG micelles as long as the micelles remain intact. In contrast, at pH 8.8, sedimentation of PTX aggregates was observed together with an increase of scattering intensity followed by a sharp decrease as a result of the release of PTX from the micelles after 8 hours of incubation, showing that the release indeed occurs concomitantly with the dissolution of the micelles. At physiological pH, PTX-loaded pHPMAmDL-*b*-PEG micelles were stable for about 200 hours, which is in good agreement with the predicted time calculated from the result at pH 8.8. It was also shown that the presence of serum proteins

did not have an adverse effect on the stability of the micelles, likely due to the dense layer of PEG surrounding the micelles as demonstrated in Chapter 3. An *in vitro* release study using a dialysis method, which simulated sink conditions for PTX, showed that 70 % of PTX incorporated into pHPMAmDL-*b*-PEG micelles was released during 20 hours at 37 °C and pH 7.4. PTX-loaded pHPMAmDL-*b*-PEG micelles showed a comparable *in vitro* cytotoxicity as Taxol (clinically used formulation of PTX in a 50:50 mixture of Cremophor EL and ethanol) against B16F10 cells. On the other hand, the non-loaded pHPMAmDL-*b*-PEG micelles were far less cytotoxic than the Cremophor EL vehicle, which is beneficial for *in vivo* applications. Finally, to get insight into the cellular processing of the PTX-loaded micelles, confocal laser-scanning microscopy (CLSM) and fluorescence activated cell sorting (FACS) analysis of fluorescently labelled micelles were performed and it was shown that pHPMAmDL-*b*-PEG micelles were internalized by the B16F10 cells.

In **Chapter 5**, *in vivo* studies of pHPMAmDL-*b*-PEG micelles and PTX-loaded pHPMAmDL-*b*-PEG micelles are reported. When administered intravenously into rats, pHPMAmDL-*b*-PEG micelles showed a relatively long blood circulation time with 20 % of the injected dose still circulating in the bloodstream after 24 hours, which is sufficient to achieve passive targeting. The liver was the major organ responsible for the uptake of the micelles, while the uptake of the micelles by spleen and lung was low. It is suggested that, due to their small size of approximately 60 nm, pHPMAmDL-*b*-PEG micelles were not only taken up by cells of the mononuclear phagocyte system (MPS) in the liver, but also entered the space of Disse (the space between the fenestrated endothelium and the parenchyma of the liver), which could result in additional uptake of micelles by hepatocytes. In mice, pHPMAmDL-*b*-PEG micelles were cleared more rapidly from the bloodstream than in rats while liver uptake was lower. Faster clearance of colloidal drug delivery systems in mice compared to rats has been reported previously, but can usually be attributed to increased uptake by the MPS. Further investigations are necessary to understand the species differences in biodistribution. Opposite to the empty micelles, PTX that was loaded into pHPMAmDL-*b*-PEG micelles was cleared quite rapidly after intravenous administration in mice with only 0.9 % of the injected PTX-dose remaining in the circulation after 1 hour, suggesting that PTX was not stably associated with the micelles in the circulation and was likely to be extracted from the micelles by blood proteins. The therapeutic efficacy of PTX-loaded pHPMAmDL-*b*-PEG micelles, evaluated in mice with B16F10 melanoma carcinoma after intravenous administration and with OVCAR-3 human ovarian carcinoma after intraperitoneal administration, was found to be comparable to Taxol at the same PTX dose. In addition, mice injected with Taxol showed local inflammation at the site of injection after repeated administrations, in contrast to mice injected with PTX-loaded pHPMAmDL-*b*-PEG micelles, indicating that

pHPMAmDL-*b*-PEG micelle are superior in terms of preventing local toxicity *in vivo*.

Perspectives

This Thesis reports on a novel class of thermosensitive and biodegradable polymers, poly(HPMAm-lactate), and polymeric micellar system consisting of pHPMAmDL-*b*-PEG block copolymers. pHPMAmDL-*b*-PEG micelles showed controlled destabilization profiles by “hydrophobic to hydrophilic” conversion in time, which would enable controlled release of entrapped drugs at their site of action. Furthermore, the suitability of pHPMAmDL-*b*-PEG micelles as vehicles for a hydrophobic model drug (PTX) was demonstrated. Here, suggestions are made for future investigations to further improve these novel polymeric micellar systems towards clinically applicable drug delivery vehicles.

The block copolymers of pHPMAmDL and PEG were synthesized by the macroinitiator route. However, it can not be excluded that besides the aimed pHPMAmDL-*b*-PEG block copolymer, also pHPMAmDL is formed e.g. by chain transfer reactions. The molecular weights and molecular weight distribution of the synthesized polymers were determined by gel permeation chromatography (GPC). However, it is not possible to establish the presence of the homopolymer of pHPMAmDL with this technique. The amount of the homopolymer should be minimized to avoid the formation of the water-insoluble aggregates, which will precipitate or be dissolved in the hydrophobic core of the micelles and thereby increase their size. One approach to obtain a well-defined A-B block copolymer is the use of chain transfer agents [15]: e.g. amine-terminated pHPMAmDL homopolymer can be synthesized by radical polymerization of HPMAmDL in the presence of 2-aminoethanethiol hydrochloride. In a subsequent step, this amine-terminated polymer might be coupled using e.g. carbodiimide chemistry to PEG with a terminal carboxylic acid group. Likely, this synthesis method can not be simply applied to pHPMAmDL-*b*-PEG due to the hydroxyl groups of the pHPMAmDL block, which might also react with the activated carboxylic acid terminus of PEG. To circumvent this side reaction, the hydroxyl groups of the pHPMAmDL block have to be protected before the coupling reaction, and be deprotected thereafter. It is also desirable to obtain block copolymers with narrower size distribution. Such polymers will give a better control over the size of the micelles and their size distribution. Controlled living radical polymerization is a technique that allows good control over molecular weight and molecular weight distribution of polymers as well as allows the preparation of well-defined block copolymers. Examples of such techniques include atom transfer radical polymerization (ATRP) and reversible addition-fragmentation transfer polymerization (RAFT).

A few examples have been reported where PEG macro-RAFT agents were utilized for the synthesis of block copolymers [16,17]. Pan et al. synthesized dithiobenzoyl-terminated PEG as a chain-transfer agent and RAFT polymerization of *N*-isopropylacrylamide (NIPAAm) with the PEG macro-RAFT agent was conducted in the presence of α , α' -azoisobutyronitrile (AIBN) [17]. The obtained PNIPAAm-*b*-PEG block copolymer indeed possessed narrow size distribution ($M_w/M_n = 1.12$). This methodology is also applicable for the synthesis of pHPMAmDL-*b*-PEG. Controlled living radical polymerization is a useful technique also for the synthesis of well-defined block copolymers of two (or more) different (meth)acrylated polymers. This may allow the synthesis of e.g. a pHPMAmDL-*b*-pHPMAm block copolymer, which is an amphiphilic polymer that could be attractive as a material for thermosensitive polymeric micelles because it would degrade into the non-toxic and water-soluble homopolymer pHPMAm.

In this Thesis the concept of the destabilization of micelles due to hydrophilization of the core was clearly demonstrated. However, the time required for destabilization at physiological conditions (pH 7.4 and 37 °C, around 200 hours for PTX-loaded micelles) is rather long for the targeted delivery to tumors of cytostatic drugs. Typically, long-circulating nanosized drug carriers are cleared from the blood circulation and passively accumulate in tumor within 24 hours after *i.v.* administration. In fact, when intravenously administered into mice, it was demonstrated in Chapter 5 that 75 % of pHPMAmDL-*b*-PEG micelle dose was already eliminated from the circulation in 24 hours. This implies that the destabilization of the micelles should occur shortly thereafter at physiological conditions, especially for drugs for which effect is primarily correlated with peak concentrations such as doxorubicin. One approach for shortening destabilization time of the thermosensitive block is copolymerizing HPMAmDL with HPMAm-monolactate (HPMAmML). It was shown in Chapter 2 that the CP of the copolymers increases with increasing molar ratio of HPMAmML. Consequently, the CMT of poly(HPMAmML-*co*-HPMAmDL)-*b*-PEG is higher than that of pHPMAmDL-*b*-PEG, and the time in which the CMT reaches 37 °C and the micelles destabilize is shortened. Theoretically it is possible to choose the molar ratio of HPMAmML/HPMAmDL so that the destabilization occurs within 24 hours at physiological conditions. Drawbacks of this approach are the likely decreased physical stability and drug retention capacity of the micelles caused by the greater hydrophilicity of poly(HPMAmML-*co*-HPMAmDL) core as compared to the pHPMAmDL core. A more sophisticated strategy is to introduce hydrolyzable groups which are degraded more rapidly. Very recently it was shown in our group that the hydrolysis kinetics of *N*-(2-hydroxyethyl) methacrylamide dilactate (HEMAmDL) is three times faster than that of HPMAmDL, with a

half-life of 5.6 hours at physiological conditions [18]. This fast kinetics is attributed to less steric hindrance of the ester bond between the HEMAm and dilactate unit (primary alcohols for HEMAm versus secondary alcohols for HPMAm) in the alkaline catalyzed hydrolysis of esters [18]. Accordingly, polymeric micelles whose core consists of 80 mol % HEMAmDL and 20 mol % *N*-(2-hydroxyethyl) methacrylamide tetralactate destabilized within 8 hours at physiological conditions [18]. For tumor targeting, acid-catalyzed degradation might be an interesting approach, since the extracellular pH of tumors is often lower than that of blood and normal tissues. This approach is also attractive for the intracellular delivery of drugs loaded into polymeric micelles, since we demonstrated in Chapter 4 that pHPMAmDL-*b*-PEG micelles are taken up by living cells and likely end up in acidic endosomal and lysosomal compartments of the cells [19]. Acid sensitive groups e.g. acetal and ketal are likely candidates for such an approach. Indeed Frechet et al. recently demonstrated that a block copolymer of PEG and poly(aspartic acid) functionalized with trimethoxybenzylidene acetals formed polymeric micelles which dissolved at pH 5 due to the hydrolysis of the acetal bonds and resulting hydrophilization of the polymer [20].

The thermosensitivity of pHPMAmDL block allows very simple preparation method of pHPMAmDL-*b*-PEG micelles, which only requires heating of an aqueous polymer solution from below to above the CMT. This is an important advantage of our system since most of micelles preparation methods (e.g. o/w emulsion and dialysis) require toxic organic solvents (e.g. chloroform and acetonitrile) whose removal is time-consuming and inconvenient. In particular, the loading of the hydrophobic PTX into pHPMAmDL-*b*-PEG micelles was done using this principle, which consists of heating of a mixture of an aqueous polymer solution and a small volume of PTX/ethanol from below to above the CMT. Although significantly high levels of PTX loading were achieved by this loading procedure (up to 2 mg/mL), some improvements would be favourable for further *in vivo* applications. Firstly, it was shown in Chapter 5 that the therapeutic efficacy of PTX-loaded pHPMAmDL-*b*-PEG micelles and Taxol are comparable at the same PTX dose of 20 mg/kg mice (the MTD of Taxol). This is consistent with the *in vivo* results of other PTX-loaded micellar systems. The superior antitumor effect of PTX formulated with PLA-*b*-PEG micelles over Taxol was observed only when they are injected at higher dose than Taxol (e.g. 100 mg/kg mice) by taking advantage of the lower toxicity of these vehicles [21,22]. The maximum *i.v.* dose of PTX with 2 mg/mL PTX-loaded pHPMAmDL-*b*-PEG micelles is around 20 mg/kg mice due to the maximum volume for bolus injection. Therefore, the concentration of PTX in pHPMAmDL-*b*-PEG micellar formulation has to be increased to allow administration of a higher dose of PTX. Secondly, the PTX- pHPMAmDL-*b*-PEG micellar formulation contains 10 % (v/v) of ethanol, which could be a

dose-limiting factor when higher doses are to be administered. Ethanol should be removed from the formulation to avoid toxicity and to increase the MTD of the formulation. Freeze-drying is a procedure of choice to remove ethanol and to increase the concentration of PTX in our micellar formulation. Freeze drying has been used for the preparation of drug-loaded polymeric micellar formulations to ensure the long-term stability and to increase the drug concentration in the formulation. Generally, organic solvents have to be removed from polymeric micelles prepared by o/w emulsion or dialysis method before freeze-drying. Recently, a straightforward approach was reported by Leroux et al, where a *tert*-butanol/water mixture containing PTX and polymer (PLA-*b*-PVP) was freeze-dried to form drug-loaded micelles [23]. This approach, in principle, is also applicable for the ethanol/water mixture of PTX-loaded pHPMAmDL-*b*-PEG micelles. Ethanol might not be suitable for freeze-drying due to its low melting point of -114 °C. But, *tert*-butanol, suitable for freeze-drying owing to its relatively high melting point of 24 °C, is an option for the solvent of PTX as utilized by Leroux et al [23].

The most challenging and important aspect to be improved for *in vivo* application of pHPMAmDL-*b*-PEG micelles is the stable retention of the drug in the micelles as well as the stabilization of the micelles themselves during circulation in the bloodstream. In contrast to our expectations, more than 95 % of PTX was released from the pHPMAmDL-*b*-PEG micelles within 1 hour after *i.v.* administration into mice. This rapid release of PTX might be from intact micelles by e.g. extraction by blood proteins, or might be caused by dissociation of the micelles. It is not likely that dissociation is the main factor contributing to the release, since the calculated initial concentration of pHPMAmDL(13600)-*b*-PEG in the bloodstream in mice (0.9 mg/mL) is far above the CMC of this polymer (0.015 mg/mL, Chapter 3) and the micelles are quite stable *in vitro* in the presence of serum (Chapter 4). Such a rapid release of PTX from polymeric micelles was also observed for PTX-loaded PLA-*b*-PEG micelles and PLA-*b*-PVP micelles [24,25]. In contrast, polymeric micelles with a core of polyaspartate modified with 4-phenyl-1-butanol significantly increased the plasma and the tumor AUC of PTX, reaching 90-fold and 25-fold increases when compared to Taxol, respectively [26]. These observations suggest that the physical interaction between lactic acid-based micellar core (including pHPMAmDL core) and PTX is not strong enough to oppose extraction of PTX by blood components. Consequently more hydrophobic and more compatible groups to PTX (e.g. phenyl groups) have to be introduced to the core segments for stable drug retention *in vivo*. The presence of free hydroxyl groups in pHPMAmDL is an advantage in terms of chemical modification of the polymer, to which phenyl compounds with carboxyl groups such as benzoic acid can be conjugated. This conjugation can be performed either with the HPMAmDL

monomers or with pHPMAmDL-*b*-PEG block copolymers. To maintain controlled instability of the micelles, the degree of conjugation has to be balanced between sufficient hydrophobicity for the drug retention and the degradation time required for increasing the CMT above body temperatures. It is desirable that the CMT of the modified block copolymers is still above 0 °C so that the simple drug loading method (mixing an aqueous solution of the polymer and a small amount of drug-containing organic solvent and subsequent heating from below to above the CMT) can still be utilized. Another strategy to retard release of drug from polymeric micelles is the chemical conjugation of drugs to the hydrophobic core segments. The free hydroxyl groups in pHPMAmDL can again be utilized to exploit this strategy. The choice of linkers between the drugs and the polymers is very important, since a too stable conjugation via e.g. amide bonds may result in an insufficient release of drugs and consequently limits therapeutic effect [27]. Biodegradable peptide linkers such as Gly-Phe-Leu-Gly, a substrate for a lysosomal cathepsin B, are interesting candidates for accelerating drug release at the target site [28]. It should be noted that the conjugation of hydrophobic drugs is likely to decrease of the CMT of pHPMAmDL-*b*-PEG and in a positive sense affects the physical stability of the micelles. When the extent of grafting drugs is controlled so that the CMT is above body temperatures after the hydrolysis of the lactic acid side chains, the following strategy of drug targeting would be possible. First step includes stable retention of pHPMAmDL-*b*-PEG with chemically conjugated drugs in the circulation and passive accumulation in tumor tissues by the EPR effect, which is expected to be enhanced with respect to single chain polymers like pHPMAm-drug conjugates (e.g. PK1). Second step after tumor accumulation: destabilization of the micelles into single chain polymers due to the hydrophilization of the core. Third step: cellular internalization of single-chain polymers (or the micelles). Fourth step, cleavage of the tetrapeptide linkers by cathepsin B in lysosomes and the liberation of the drugs. An alternative strategy is that the drugs are liberated from the polymer extracellularly and the free drugs enter the cells. Regarding the preparation method, when the drug conjugated pHPMAmDL-*b*-PEG is soluble in water above 0 °C, a very simple micelle formation procedure by heating above the CMT is applicable similarly as non-loaded pHPMAmDL-*b*-PEG micelles. This is certainly a distinguished feature of our systems, since to our knowledge there has been no example of preparation of polymeric micelles loaded with hydrophobic drugs without any use of organic solvents.

For the stabilization of the micelles, chemical crosslinking of their core has proven to be an effective approach. Kissel et al. prepared core-crosslinked PCL-*b*-PEG micelles by radical polymerization of double bonds which were introduced in the PCL block. The polymeric micelles indeed showed an

enhanced *in vitro* stability: the micelles were not destabilized upon 1,000-fold dilution in water [29]. Crosslinking of the micellar core of pHPMAmDL-*b*-PEG micelles could be performed via derivatization of the free hydroxyl groups in the pHPMAmDL blocks.

The results of the *in vivo* biodistribution study performed in rats may suggest that some pHPMAmDL-*b*-PEG micelles entered the space of Disse in the liver. To substantiate this hypothesis, it would be interesting to investigate the cellular distribution of the micelles in the liver. If the micelles are distributed into hepatic parenchymal cells, this may open up possibilities to treat hepatocyte-related diseases like hepatitis B.

In addition to passive targeting by the EPR effect, active targeting with target-specific ligands such as antibodies, to achieve receptor-mediated binding to the target cells and subsequent internalization into the cells, may enhance the therapeutic index. In fact Torchilin et al. prepared micelles composed of a core of phosphatidylethanolamine (PE) and a shell of PEG, with cancer-specific monoclonal antibody 2C5 to the surface. The immunomicelles loaded with PTX showed an enhanced accumulation in tumors and inhibition of tumor growth in mice compared to PTX-loaded micelles without the antibody [30]. Coupling of targeting ligands to the surface of pHPMAmDL-*b*-PEG micelles should be possible by use of e.g. succinimidyl active PEG esters in preparing PEG₂-ABCPA macroinitiator. Then ligands with amine groups can be coupled to the ends of the PEG chains either before or after the formation of the micelles.

Apart from their use for polymeric micelles, poly(HPMAm-mono/di lactate) would also be a very attractive material for hydrogel-based drug delivery systems. Typically, thermosensitive hydrogels are prepared by physical crosslinking of triblock copolymers and these polymers include PEG-*b*-PL(G)A-*b*-PEG [31,32] and PL(G)A-*b*-PEG-*b*-PL(G)A [33,34]. The hydrogels are formed above the CP of the thermosensitive polymers by hydrophobic interactions between the collapsed polymers, in which drugs (from small molecules to proteins) can be held in a large quantity [33,34]. The following advantages of poly(HPMAm-mono/di lactate) as hydrogel forming materials are foreseen. Firstly, by the monomer ratio of HPMAmML and HPMAmDL, the gelation temperature of poly(HPMAm-mono/di lactate) can be adjusted around 30 °C. Then, *in situ* formation of the hydrogels is possible after injection. Secondly, the release of the entrapped drugs (low molecular weight as well as pharmaceutically active peptides and proteins) from the hydrogels can be controlled by the degradation of the lactic acid side chain of the polymers. The relatively long degradation time of HPMAmDL can be advantageous for the sustained release of drugs and other therapeutically relevant molecules for weeks. Thirdly, the biocompatibility of the materials is an important issue for hydrogel-based drug delivery systems as well as for polymeric micellar drug delivery systems. As mentioned above, poly(HPMAm-mono/di lactate), which

are eventually degraded into pHPMAm and lactic acid, is supposed to possess good biocompatibility. Thus, hydrogels seems to be a promising application of poly(HPMAm-mono/di lactate). Preliminary results indeed showed that pHPMAmDL-*b*-PEG-*b*-pHPMAmDL triblock copolymers formed hydrogels in an aqueous solution by heating above the CP of pHPMAmDL.

In conclusion, the work presented in this Thesis indicates that pHPMAmDL-*b*-PEG polymeric micelles have promising features as vehicles for hydrophobic drugs owing to their controlled instability.

References

1. S. Forster, T. Plantenberg. *Angew Chem Int Ed Engl* 41 (2002) 689-714.
2. G. Riess. *Prog Polym Sci* 28 (2003) 1107-1170.
3. H. Maeda, J. Wu, T. Sawa, Y. Matsumura, K. Hori. *J Control Release* 65 (2000) 271-284.
4. K. Kataoka, A. Harada, Y. Nagasaki. *Adv Drug Deliv Rev* 47 (2001) 113-131.
5. G.S. Kwon. *Crit Rev Ther Drug Carrier Syst* 20 (2003) 357-403.
6. Y. Matsumura, T. Hamaguchi, T. Ura, K. Muro, Y. Yamada, Y. Shimada, K. Shirao, T. Okusaka, H. Ueno, M. Ikeda, N. Watanabe. *Br J Cancer* 91 (2004) 1775-1781.
7. N. Rapoport, W.G. Pitt, H. Sun, J.L. Nelson. *J Control Release* 91 (2003) 85-95.
8. J.E. Chung, M. Yokoyama, T. Okano. *J Control Release* 65 (2000) 93-103.
9. Y. Bae, S. Fukushima, A. Harada, K. Kataoka. *Angew Chem Int Ed Engl* 42 (2003) 4640-4643.
10. Y. Kakizawa, A. Harada, K. Kataoka. *Biomacromolecules* 2 (2001) 491-497.
11. A. Napoli, M.J. Boerakker, N. Tirelli, R.J. Nolte, N.A. Sommerdijk, J.A. Hubbell. *Langmuir* 20 (2004) 3487-3491.
12. E.R. Gillies, T.B. Jonsson, J.M. Frechet. *J Am Chem Soc* 126 (2004) 11936-11943.
13. D. Neradovic, C.F. van Nostrum, W.E. Hennink. *Macromolecules* 34 (2001) 7589-7591.
14. D. Neradovic, M.J. van Steenberg, L. Vansteelant, Y.J. Meijer, C.F. van Nostrum, W.E. Hennink. *Macromolecules* 36 (2003) 7491-7498.
15. G. Chen, A.S. Hoffman. *Nature* 373 (1995) 49-52.
16. L. Shi, T.M. Chapman, E.J. Beckman. *Macromolecules* 36 (2003) 2563-2567.
17. C.Y. Hong, Y.Z. You, C.Y. Pan. *J Polym Sci Part A: Polym Chem* 42 (2004) 4873-4881.
18. C.J. Rijcken, T.F.J. Veldhuis, A. Ramzi, J.D. Meeldijk, C.F. van Nostrum, W.E. Hennink. *Biomacromolecules* 6 (2005) 2343-2351.
19. R. Haag. *Angew Chem Int Ed Engl* 43 (2004) 278-282.
20. E.R. Gillies, J.M. Frechet. *Chem Commun (Camb)* (2003) 1640-1641.
21. S.C. Kim, D.W. Kim, Y.H. Shim, J.S. Bang, H.S. Oh, S.W. Kim, M.H. Seo. *J Control Release* 72 (2001) 191-202.

22. X. Zhang, H.M. Burt, D. Von Hoff, D. Dexter, G. Mangold, D. Degen, A.M. Oktaba, W.L. Hunter. *Cancer Chemother Pharmacol* 40 (1997) 81-86.
23. E. Fournier, M.H. Dufresne, D.C. Smith, M. Ranger, J.C. Leroux. *Pharm Res* 21 (2004) 962-968.
24. H.M. Burt, X.C. Zhang, P. Toleikis, L. Embree, W.L. Hunter. *Colloids Surf B: Biointerfaces* 16 (1999) 161-171.
25. D. Le Garrec, S. Gori, L. Luo, D. Lessard, D.C. Smith, M.A. Yessine, M. Ranger, J.C. Leroux. *J Control Release* 99 (2004) 83-101.
26. T. Hamaguchi, Y. Matsumura, M. Suzuki, K. Shimizu, R. Goda, I. Nakamura, I. Nakatomi, M. Yokoyama, K. Kataoka, T. Kakizoe. *Br J Cancer* 92 (2005) 1240-1246.
27. M. Yokoyama, T. Okano, Y. Sakurai, K. Kataoka. *J Control Release* 32 (1994) 269-277.
28. R. Duncan. *Nat Rev Drug Discov* 2 (2003) 347-360.
29. X. Shuai, T. Merdan, A.K. Schaper, F. Xi, T. Kissel. *Bioconjug Chem* 15 (2004) 441-448.
30. V.P. Torchilin, A.N. Lukyanov, Z. Gao, B. Papahadjopoulos-Sternberg. *Proc Natl Acad Sci U S A* 100 (2003) 6039-6044.
31. B. Jeong, Y.H. Bae, D.S. Lee, S.W. Kim. *Nature* 388 (1997) 860-862.
32. B. Jeong, Y.K. Choi, Y.H. Bae, G. Zentner, S.W. Kim. *J Control Release* 62 (1999) 109-114.
33. G.M. Zentner, R. Rathi, C. Shih, J.C. McRea, M.H. Seo, H. Oh, B.G. Rhee, J. Mestecky, Z. Moldoveanu, M. Morgan, S. Weitman. *J Control Release* 72 (2001) 203-215.
34. M. Qiao, D. Chen, X. Ma, Y. Liu. *Int J Pharm* 294 (2005) 103-112.

Appendices

Nederlandse samenvatting

List of abbreviations

List of publications

Curriculum vitae

Acknowledgements

Nederlandse samenvatting

Veel potentieel therapeutisch actieve stoffen komen niet tot klinische toepassing vanwege hun slechte biofarmaceutische eigenschappen. Zo worden deze stoffen snel uit de bloedcirculatie verwijderd, ze worden snel door de lever in inactieve metabolieten omgezet en/of ze zijn niet in staat de juiste cellen te bereiken. Deze slechte eigenschappen van (potentiële) farmaca kunnen gemaskeerd worden door deze stoffen te encapsuleren in nanodeeltjes. Een veelbelovende categorie van nanodeeltjes is die van de polymere micellen. Deze bestaan uit amfifiele blokcopolymeren. Polymere micellen hebben een zogenaamde “core-shell” structuur en worden in water gevormd door spontane assemblage van amfifiele blokcopolymeren. Het hydrofiele segment van een blokcopolymeer vormt de “shell” en stabiliseert de micellaire structuur terwijl het hydrofobe segment de “core” van de micellen vormt. De hydrofobe core kan beladen worden met een grote variëteit aan met name hydrofobe farmaca. Door hun geringe afmeting (10-100 nm) zijn deze micellen geschikt om via de intraveneuze route toegediend te worden aan patiënten. Bovendien zijn ze in staat om pathologische weefsels, bijvoorbeeld tumoren of andere ontstekingshaarden, te bereiken door de lokaal verhoogde capillaire permeabiliteit. In de laatste decennia zijn er verschillende typen polymere micellen als drager voor therapeutisch actieve stoffen bestudeerd. In dit proefschrift zijn polymere micellen onderzocht als afgiftesysteem voor het hydrofobe cytostaticum paclitaxel. De onderzochte micellen bestaan uit blokcopolymeren van *N*-(2-hydroxypropyl) methacrylamide-lactaat (HPMAM-lactaat) en poly(ethyleen glycol) (PEG). Het poly(HPMAM-lactaat) heeft temperatuur-gevoelige eigenschappen, hetgeen wil zeggen dat dit polymeer oplosbaar is in water beneden de troebelings temperatuur (“cloud point”, CP) maar onoplosbaar is boven deze temperatuur. Blokcopolymeren van poly(HPMAM-lactaat) en het hydrofiele PEG zijn oplosbaar in water beneden de troebelings temperatuur van het poly(HPMAM-lactaat) blok, terwijl boven deze temperatuur “core-shell” micellen worden gevormd. De lactaat zijgroepen zijn via esterbindingen aan het polymeer gebonden. Het valt te verwachten dat deze bindingen langzaam zullen hydrolyseren waardoor uiteindelijk een blokcopolymeer van PEG en poly(*N*-(2-hydroxypropyl) methacrylamide) gevormd zal worden; een polymeer dat goed in water oplosbaar is en daardoor geen micellen vormt. Door de hydrolyse zullen de micellen dus geleidelijk uiteenvallen waardoor het ingesloten farmacon vrijkomt.

Hoofdstuk 1 van dit proefschrift geeft een overzicht betreffende polymere micellen als dragersysteem voor farmaca. Ook worden het doel en de opzet van dit proefschrift besproken. **Hoofdstuk 2** rapporteert over poly(*N*-(2-hydroxypropyl) methacrylamide mono/di-lactaat) als een nieuwe klasse van temperatuur-gevoelige polymeren. Er werd gevonden dat de

troebelings temperatuur van deze polymeren ingesteld kon worden tussen de 13 en 65 °C door de verhouding mono- en di-lactaat in het copolymeer te variëren. In **Hoofdstuk 3** worden amfifiele blokcopolymeren van poly(*N*-(2-hydroxypropyl) methacrylamide di-lactaat) en PEG bestudeerd. Deze polymeren vormen boven de troebelings temperatuur van het temperatuur-gevoelige poly(HPMAM-lactaat) blok (13 °C) micellen in water met een afmeting van ongeveer 50 nm. Met verschillende technieken werd aangetoond dat deze micellen bestaan uit een dicht gepakte “core” van poly(HPMAM-lactaat) en een corona van gezwollen PEG ketens. Hydrolyse-studies toonden aan dat de micellen inderdaad uiteenvallen; de berekende destabilisatietijd onder fysiologische condities bedraagt ongeveer 160 uren. In **Hoofdstuk 4** is aangetoond dat polymere micellen die bestaan uit poly(*N*-(2-hydroxypropyl) methacrylamide di-lactaat) en PEG zeer goed beladen kunnen worden met paclitaxel, een zeer hydrofoob cytostaticum. Deze micellen beladen met paclitaxel vertoonden een vergelijkbare *in vitro* celtoxiciteit als Taxol (een oplossing van paclitaxel in Cremophor EL, de klinisch gebruikte formulering van paclitaxel). Een opmerkelijk voordelig effect was dat de niet-beladen micellen een aanzienlijk geringere toxiciteit dan Cremophor EL bezitten. In **Hoofdstuk 5** worden *in vivo* studies beschreven van micellen die bestaan uit blokcopolymeren van poly(*N*-(2-hydroxypropyl) methacrylamide di-lactaat) en PEG. Aangetoond werd dat deze micellen na intraveneuze toediening relatief lang in de circulatie bleven. Therapeutische studies in tumor-dragende muizen toonden aan dat de paclitaxel beladen micellen een gelijke anti-tumor activiteit vertoonden als Taxol. De polymere micellen hadden wel het voordeel van een veel geringere toxiciteit vergeleken met die van de Taxolformulering.

Concluderend kan vastgesteld worden dat het werk beschreven in dit proefschrift heeft aangetoond dat polymere micellen die gebaseerd zijn op blokcopolymeren van poly(*N*-(2-hydroxypropyl) methacrylamide di-lactaat) en PEG veelbelovende dragersystemen zijn voor met name hydrofobe farmaca.

List of abbreviations

ABCPA	4,4-azobis(4-cyanopentanoic acid)
AFM	atomic force microscopy
AIBN	α, α' -azoisobutyronitrile
AMA	<i>N</i> -(3-aminopropyl) methacrylamide hydrochloride
ATRP	atom transfer radical polymerization
AUC	area under the curve
CDCl ₃	deuterated chloroform
CLSM	confocal laser-scanning microscopy
CMC	critical micelle concentration
CMT	critical micelle temperature
CP	cloud point
DENA monomer	2-(4-vinylbenzyloxy)- <i>N,N</i> -diethylnicotinamide
DDS	drug delivery systems
DLS	dynamic light scattering
DMAAm	dimethylacrylamide
DMEM	Dulbecco's modification of Eagle's Medium
D ₂ O	deuterated water
DOX	doxorubicin
DSC	differential scanning calorimetry
EDTA	ethylenediaminetetraacetic acid
EPR	enhanced permeability and retention
FACS	fluorescence activated cell sorting
FCS	fetal calf serum
FDA	Food and Drug Administration
FT-IR	Fourier transform infrared spectroscopy
GMP	good manufacturing practice
GOx	glucose oxidase
GPC	gel permeation chromatography
HEMAmDL	<i>N</i> -(2-hydroxyethyl) methacrylamide dilactate
[³ H]-NSP	<i>N</i> -succinimidyl[2,3- ³ H]-propionate
HPLC	high performance liquid chromatography
HPMAm	<i>N</i> -(2-hydroxypropyl) methacrylamide
HPMAm-lactate	<i>N</i> -(2-hydroxypropyl) methacrylamide lactate
<i>i.p.</i>	intraperitoneal
<i>i.v.</i>	intravenous
LCST	lower critical solution temperature
MALLS	multi-angle laser light scattering
M _n	number average molar weight
MPS	mononuclear phagocyte system
MTD	maximum tolerated dose

M_w	weight average molar weight
M_w (mic)	weight average molecular weight of micelles
N_A	Avogadro's constant
N_{agg}	aggregation number of micelles
NIPAAm	<i>N</i> -isopropylacrylamide
NMR	nuclear magnetic resonance spectroscopy
NNDNA	<i>N,N</i> -diethylnicotinamide
pAsp(DOX)	poly(aspartic acid) with chemically conjugated doxorubicin
PBLA	poly(β -benzyl-L-aspartate)
PBMA	poly(butyl methacrylate)
PBS	phosphate buffered saline
PCL	poly(ϵ -caprolactone)
PD	polydispersity index
PDENA	poly(2-(4-vinylbenzyloxy)- <i>N,N</i> -diethylnicotinamide)
PE	phosphatidylethanolamine
PEG	poly(ethylene glycol)
pHis	poly(L-histidine)
PHSA	poly(<i>N</i> -(6-hexylstearate)-L-aspartamide)
PLA	poly(lactic acid)
PNIPAAm	poly(<i>N</i> -isopropylacrylamide)
PPO	poly(propylene glycol)
PPS	poly(propylene sulfide)
PS	polystyrene
PTX	paclitaxel
PVP	poly(<i>N</i> -vinyl-2-pyrrolidone)
RAFT	reversible addition-fragmentation transfer polymerization
R_g	radius of gyration
R_{hyd}	hydrodynamic radius
RI	refractive index
RITC	rhodamine B isothiocyanate
SLS	static light scattering
TEM	transmission electron microscopy
T_g	glass transition temperature
UV	ultraviolet
XTT	sodium 3'-[1-(phenylaminocarbonyl)-3,4-tetrazolium]-bis(4-methoxy-6-nitro)benzene sulfonic acid hydrate
Z_{ave}	<i>z</i> -averaged particle size determined by DLS
ρ_{mic}	density of a micelle

List of publications

Papers

D. Neradovic, O. Soga, C.F. van Nostrum, W.E. Hennink. The effect of the processing and formulation parameters on the size of nanoparticles based on block copolymers of poly(ethylene glycol) and poly(*N*-isopropylacrylamide) with and without hydrolytically sensitive groups. *Biomaterials* 25 (2004) 2409-2418.

O. Soga, C.F. van Nostrum, W.E. Hennink. Poly(*N*-(2-hydroxypropyl) methacrylamide mono/di lactate): a new class of biodegradable polymers with tuneable thermosensitivity. *Biomacromolecules* 5 (2004) 818-821.

O. Soga, C.F. van Nostrum, A. Ramzi, T. Visser, F. Soulimani, P.M. Frederik, P.H. Bomans, W.E. Hennink. Physicochemical characterization of degradable thermosensitive polymeric micelles. *Langmuir* 20 (2004) 9388-9395.

O. Soga, C.F. van Nostrum, M.H.A.M. Fens, C.J.F. Rijcken, R.M. Schiffelers, G. Storm, W.E. Hennink. Thermosensitive and biodegradable polymeric micelles for paclitaxel delivery. *Journal of Controlled Release* 103 (2005) 341-353.

O. Soga, C.F. van Nostrum, C.J. Snel, M.H.A.M. Fens, R.M. Schiffelers, G. Storm, W.E. Hennink. *In vivo* efficacy of paclitaxel-loaded thermosensitive and biodegradable polymeric micelles. *Manuscript in preparation*.

C.F. van Nostrum, C.J.F. Rijcken, O. Soga, W.E. Hennink. *Manuscript in preparation (Review article)*.

Book chapter

C. F. van Nostrum, D. Neradovic, O. Soga, W. E. Hennink. Polymeric micelles with transient stability: a novel drug delivery concept. In *Polymeric Drug Delivery Volume I - Particulate Drug Carriers*, S. Svenson (Ed.), ACS Symposium Series, Vol. 923, American Chemical Society, Washington, DC (2006).

Patent

W.E. Hennink, C.F. van Nostrum, O. Soga, M.J. van Steenberg. Temperature sensitive polymers. *US Patent Application* No. 10/804,302.

Abstracts

O. Soga, D. Neradovic, C.F. van Nostrum, W.E. Hennink. Size control and pyrene loading of nanoparticles based on block copolymers of *N*-isopropylacrylamide and ethylene glycol. *Proceedings of the 30th International Symposium on Controlled Release of Bioactive Materials* (2003).

O. Soga, C.F. van Nostrum, W.E. Hennink. Thermosensitive and biodegradable polymeric micelles with transient stability. *Proceedings of the 8th European Symposium on Controlled Drug Delivery* (2004).

O. Soga, C.F. van Nostrum, M.H.A.M. Fens, C.J. Snel, C.J.F. Rijcken, R.M. Schiffelers, G. Storm, W.E. Hennink. Thermosensitive and biodegradable polymeric micelles for paclitaxel delivery. *Proceedings of the 12th International Symposium on Recent Advances in Drug Delivery Systems* (2005).

C.F. van Nostrum, O. Soga, C.J.F. Rijcken, A. Ramzi, T.F.J. Veldhuis, W.E. Hennink. Biodegradable polymeric micelles based on thermosensitive poly((methacrylamido)alkyl oligolactate) for delayed drug delivery. *Cellular & Molecular Biology Letters* 10 (2005) 59-61.

C.F. van Nostrum, O. Soga, C.J.F. Rijcken, A. Ramzi, T.F.J. Veldhuis, W.E. Hennink. Delayed drug delivery from degrading polymeric micelles based on thermosensitive poly(methacrylamide-lactate) derivatives. *Proceedings of the 32nd International Symposium on Controlled Release of Bioactive Materials* (2005).

Curriculum vitae

Osamu Soga was born on December 29th, 1970 in Gifu, Japan. In 1995 he received his master's degree in Engineering at the Research Division in Engineering, Synthetic Chemistry and Biological Chemistry Course of the postgraduate School, Kyoto University. In the same year he joined Mitsubishi Chemical Corporation (presently Mitsubishi Pharma Corporation), and was engaged in the pharmaceutical process development of MCC-465, an immunoliposomal formulation of doxorubicin, for seven years. In 2002 he joined the Department of Pharmaceutics at the Utrecht University as a guest researcher funded by the scholarship program of Mitsubishi Pharma Corporation, and started his Ph D project under supervision of Prof. Dr. Ir. W.E. Hennink, Prof. Dr. G. Storm, Dr. C.F. van Nostrum and Dr. R.M. Schiffelers. The results of this project are described in this thesis. In 2004 he returned to Mitsubishi Pharma Corporation, since then he works on formulation development of parenteral dosage forms.

Acknowledgements

It is nearly four years ago since I first visited the Netherlands in March 2002. At that time having a Ph D in Utrecht seemed a kind of dream to me. It was indeed a big challenge, but finally the dream became true. Now, thinking back with gratitude on the wonderful time I had in Utrecht, I again realize that my thesis work has been supported by so many people. I want to use the last pages to express my heartfelt thanks to them.

First of all, I would like to express my sincere gratitude to my promotor Prof. Dr. Wim Hennink for being my supervisor throughout this work and for his continuous hearty support for these four years. Wim, you have encouraged and motivated me to obtain a Ph D in Utrecht since our first meeting at your office. You were always positive and optimistic about my results, even when they were in contradiction to our expectations. In this way you inspired me to reach my goal. I really appreciate your guidance, not only in doing my research in Utrecht, but also in writing the thesis in Japan. Thank you very much also for your hospitality to Rie and me, as well as to my colleagues from Japan.

I also would like to thank my other promotor, Prof. Dr. Gert Storm, for guiding the biological part of my research. Gert, I appreciate your constructive criticism towards our *in vivo* results. I again realized that it is a big “challenge” to develop a drug targeting system which really works *in vivo*. Back to the year 2000; the lecture you gave at our company attracted me to your lab. Without your visit to Japan, I would not have had a chance to work in Utrecht and to write this thesis. So, thank you also for that.

I am very grateful to my copromotores, Dr. Rene van Nostrum and Dr. Raymond Schiffelers, for their advice and help in my research. Rene, I appreciate your sharp and useful comments on the results I obtained and the generosity in answering my questions on the chemical part of the work. I wish you further success in your research on polymeric micelles as well as in your other innovative research projects. Raymond, thank you for giving me a lot of helpful advice on the biological part of the project. I also appreciate your kind help after I returned to Japan. You were also a pleasant room-mate; your cheerful character always made me feel comfortable in our office.

I would like to express my appreciation to Prof. Dr. Daan Crommelin for opening the door for me to work in his lab. Daan, although I was not under your direct supervision, you kindly showed involvement in my research. I was really delighted when I occasionally obtained a compliment from you, since I know it is not easy to obtain positive remarks from you. I also appreciated your

continuous encouragement to obtain my Ph D. The meeting we had at your house to set up the plan for my thesis was a very fruitful and valuable, and on the other hand an exhausting experience for me.

I would like to extend my special thanks to Dr. Herre Talsma for his kind support and hospitality during our stay in Utrecht. You generously took care of us when starting our Dutch life; any problems Rie and I met (most of them were bureaucratic things) were solved by your help. During my first month in the Netherlands, when Rie was still in Japan, I had dinners quite often at your house, and spent weekends with you and your wonderful family. These are all great memories for me. I really appreciate all the things you did for us!

I am thankful to my collaborators, who greatly contributed to complete this thesis: Dragana, I was really lucky to succeed your interesting project. I appreciate your collaboration and help during my first year. I hope you like what I have achieved based on your system. Mies, I am very grateful to you for all your help throughout my research. Thank you very much also for your efforts on our hydrogel project. Although your name does not appear on any of the chapters of my thesis, I very much appreciate the many things you did for me to complete my work. In addition, your “sunshiny” personality always made me relaxed and cheered up. I really think you are a most indispensable person in your lab! Cor and Marcel, thanks a lot for so many biological experiments you performed for me, as well as the friendly mood you always created in our collaboration. Chapter 5 is definitely based on your valuable contribution. Marcel, thank you also for inviting Rie and me to your Shin Tai Ryu Riki Bu Dojo and to your house. I know you are more “Japanese” than I am! Cristianne, thanks for 2-weeks DLS experiments for me after I left for Japan. I hope you will develop our micellar system into more advanced and useful ones. Aissa, you helped me imagine what our micelles look like. Your SLS results added special value to Chapter 3. Tom and Fouad, thank you for your temperature-controlled FT-IR measurements and valuable discussions on the results. Peter and Paul, I appreciate your collaboration in the cryo-TEM measurements with your innovative Vitrobot technology. It was really an exciting moment for me when I observed beautiful spherical micelles through your microscope.

My hearty thanks go to my ex-room-mates in the lab for their friendship: Gerben, I can not express how grateful I am for your generosity and hospitality to Rie and me. You kindly did so many things for us, among which the time we spent with you, Miranda and your lovely kids at your house was a most enjoyable time for us. You must be a really happy man with your wonderful family! Marc, thank you very much for being my nice room-mate during my last year in Utrecht. You were always warm, sincere and very kind to me, creating a

pleasant atmosphere in our office. I appreciate all your help as well as your scientific advice. Carmen, thank you for the very pleasant time at your house with you and Michiel. We are also glad that you really liked our Japanese food, as we loved the Spanish food you cooked for us. Bart, we enjoyed ourselves very much in Amsterdam with you and Ingrid. Thank you also for inviting us to your house. I am impressed by your energy to start an enterprise. I hope you have great success in your liposome company!

I would like to express my warm thanks to Marc and Mies again, for being my “paranimfs”. For the last three months, you kindly supported a lot of the preparations for my thesis defense. Since I live far from Utrecht, your cooperation was extremely helpful. Thank you so much!

Other than my collaborators, I am thankful to the following people in the lab: Jan Hein for guiding me in amphotericin B project during my trainee period; Wim Jiskoot and Christien for your useful suggestions; Judith, Suzanne, Arjen, Mark, Jordy, Karin, Theo, Adrienne, Louis, Marieke, Marjan (sorry if I miss some of your names) for helping my experiments such as NMR, DSC and FT-IR etc. Barbara, thank you for all your help in the procedures for my Ph D.

To all the people in the lab: thanks to you I really enjoyed my stay in Utrecht. I am very happy to have been a member of such a great lab with you wonderful people!

Here in Japan, I would like to express my sincere gratitude to Mitsubishi Pharma Corporation for providing me an opportunity to study and work in Utrecht for two years, and for their financial supports for my research. Especially I would like to thank Tezuka-san, Morimoto-san, and Chiba-san for encouraging me to study abroad and giving me this opportunity. It was really a great and valuable experience for me to work with people having a different language and cultural background. I also would like to thank Ozaki-san for his support during my stay in the Netherlands, as well as for generously allowing me to continue my thesis work after returning to Japan.

Finally, I would like to dedicate this thesis to my wife, Rie. Thank you so much for your continuous support in these four years. Without you this thesis would have never been realized.

Iedereen ontzettend bedankt!

Osamu